

Contrails

FOREWORD

This report presents the results of an investigation on the effects of elastic deformation on the stability and control of airframes, and in particular the effects on the modifications to the longitudinal transfer functions caused by coupling of the elastic modes. The research reported was sponsored by the Flight Control Laboratory of the Aeronautical Systems Division under Project No. 8219, Task No. 821901. It was started 1 November 1960 and completed 15 February 1962 at Systems Technology, Inc., under Contract No. AF 33(616)-7657. The ASD project engineer has been Mr. H. M. Davis of the Flight Control Laboratory, and the project engineer at Systems Technology, Inc., has been Mr. I. L. Ashkenas and Mr. B. F. Pearce, successively.

The authors are indebted to Mr. I. L. Ashkenas for this guidance and numerous suggestions, and to Mr. R. Walton for his contribution to the section on single sensor control loop systems. Acknowledgment is also given to the production staff for their help in preparing this report.

ASD-TDR-62-279

Contracts

ABSTRACT

This report presents results of a study on elastic-airframe dynamics that are important from the standpoint of flight control system design. Approximate transfer functions are given in literal terms for three classes of vehicles. These are of such a form that the important poles and zeros are related directly to simple functions of aerodynamic, elastic, and inertial properties. The aero-elastic corrections required to account for the flexibility influences of all modes not included in the equations of motion are discussed, and a rigorous method for applying these corrections is presented.

PUBLICATIONS REVIEW

This report has been reviewed and is approved.

FOR THE COMMANDER:



C. B. WESTBROOK
Chief, Aerospace Mechanics Branch
Flight Control Laboratory

Contracts

CONTENTS

	<u>Page</u>
I INTRODUCTION.	1
A. General	1
B. Outline of the Report	3
II EQUATIONS OF MOTION	5
A. General Equations of Motion	5
B. Elimination of the High-Frequency Modes	15
C. Aerodynamic Forces	20
D. Final Equations of Motion	24
III FLEXIBLE AIRFRAME APPROXIMATE TRANSFER FUNCTIONS.	28
A. Discussion of Methods of Derivation.	28
B. Approximate Factors	30
C. Adequacy of One- and Two-Elastic-Mode Representations.	30
D. Numerical Comparisons of Exact and Approximate Factors	40
IV SINGLE SENSOR CONTROL LOOP SYSTEMS	41
A. Introduction	41
B. Sensor Output	41
C. Closed-Loop Considerations.	43
D. Optimum Sensor Location.	45
V RECOMMENDATIONS FOR FUTURE INVESTIGATIONS	52
REFERENCES.	55
APPENDIX A - AEROELASTIC CORRECTIONS	56
APPENDIX B - ANALYTICAL METHODS OF APPROXIMATE FACTORIZATION	69
APPENDIX C - DESCRIPTION OF CONFIGURATION	78
APPENDIX D - NUMERICAL EQUATIONS OF MOTION, APPROXIMATE FACTORS AND EXACT FACTORS	95

Contrails

ILLUSTRATIONS

		<u>Page</u>
1	Flexible Airframe Represented by n Control Points.	8
2	Mode Displacement Curves; $q_i = \sum_{j=1}^n \phi_{ij} \xi_j$	10
3	Derivation of the [W] Matrix.	14
4	Bode (j ω) Amplitude for Typical θ/δ with Lead Equalization.	44
5	Bode (j ω) Amplitude for θ/δ with $\omega_{1e} < \omega_{\theta 1}$ and ω_{sp} Near ω_{1e}	44
6	Bode (j ω) Amplitude for $A_{\xi 4} N_{\xi 3} / A_{\xi 3} N_{\xi 4}$	47
7	Bode (j ω) Amplitude for $A_{\theta} N_{\xi 4} / A_{\xi 4} N_{\theta}$	47
8	Variation of Mode Slopes Along the Fuselage.	48
9	Locus of Roots for First Closure, $A_{\xi 4} N_{\xi 3} / A_{\xi 3} N_{\xi 4}$	50
10	Pole Zero Configuration for Second Closure, $\frac{A_{\theta} N_{\xi 4}}{A_{\xi 4} N_{\theta}} \left(1 + \frac{\phi'_{13} N_{\xi 3}}{\phi'_{14} N_{\xi 4}} \right)$	50
A-1	Mechanical Model.	58
C-1	Elastic Modes for Configuration 2	80
C-2	Elastic Modes for Configuration 3	82
C-3	Elastic Modes for Configuration 4	84
C-4	Configuration 2	90
C-5	Configuration 3	91
C-6	Aerodynamic Strips for Configuration 3	92
C-7	Configuration 4	93
C-8	Aerodynamic Strips for Configuration 4	94
D-1	Equations of Motion in Numerical Terms, Configuration 2.	96
D-2	Equations of Motion in Numerical Terms, Configuration 3.	97
D-3	Equations of Motion in Numerical Terms, Configuration 4.	98

Contrails

TABLES

	<u>Page</u>
I Summary of Transfer Function Factored Forms	29
II Transfer Function Approximate Factors, Configuration 2, 3 Modes	31
III Transfer Function Approximate Factors, Configuration 3, 3 Modes	32
IV Transfer Function Approximate Factors, Configuration 4, 3 Modes	33
V Transfer Function Approximate Factors, Configuration 2, 4 Modes	34
VI Transfer Function Approximate Factors, Configuration 3, 4 Modes	36
VII Transfer Function Approximate Factors, Configuration 4, 4 Modes	38
C-I Description of Configurations.	79
C-II Mode Shapes and Frequencies, Configuration 2.	81
C-III Mode Shapes and Frequencies, Configuration 3.	83
C-IV Mode Shapes and Frequencies, Configuration 4.	85
C-V $[X_{(f+\infty)}] \times 10^6$, Configuration 2	86
C-VI $[X_{(f+\infty)}] \times 10^6$, Configuration 3	87
C-VII $[X_{(f+\infty)}] \times 10^6$, Configuration 4	88
C-VIII Flight Conditions.	89
D-I Numerical Values for Exact and Approximate Transfer Function Factors, Configuration 2	99
D-II Numerical Values for Exact and Approximate Transfer Function Factors, Configuration 3	100
D-III Numerical Values for Exact and Approximate Transfer Function Factors, Configuration 4	101

Contrails

LIST OF SYMBOLS

a_{ij}	Constant coefficient
a_{ij}	Lift at the $1/4$ chord of the i^{th} aerodynamic surface due to unit vertical displacement of the $3/4$ chord of the j^{th} surface (lb/ft)
[a]	Matrix of a_{ij} 's
A_w	Root locus gain of w/δ transfer function (ft/sec ²)
A_θ	Root locus gain of θ/δ transfer function (rad/sec ²)
A_{ξ_r}	Root locus gain of ξ_r/δ transfer function (ft/sec ²)
b_{ij}	Constant coefficient
b_{ij}	Lift at the $1/4$ chord of the i^{th} aerodynamic surface due to unit rigid rotation of the chord of the j^{th} surface (lb)
[b]	Matrix of b_{ij} 's
B	Polynomial coefficient
c	Local chord (ft)
c.g.	Center of gravity
c.p.	Center of pressure
cps	Cycles per sec
c_{ij}	Moment on the i^{th} aerodynamic surface due to unit vertical displacement of the $3/4$ chord of the j^{th} surface (ft-lb)
[c]	Matrix of c_{ij} 's
C	Polynomial coefficient
\mathcal{C}	Centerline
C_{ij}	Flexibility influence coefficient giving the physical displacement at the i^{th} point caused by a unit physical force (i.e., a force or a moment) at the j^{th} point (ft/lb)
$C_{L\alpha}$	Lift coefficient per unit α (per rad)
$C_{m\dot{\theta}}$	Pitching moment coefficient per unit $\dot{\theta}c/2U_0$
db	Decibels ($20 \log_{10}$ amplitude ratio)
d_{ij}	Moment on the i^{th} aerodynamic surface due to unit rigid rotation of the chord of the j^{th} surface (ft-lb)

Contrails

[d]	Matrix of d_{ij} 's
D	Polynomial coefficient
D	Damping energy of system (ft-lb/sec)
E	Polynomial coefficient
EI	Stiffness (Young's modulus times section moment of inertia)(lb-ft ²)
$F_{q_{\xi_r}}$	Generalized force in q^{th} mode per unit deflection in r^{th} generalized coordinate (lb/ft)
$F_{q_{\dot{\xi}_r}}$	Generalized force in q^{th} mode per unit velocity in r^{th} generalized coordinate (lb/ft/sec)
F_r	Generalized force in r^{th} mode (lb)
F_1	Generalized force in the first mode, Z_m (lb)
F_2	Generalized force in the second mode, MI_y (ft-lb)
{F}	Column matrix of modal forces
[F_{ξ}]	Modal forces per unit deflections in { ξ } (and unit velocities in { $\dot{\xi}$ }, etc.)
h	Rigid-body displacement (positive down) (ft)
I_y	Total pitch inertia of the system (slug ft ²)
I_2	Pitch inertia of mass two (example in Appendix A) (slug ft ²)
[I]	The identity matrix
k_{ij}	Stiffness influence coefficient giving the set of generalized forces, Q_i , required to make $q_r = 1$ and $q_i = 0$ for $i \neq r$ (lb/ft)
[k]	Matrix of stiffness influence coefficients
K_i	Stiffness influence coefficient of the i^{th} mode (lb/ft)
[K]	Stiffness matrix in modal coordinates
l	Length (ft)
l_{n_k}	Distance from the airframe center of gravity to the k chord of the n^{th} aerodynamic surface, positive aft (ft)
L	Z force (positive down) (lb)
L	T - U (ft-lb)
m	Total mass of the system (slugs)

Contrails

m_i	Physical mass at the i^{th} point (slugs)
$[m]$	Matrix of masses
M	Aerodynamic moment (ft-lb)
M	Rotational acceleration (rad/sec ²)
M_q	Pitching acceleration per unit pitching velocity (1/sec)
M_w	Pitching acceleration per unit w (sec/ft)
M_r	Generalized mass of r^{th} normal mode (slugs)
M_{ξ_k}	Rotational acceleration per unit deflection of k^{th} mode ($\frac{\text{rad/sec}^2}{\text{ft}}$)
M'_{ξ_k}	Rotational acceleration per unit velocity of k^{th} mode (rad/ft-sec)
MAC	Mean aerodynamic chord
$[M]$	Matrix of generalized modal masses
N_w	Numerator of w/δ transfer function
N_θ	Numerator of θ/δ transfer function
N_{ξ_r}	Numerator of ξ_r/δ transfer function
$P(s)$	Polynomial in s
q	Dynamic pressure (lb/ft ²)
q_i	Physical displacement (which may be either a translation or a rotation) at the i^{th} point (ft)
$\{q\}$	Column matrix of q_i 's
Q_i	Physical force (i.e., a force or a moment) applied at the i^{th} point (lb)
Q_{ai}	Physical aerodynamic force at the i^{th} point (lb)
Q_{ei}	Physical elastic force at the i^{th} point (lb)
Q_{in}	Physical aerodynamic force input caused by a movement of control surfaces (lb)
$\{Q\}$	Column matrix of physical forces
$\{Q_{in}\}$	Column matrix of Q_{in} 's
rad	Radians
R_{ij}	Physical aerodynamic force at point i caused by a unit movement of point j (lb/ft)

Contrails

$R_1(s)$	Polynomials in s
$R_2(s)$	
$[R]$	Aerodynamic matrix with elements R_{ij}
s	Laplace transform variable (1/sec)
sec	Second(s)
S	Wing area (ft ²)
t	Time (sec)
T	Kinetic energy of system (ft-lb)
T_k	$1/T_k$ is the position of the zero associated with k (1/sec)
U	Potential energy of system (ft-lb)
U_0	Forward velocity of the vehicle (ft/sec)
w	Rigid-body velocity measured normal to instantaneous body reference line (ft/sec)
$[W]$	Transformation matrix whereby h is transformed to w and all other modal coordinates remain unchanged
x	Variable
$[X]$	$[\Phi] [Y]^{-1} [\Phi]^T$
y	Variable
y_i	Vertical deflection of elastic vehicle at point i (ft)
y_i	Vertical displacement of i^{th} mass (ft)
$[Y]$	$[Ms^2 + K]$
Z	Vertical acceleration, along the Z axis (ft/sec ²)
Z_q	Vertical acceleration per unit pitching velocity (ft/sec)
Z_w	Vertical acceleration per unit w (1/sec)
Z_{ξ_k}	Vertical acceleration per unit deflection in k^{th} mode (1/sec ²)
$Z_{\dot{\xi}_k}$	Vertical acceleration per unit velocity in k^{th} mode (1/sec)
α	Angle of attack, w/U_0 (rad)
α, β	Variables

Contrails

δ	Control surface deflection (rad)
δ_{ij}	Kronecker delta ($\delta_{ij} = 0, i \neq j; \delta_{ij} = 1, i = j$)
Δ	Denotes finite increment in quantity
Δ	Transfer function denominator
ζ	Damping ratio
ζ_{ke}	Damping ratio of the k^{th} coupled elastic mode
ζ_r	Effective structural damping ratio of the r^{th} mode
θ	Rigid-body rotation (rad)
θ_i	Rotation of elastic fuselage at point i (rad)
ξ_r	Generalized coordinate or displacement of the r^{th} mode (ft)
$\dot{\xi}_1$	Time rate of change of the generalized coordinate of the first mode, w (ft/sec)
ξ_2	Generalized coordinate of the second mode, θ (rad)
ρ	Air density (slugs/ft ³)
ϕ_{ir}	Translation of i^{th} point in r^{th} normal mode (ft)
Φ_{ir}	Normalized translation of i^{th} point in r^{th} mode
Φ'_{ir}	Normalized rotation of surface at i^{th} point in r^{th} normal mode
Φ_r	Normalized shape of the r^{th} normal mode
$[\Phi]$	Modal matrix, formed with Φ_r 's as columns
ω	Frequency (rad/sec)
ω_{ke}	Frequency of the k^{th} coupled elastic mode (rad/sec)
ω_r	Eigenvalue of the r^{th} normal mode (rad/sec)
\doteq	Approximately equal to
\equiv	Is defined as
\ll	Much less than
\gg	Much greater than
Σ	Summation
$(\dot{\quad})$	Dot over quantity denotes time derivative

Contrails

$[]$	Matrix
$[]$	Diagonal matrix
$[]$	Row matrix
$\{ \}$	Column matrix
$[]^T$	Transpose
$[]^{-1}$	Inverse
$()'$	Prime denotes differentiation with respect to fuselage station

Subscripts

a	Aerodynamic force
a	Acceleration deflections
f	Associated with modes of nonzero frequency which are of interest
g	Grounded coordinates
ke	Associated with k th elastic mode
m	Movable coordinates
o	Associated with modes of zero frequency
rot	Rotation
sp	Short period
trans	Translation
w_k	k th root of w transfer function numerator
θ_k	k th root of θ transfer function numerator
$\xi_{r,k}$	k th root of ξ_r transfer function numerator
∞	Associated with modes of nonzero frequency which are not of interest
1/4	Designates the c.p. (ordinarily at 1/4 chord)
3/4	Three-quarter point of chord

Contrails

SECTION I

INTRODUCTION

A. GENERAL

The high-speed capabilities of modern airplanes depend on (among other things) the use of extremely low thickness ratios for lifting surfaces and on very high fineness ratios for bodies. Coupled with desired payload and range capabilities, which impose natural restrictions on weight, this dependence leads to fairly flexible structures and relatively low frequencies for the structural oscillatory modes. For certain flight conditions, these modes tend to couple with the rigid-body, short-period motions; in some cases, this tendency is greatly exaggerated by the action of the autopilot. The danger of such autopilot-flexible airframe coupling generally increases as the structure is lightened to reflect reduced stiffness requirements. In such cases, the incipient airframe-autopilot instability must be checked by analyses which may require, in addition to the normal rigid-body modes, consideration of

1. as many as the first three or four coupled normal ("free-free") modes, which, in general, comprise fuselage, wing, and tail deflections
2. structural damping effects, usually included as an equivalent viscous damping
3. contributions of the structural modes to the sensor output
4. control system nonlinearities and more detailed treatment of control system dynamics than necessary for rigid situations
5. nonstationary aerodynamic effects.

Regardless of its complexity, the closed-loop system must be stable for each of the flight regimes to be encountered. Additionally, it must accept the required guidance inputs, and must cope with undesired inputs, such as atmospheric turbulence and noise generated by the airframe-autopilot system itself, and must not exceed structural or other limits. Preferably, this is to be accomplished with a simple control system.

Manuscript released by the authors April 1962 for publication as an ASD
Technical Documentary Report

Contrails

Ad hoc solutions to the problem posed above have been obtained by increasingly complex multidegree-of-freedom analyses which involve the use of large computer facilities. Such analyses provide little insight into the physics of the problem; consequently, interpretation of the results to obtain more than a yes-no answer and an extension of the findings to slightly modified situations is difficult. Furthermore, there is little carry-over from system to system, so that, for example, the number and types of basic degrees of freedom required to yield the critical situation for a new design cannot readily be assessed a priori. The design process suffers accordingly. Not only is an undesirably long time required to select (and perhaps later modify) the pertinent degrees of freedom, and to set up and run the problem, but also modifications required to cure discovered problem areas are difficult to explain to a design group affected or to management. For these reasons, it is desirable to obtain simple literal approximations to the airframe transfer function factors. Such approximations relating the important poles and zeros directly to simple functions of aerodynamic, elastic, and inertial properties can provide an invaluable design guide.

This report presents the results of a 1-year study devoted to the analytical approximation of flexible airframe transfer functions. In this study, three classes of vehicles were represented by typical configurations, and the influence of elastic modes on the longitudinal transfer functions was examined (the three configurations were also subjected to a parallel study, Ref. 1, which yielded the basic information, i.e., mode shapes, etc., used in this study). Each of the configurations is shown to possess transfer function factors which can be simply approximated by a few major terms when interest is confined to only the first two elastic modes. (The results of Ref. 1 show that additional higher-frequency modes do not appreciably affect the two-elastic-mode transfer function in the frequency range that is important for flight control analysis.)

The first configuration studied (Configuration 2) is a missile-like vehicle with canard control, capable of supersonic speeds at low altitudes. Configuration 3 is a swept-wing, high-aspect-ratio arrangement, while Configuration 4 is a supersonic delta-wing vehicle. All three configurations are described in detail in Appendix C.

B. OUTLINE OF THE REPORT

The report is divided into five sections followed by four appendices. Most of the analytical work is presented in Sections II through IV, while the numerical data are included in the appendices.

Section II presents a derivation of the equations which are used to form the transfer functions. The static aeroelastic effect of the truncated high-frequency modes on the aerodynamic inputs is discussed and the method of inclusion is shown. The derivation of the matrix required in this method is presented in Appendix A.

The transfer function factored forms are presented in Section III, along with the approximation formulas for the three configurations studied. All of these approximations were derived by one of the methods presented in Appendix B.

Section IV discusses the problem of sensor location for closed-loop operation. The effect of sensor location on a particular configuration is shown, and a method for "optimum" placement is suggested. ("Optimum" here implies that the effect of the elastic modes is minimized with respect to the rigid-body pitch degree of freedom.)

As noted, Appendix A presents a derivation of a proper method of accounting for the elastic modes not included in the equations. This method was derived in Ref. 1, and Appendix A parallels that presentation. An example is included which utilizes the method, and shows the exactness of the results obtained.

Appendix B presents the several methods that were used to derive the transfer function approximation formulas of Section III. No one method could be found which consistently produced the simplest approximations; hence, the approximations were derived by the best of those in Appendix B for the case at hand.

A detailed description of the configurations studied is presented in Appendix C, along with the normal mode shapes used.

The numerical equations of motion for each configuration are included in Appendix D, as are the exact transfer functions that these equations yielded. The equations and the transfer functions were calculated by a digital computer according to the equations outlined in Section II. The transfer functions obtained with the approximation formulas of Section III are also presented in

Contrails

Appendix D as an indication of their accuracy. All of these data are presented for a range of dynamic pressures for each configuration with one and two elastic modes included.

SECTION II EQUATIONS OF MOTION

The equations will first be derived in terms of the physical coordinates of the airframe, and will then be converted to modal coordinates to allow a reduction in degrees of freedom and coupling terms by the use of orthogonal modes. The high-frequency modes will then be eliminated and the equations reduced to a set involving a limited number of flexible modes. Detailed consideration of the aerodynamic forces will then give the form of various coefficients involved in the final equations of motion.

A. GENERAL EQUATIONS OF MOTION

The methods for the development of expressions for the inertial and elastic forces on a flexible airframe differ, depending on whether the inertial and external loadings are considered to be distributed or concentrated. If they are considered to be concentrated at a finite number of points, then the displacement of any point, q_i , can be written

$$q_i = \sum_{j=1}^n C_{ij} Q_j \quad (1)$$

where q_i is the physical displacement (which may be either a translation or a rotation) at the i^{th} point
 C_{ij} is the flexibility influence coefficient giving the physical displacement at the i^{th} point caused by a unit physical force (i.e., a force or a moment) at the j^{th} point
 Q_j is the physical force applied at the j^{th} point

A force and a moment can be applied simultaneously at any given location merely by making two of the n points of application coincident; e.g., the first and second of the n points will be the same if Q_1 is a force applied at some location, and Q_2 is a moment applied at the same location.

The physical elastic force at point i due to any arbitrary set of physical displacements, q_j , can be expressed as

Contrails

$$Q_{e_i} = - \sum_{j=1}^n k_{ij} q_j \quad (2)$$

where k_{ij} is a stiffness influence coefficient. For any j (e.g., $j = r$), the set of k_{ir} 's is equal to the set of forces, Q_i , required to make $q_r = 1$ and $q_i = 0$ for $i \neq r$.

If the distributed air loads over the airframe are considered to act as a set of concentrated forces, the sum of the elastic and aerodynamic forces at the i th mass may be equated to the inertial force at that point, yielding (neglecting structural damping)

$$m_i \frac{d^2 q_i}{dt^2} = Q_{e_i} + Q_{a_i} \quad (3)$$

where m_i is the physical mass at the i th point
 Q_{a_i} is the physical aerodynamic force at the i th point

The aerodynamic force may be considered to be generated by the displacement of a finite number of physical coordinates on the airframe.

$$Q_{a_i} = \sum_{j=1}^n R_{ij} q_j \quad (4)$$

where R_{ij} is the physical aerodynamic force at point i caused by a unit movement of point j . R_{ij} will generally be a polynomial in the differential operator (or Laplace variable), s

Using matrix notation, it is possible to write Eq 2 and 4 as

$$\{Q_e\} = -[k]\{q\} \quad (5)$$

and

$$\{Q_a\} = [R]\{q\} \quad (6)$$

Contrails

Equation 3 now becomes

$$[ms^2] \{q\} = -[k] \{q\} + [R] \{q\} \quad (7)$$

It is customary to combine the elastic and inertial forces because these do not vary with dynamic pressure:

$$[ms^2 + k] \{q\} = [R] \{q\} \quad (8)$$

If movement of the control surfaces, while introducing aerodynamic forces into the system, does not introduce significant inertial or elastic force, it is reasonable to separate control surface deflections from the rigid-body and elastic deflections, and to write Eq 8 as

$$[ms^2 + k] \{q\} = [R] \{q\} + \{Q_{in}\} \quad (9)$$

where Q_{in} is the physical aerodynamic force input caused by the movement of control surfaces. Gust loads, nonuniform wind conditions, etc., will create forces which can also be included in the Q_{in} term

Equation 9, when expanded, appears as follows:

$$\begin{aligned} m_1 s^2 q_1 + k_{11} q_1 + k_{12} q_2 + \dots + k_{1n} q_n &= R_{11} q_1 + R_{12} q_2 + \dots + R_{1n} q_n + Q_{in1} \\ m_2 s^2 q_2 + k_{21} q_1 + k_{22} q_2 + \dots + k_{2n} q_n &= R_{21} q_1 + R_{22} q_2 + \dots + R_{2n} q_n + Q_{in2} \\ \vdots & \vdots \\ m_n s^2 q_n + k_{n1} q_1 + k_{n2} q_2 + \dots + k_{nn} q_n &= R_{n1} q_1 + R_{n2} q_2 + \dots + R_{nn} q_n + Q_{inn} \end{aligned} \quad (10)$$

Equations 10, then, are the equations of motion (for perturbations from a trimmed condition) for a flexible airframe represented by n control points (see Fig. 1). The degree of accuracy employed in the construction of the $[R]$ matrix, and the number and location of discrete mass points chosen, will determine the adequacy of these equations in representing the actual system. Because a great number of q_1 's is generally required for an adequate representation of a

Contrails

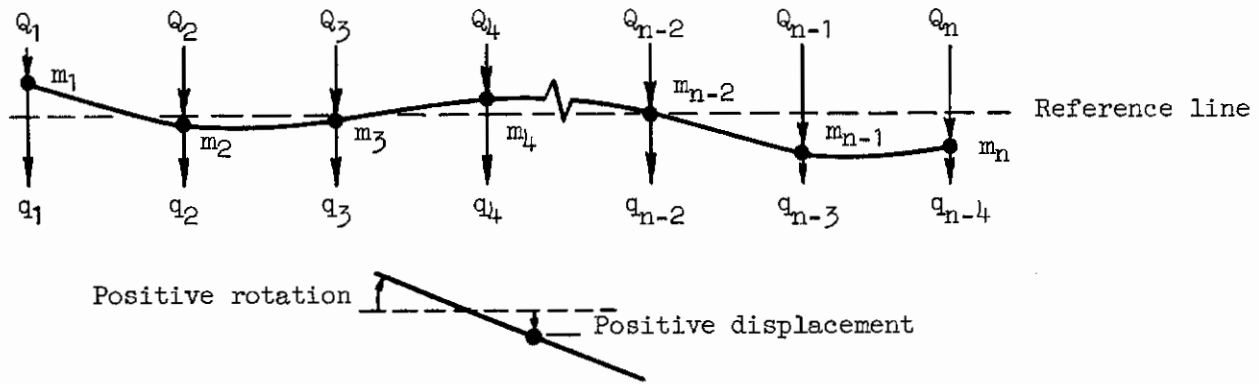


Figure 1. Flexible Airframe Represented by n Control Points

continuous airframe with a continuous loading, it is impractical to work directly with Eq 10 to achieve simple approximate methods. As an equation-reducing alternative, airframe motion is often represented by a few normal modes; then, each of the q_i 's consists of the superposition of the motion of the modal coordinates; i.e.,

$$q_i = \sum_{j=1}^n \Phi_{ij} F_j(t) \quad (11)$$

Defining

$$\varphi_{ij} = \frac{\Phi_{ij}}{\Phi_{ij_{ref}}} \quad (12)$$

Then,

$$q_i = \sum_{j=1}^n \varphi_{ij} \Phi_{ij_{ref}} F_j(t) \quad (13)$$

Defining

$$\xi_j = \Phi_{ij_{ref}} F_j(t) \quad (14)$$

Then,

$$q_i = \sum_{j=1}^n \varphi_{ij} \xi_j \quad (15)$$

where q_i is the physical displacement at the i th point on the airframe
 Φ_{ij} is the physical displacement of the i th point caused by a unit generalized displacement of the j th normal mode
 φ_{ij} is the physical normalized displacement at the i th point caused by a unit generalized deflection of the j th normal mode. The collection of all the φ_{ij} 's for any given j represents the mode shape for the j th normal mode.

Contrails

ξ_j is the generalized displacement or coordinate of the j^{th} normal mode; i.e., ξ_j is a scale factor for the j^{th} normal mode, given by the normalized physical displacement (resulting from deflection of the j^{th} normal mode, and no other) of a preselected point on the airframe.

Thus,

$$\begin{aligned} q_1 &= \varphi_{11}\xi_1 + \varphi_{12}\xi_2 + \cdots + \varphi_{1n}\xi_n \\ q_2 &= \varphi_{21}\xi_1 + \varphi_{22}\xi_2 + \cdots + \varphi_{2n}\xi_n \\ &\vdots \\ q_n &= \varphi_{n1}\xi_1 + \varphi_{n2}\xi_2 + \cdots + \varphi_{nn}\xi_n \end{aligned} \tag{16}$$

This may be written in matrix form as

$$\{q\} = [\Phi] \{\xi\} \tag{17}$$

Henceforth, $[\Phi]$ will be referred to as the modal matrix. A typical graphical presentation of Eq 16 is given in Fig. 2.

The n columns of $[\Phi]$, i.e., the mode shapes, are found by assuming simple harmonic motion ($s = j\omega$) and substituting Eq 17 into Eq 9,

$$[k - m\omega^2] \{\varphi_i\} = \{0\} \tag{18}$$

which can also be written

$$[k] \{\varphi_i\} - [m\omega_i^2] \{\varphi_i\} = 0 \tag{19}$$

$$[k] \{\varphi_i\} - [m] \omega_i^2 \{\varphi_i\} = 0 \tag{20}$$

$$[m]^{-1} [k] \{\varphi_i\} = \omega_i^2 \{\varphi_i\} \tag{21}$$

The form of Eq 21 makes it clear that the ω_i^2 's are eigenvalues of $[m]^{-1} [k]$, and the φ_i 's are the associated eigenvectors.

For any two linearly independent eigenvectors, it is possible to write (Eq 20)

Contrails

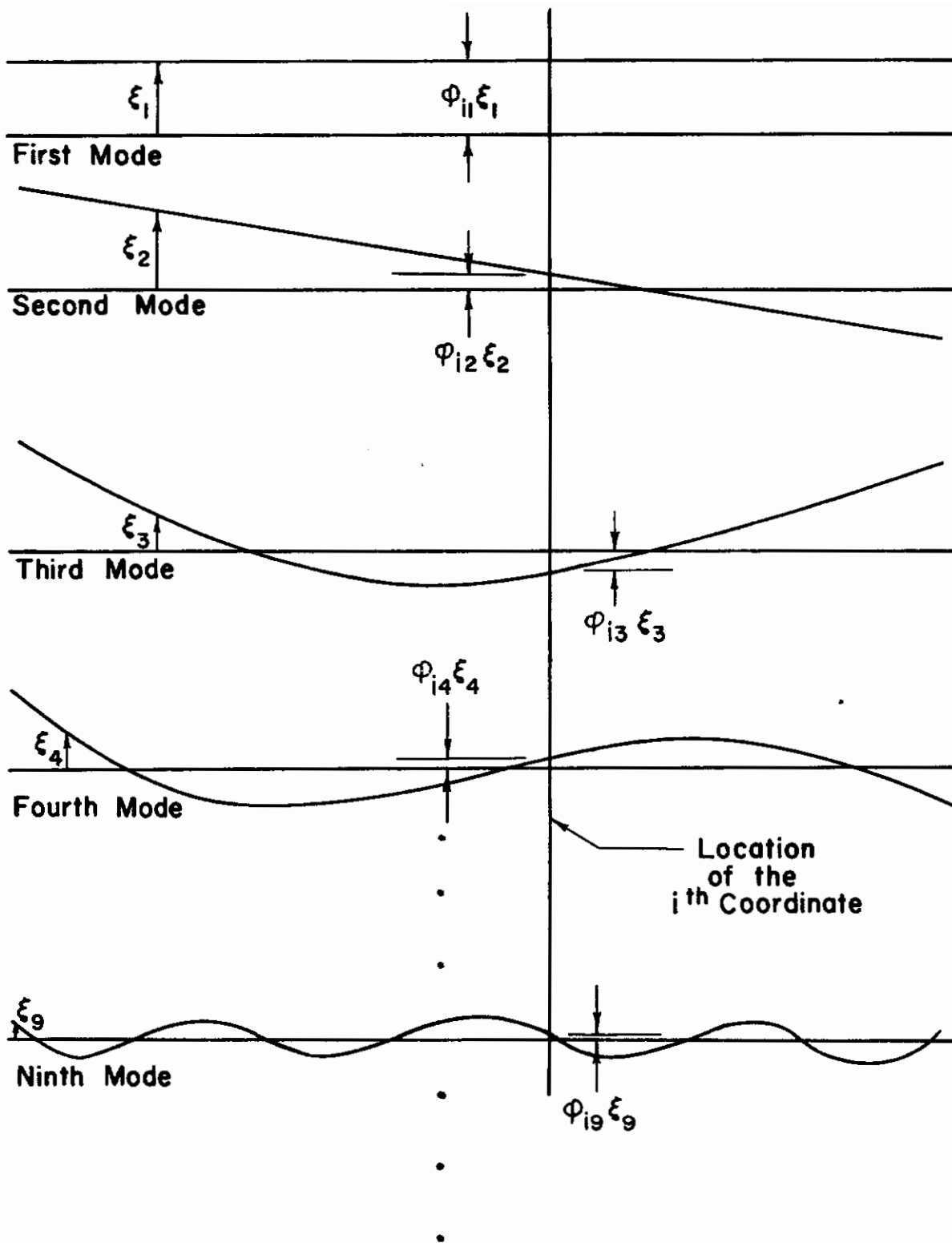


Figure 2. Mode Displacement Curves; $q_i = \sum_{j=1}^n \phi_{ij} \xi_j$

Contrails

$$[k] \{\varphi_a\} = \omega_a^2 [m] \{\varphi_a\} \quad (22)$$

$$[k] \{\varphi_b\} = \omega_b^2 [m] \{\varphi_b\} \quad (23)$$

When both sides of Eq 22 are transposed,

$$[\varphi_a^T] [k]^T = \omega_a^2 [\varphi_a^T] [m]^T$$

Therefore, $[\varphi_a^T] [k]^T \{\varphi_b\} = \omega_a^2 [\varphi_a^T] [m]^T \{\varphi_b\}$

But $[k]$ and $[m]$ are symmetric, whereby

$$[\varphi_a^T] [k] \{\varphi_b\} = \omega_a^2 [\varphi_a^T] [m] \{\varphi_b\} \quad (24)$$

Now, premultiplying both sides of Eq 23 by $[\varphi_a^T]$,

$$[\varphi_a^T] [k] \{\varphi_b\} = \omega_b^2 [\varphi_a^T] [m] \{\varphi_b\} \quad (25)$$

A comparison of Eq 24 and 25 yields

$$\omega_a^2 [\varphi_a^T] [m] \{\varphi_b\} = \omega_b^2 [\varphi_a^T] [m] \{\varphi_b\}$$

or

$$(\omega_a^2 - \omega_b^2) [\varphi_a^T] [m] \{\varphi_b\} = 0 \quad (26)$$

If ω_a^2 and ω_b^2 are distinct, then

$$[\varphi_a^T] [m] \{\varphi_b\} = 0 \quad (27)$$

Section 1.21 of Ref. 5 considers the case where ω_a^2 and ω_b^2 are not distinct, and shows that Eq 27 above still holds. Since the implication of Eq 27 is that all off-diagonal terms are zero, then for orthogonal modes

$$[\Phi]^T [m] [\Phi] = [M] \quad (28)$$

Contrails

where $[M]$ must be diagonal. It can similarly be shown that

$$[\Phi]^T [k] [\Phi] = [K] \quad (29)$$

where $[K]$ must be diagonal.

The significance of Eq 28 and 29 is that Eq 9, combined with Eq 17, can be premultiplied by $[\Phi]^T$ to obtain

$$[\Phi]^T [ms^2 + k] [\Phi] \{\xi\} = [\Phi]^T [R] [\Phi] \{\xi\} + [\Phi]^T \{Q_{in}\} \quad (30)$$

where $[\Phi]^T [ms^2 + k] [\Phi]$ will be diagonal. Therefore, defining

$$\begin{aligned} [Ms^2 + K] &\equiv [\Phi]^T [ms^2 + k] [\Phi] \\ [F_\xi] &\equiv [\Phi]^T [R] [\Phi] \\ \{F_{in}\} &\equiv [\Phi]^T \{Q_{in}\} \end{aligned} \quad (31)$$

allows Eq 30 to take the simple form

$$[Ms^2 + K] \{\xi\} = [F_\xi] \{\xi\} + \{F_{in}\} \quad (32)$$

- where
- $[M]$ represents the generalized mass matrix in generalized coordinates
 - $[K]$ represents the generalized stiffness matrix in generalized coordinates
 - $\{\xi\}$ is a column of generalized coordinates (which are orthogonal coordinates when $[F_\xi] = 0$)
 - $[F_\xi]$ represents, in generalized coordinates, the externally applied forces per unit deflections in $\{\xi\}$ (and unit velocities in $\{\dot{\xi}\}$, etc.)

The left side of Eq 32 represents the structural dynamics of the vehicle in vacuum (neglecting structural damping), while the right side represents externally applied forces. When expanded, the left side will appear as

Contrails

$$\begin{Bmatrix} M_1 (s^2 + \omega_1^2) \xi_1 \\ M_2 (s^2 + \omega_2^2) \xi_2 \\ \vdots \\ M_n (s^2 + \omega_n^2) \xi_n \end{Bmatrix}$$

As is normal, ξ_1 and ξ_2 will be used to represent rigid-body translation and rotation, respectively. Thus,

$$\begin{aligned} M_1 &= m, \text{ the total physical mass of the system} \\ M_2 &= I_y, \text{ the total physical pitch inertia of the system} \\ \xi_1 &= h \text{ (positive down)} \\ \xi_2 &= \theta \text{ (positive nose up)} \\ \omega_1 &= \omega_2 = 0 \text{ (no structural stiffness in } \xi_1 \text{ or } \xi_2) \end{aligned} \tag{33}$$

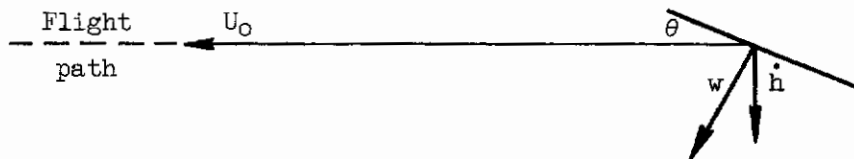
The appearance of h is not in keeping with the normal aircraft stability and control formulation of the equations of motion. Therefore, it is desirable to transform Eq 32 so that h is replaced by w . Such a transformation is representable by the matrix $[W]$, where $[W]$ is defined by

$$\begin{Bmatrix} h \\ \theta \\ \xi_3 \\ \xi_4 \\ \vdots \\ \vdots \\ \vdots \end{Bmatrix} = [W] \begin{Bmatrix} \frac{w}{s} \\ \theta \\ \xi_3 \\ \xi_4 \\ \vdots \\ \vdots \\ \vdots \end{Bmatrix} \tag{34}$$

For this case, the matrix $[W]$ can be found rather easily by using the expression

Contrails

relating w to h and θ for the assumed unperturbed condition, $\gamma_0 = 0$.



$$w = U_0 \sin \theta + \dot{h} \cos \theta$$

Figure 3. Derivation of the $[W]$ Matrix

Thus,

$$h = \begin{bmatrix} 1 & \frac{-U_0}{s} \end{bmatrix} \begin{Bmatrix} w/s \\ \theta \end{Bmatrix}$$

and the desired transformation matrix is

$$[W] = \begin{bmatrix} 1 & \frac{-U_0}{s} & 0 & 0 & & 0 \\ 0 & 1 & 0 & 0 & & 0 \\ 0 & 0 & 1 & 0 & \dots & 0 \\ 0 & 0 & 0 & 1 & & 0 \\ & \cdot & & & \cdot & \cdot \\ & \cdot & & & \cdot & \cdot \\ 0 & 0 & 0 & 0 & \dots & 1 \end{bmatrix} \quad (35)$$

Using the transformation matrix defined by Eq 35, and for convenience defining

$$[Y] \equiv [Ms^2 + K] \quad (36)$$

Eq 32 becomes

$$[Y][W]\{\xi\} = [F_\xi][W]\{\xi\} + \{F_{in}\} \quad (37)$$

Contrails

where ξ_1 is now w/s rather than h . It can be shown that $[Y][W]$ is not a diagonal matrix. It is therefore desirable to redefine $[F_\xi][W]$ to include the off-diagonal term from $[Y][W]$, thus giving a diagonal form to $[Y][W]$. This can be done by writing out the $[Y][W]$ matrix,

$$[Y][W] = \begin{bmatrix} ms^2 & -U_0ms & 0 & & 0 \\ 0 & I_y s^2 & 0 & \dots & 0 \\ 0 & 0 & M_3(s^2 + \omega_3^2) & & 0 \\ & \cdot & & \cdot & \\ & \cdot & & & \cdot \\ & \cdot & & & \\ 0 & 0 & 0 & \dots & M_n(s^2 + \omega_n^2) \end{bmatrix} \quad (38)$$

and redefining $[F_\xi][W]$ so that it includes the $-U_0ms$ term that appears in Eq 38. This will restore $[Y][W]$ to its original diagonal form.

B. ELIMINATION OF THE HIGH-FREQUENCY MODES

At this point the set of simultaneous relationships given by Eq 37 is capable of yielding results which increase in "exactness" with the number of modes considered. Since engineering interest is inevitably confined to a limited bandwidth, the importance of including higher frequency modes is measured by their effects in this bandwidth. For example, if all elastic modes are considered to lie outside the frequency region of concern and all are excluded from the equations, then the resulting solution yields only the conventional rigid-body short-period motions. But at appreciable dynamic pressures this is a gross oversimplification, because the excluded structural modes give rise then to at least an aeroelastic correction on the rigid-body stability derivatives. Such corrections can be and usually are made by considering only the static deflection properties of the structure. In this instance, the effects of all possible elastic modes have been approximated, for the frequency region of interest, by considering only static deflection characteristics. When the bandwidth of interest includes a number of low-frequency structural modes, the question arises as to

Contrails

the proper aeroelastic correction whereby to approximate the influence of the neglected modes. Clearly, now the use of the "full" aeroelastic correction will be incorrect since the modes included in the equations of motion must somehow alter the approximated contribution of all remaining modes. The proper treatment of the neglected higher-frequency modes first studied in Ref. 1 will now be outlined.

If Eq 32 is partitioned into those coordinates which are of interest (denoted ξ_{0+f} , where 0+f stands for zero frequency + finite frequency), and into those of higher frequency which are not of direct interest (denoted as ξ_{∞}), then the latter can be eliminated from the equations. This is accomplished as follows: Using Eq 31 and 36, Eq 32 is rewritten as

$$[Y]\{\xi\} = [\Phi]^T[R][\Phi]\{\xi\} + [\Phi]^T\{Q_{in}\} \quad (39)$$

where the transformation from $\xi_1 = h$ to $\xi_1 = w/s$ has not yet been made. Then, partitioning the matrices,

$$\begin{bmatrix} Y_{0+f} & \vdots & 0 \\ \dots & \dots & \dots \\ 0 & \vdots & Y_{\infty} \end{bmatrix} \begin{Bmatrix} \xi_{0+f} \\ \dots \\ \xi_{\infty} \end{Bmatrix} = \begin{bmatrix} \Phi_{0+f}^T \\ \dots \\ \Phi_{\infty}^T \end{bmatrix} [R] [\Phi_{0+f} \quad \dots \quad \Phi_{\infty}] \begin{Bmatrix} \xi_{0+f} \\ \dots \\ \xi_{\infty} \end{Bmatrix} + \begin{bmatrix} \Phi_{0+f}^T \\ \dots \\ \Phi_{\infty}^T \end{bmatrix} \{Q_{in}\} \quad (40)$$

and expanding the right side

$$\begin{aligned} \begin{bmatrix} Y_{0+f} & \vdots & 0 \\ \dots & \dots & \dots \\ 0 & \vdots & Y_{\infty} \end{bmatrix} \begin{Bmatrix} \xi_{0+f} \\ \dots \\ \xi_{\infty} \end{Bmatrix} &= \begin{bmatrix} [\Phi_{0+f}]^T [R] \\ \dots \\ [\Phi_{\infty}]^T [R] \end{bmatrix} [\Phi_{0+f} \quad \dots \quad \Phi_{\infty}] \begin{Bmatrix} \xi_{0+f} \\ \dots \\ \xi_{\infty} \end{Bmatrix} + \begin{bmatrix} \Phi_{0+f}^T \\ \dots \\ \Phi_{\infty}^T \end{bmatrix} \{Q_{in}\} \\ &= \begin{bmatrix} [\Phi_{0+f}]^T [R] [\Phi_{0+f}] & \vdots & [\Phi_{0+f}]^T [R] [\Phi_{\infty}] \\ \dots & \dots & \dots \\ [\Phi_{\infty}]^T [R] [\Phi_{0+f}] & \vdots & [\Phi_{\infty}]^T [R] [\Phi_{\infty}] \end{bmatrix} \begin{Bmatrix} \xi_{0+f} \\ \dots \\ \xi_{\infty} \end{Bmatrix} + \begin{bmatrix} \Phi_{0+f}^T \\ \dots \\ \Phi_{\infty}^T \end{bmatrix} \{Q_{in}\} \end{aligned} \quad (41)$$

Contrails

Equation 41 is equivalent to the two simultaneous matrix equations,

$$[Y_{o+f}] \{ \xi_{o+f} \} = [\Phi_{o+f}]^T [R] [\Phi_{o+f}] \{ \xi_{o+f} \} + [\Phi_{o+f}]^T [R] [\Phi_{\infty}] \{ \xi_{\infty} \} + [\Phi_{o+f}]^T \{ Q_{in} \} \quad (42)$$

and

$$[Y_{\infty}] \{ \xi_{\infty} \} = [\Phi_{\infty}]^T [R] [\Phi_{o+f}] \{ \xi_{o+f} \} + [\Phi_{\infty}]^T [R] [\Phi_{\infty}] \{ \xi_{\infty} \} + [\Phi_{\infty}]^T \{ Q_{in} \} \quad (43)$$

Equation 43 can be solved for $\{ \xi_{\infty} \}$, which can then be substituted into Eq 42. This will result in equations of motion for the modal coordinates of interest. Thus, multiplying Eq 43 by $[Y_{\infty}]^{-1}$ and solving for $\{ \xi_{\infty} \}$

$$\begin{aligned} \{ \xi_{\infty} \} = & \left[[I] - [Y_{\infty}]^{-1} [\Phi_{\infty}]^T [R] [\Phi_{\infty}] \right]^{-1} [Y_{\infty}]^{-1} [\Phi_{\infty}]^T [R] [\Phi_{o+f}] \{ \xi_{o+f} \} \\ & + \left[[I] - [Y_{\infty}]^{-1} [\Phi_{\infty}]^T [R] [\Phi_{\infty}] \right]^{-1} [Y_{\infty}]^{-1} [\Phi_{\infty}]^T \{ Q_{in} \} \end{aligned} \quad (44)$$

and using this result in Eq 42,

$$\begin{aligned} [Y_{o+f}] \{ \xi_{o+f} \} = & [\Phi_{o+f}]^T [R] [\Phi_{o+f}] \{ \xi_{o+f} \} \\ & + [\Phi_{o+f}]^T [R] [\Phi_{\infty}] \left[[I] - [Y_{\infty}]^{-1} [\Phi_{\infty}]^T [R] [\Phi_{\infty}] \right]^{-1} [Y_{\infty}]^{-1} [\Phi_{\infty}]^T [R] [\Phi_{o+f}] \{ \xi_{o+f} \} \\ & + [\Phi_{o+f}]^T [R] [\Phi_{\infty}] \left[[I] - [Y_{\infty}]^{-1} [\Phi_{\infty}]^T [R] [\Phi_{\infty}] \right]^{-1} [Y_{\infty}]^{-1} [\Phi_{\infty}]^T \{ Q_{in} \} \\ & + [\Phi_{o+f}]^T \{ Q_{in} \} \end{aligned} \quad (45)$$

Because

$$[D] [B] + [D] [C]^{-1} = [B] + [C]^{-1} [D]^{-1}$$

$$[D] [B] + [C] [B]^{-1} = [B]^{-1} [D] + [C]$$

Contrails

$$\begin{aligned}
 \text{Then } \left[[I] - [Y_{\infty}]^{-1} [\Phi_{\infty}]^T [R] [\Phi_{\infty}] \right]^{-1} [Y_{\infty}]^{-1} [\Phi_{\infty}]^T \\
 &= \left[[\Phi_{\infty}]^T [Y_{\infty}] - [R] [\Phi_{\infty}] \right]^{-1} \\
 &= [Y_{\infty}]^{-1} [\Phi_{\infty}]^T \left[[I] - [R] [\Phi_{\infty}] [Y_{\infty}]^{-1} [\Phi_{\infty}]^T \right]^{-1} \quad (46)
 \end{aligned}$$

Using this result, Eq 45 is modified to

$$\begin{aligned}
 [Y_{o+f}] \{ \xi_{o+f} \} &= [\Phi_{o+f}]^T [R] [\Phi_{o+f}] \{ \xi_{o+f} \} \\
 &+ [\Phi_{o+f}]^T [R] [\Phi_{\infty}] [Y_{\infty}]^{-1} [\Phi_{\infty}]^T \left[[I] - [R] [\Phi_{\infty}] [Y_{\infty}]^{-1} [\Phi_{\infty}]^T \right]^{-1} [R] [\Phi_{o+f}] \{ \xi_{o+f} \} \\
 &+ [\Phi_{o+f}]^T [R] [\Phi_{\infty}] [Y_{\infty}]^{-1} [\Phi_{\infty}]^T \left[[I] - [R] [\Phi_{\infty}] [Y_{\infty}]^{-1} [\Phi_{\infty}]^T \right]^{-1} \{ Q_{in} \} \\
 &+ [\Phi_{o+f}]^T \{ Q_{in} \}
 \end{aligned}$$

and collecting terms,

$$\begin{aligned}
 [Y_{o+f}] \{ \xi_{o+f} \} &= [\Phi_{o+f}]^T \\
 &\times \left[[I] + [R] [\Phi_{\infty}] [Y_{\infty}]^{-1} [\Phi_{\infty}]^T \left[[I] - [R] [\Phi_{\infty}] [Y_{\infty}]^{-1} [\Phi_{\infty}]^T \right]^{-1} \right] \\
 &\times \left[[R] [\Phi_{o+f}] \{ \xi_{o+f} \} + \{ Q_{in} \} \right] \quad (47)
 \end{aligned}$$

To simplify this further, use the following identity:

$$\begin{aligned}
 [I] + [B] \left[[I] - [B] \right]^{-1} &= [I] + [B] \left[[I] - [B] \right]^{-1} - \left[[I] - [B] \right]^{-1} + \left[[I] - [B] \right]^{-1} \\
 &= [I] - \left[[I] - [B] \right] \left[[I] - [B] \right]^{-1} + \left[[I] - [B] \right]^{-1} \\
 &= [I] - [I] + \left[[I] - [B] \right]^{-1} \\
 &= \left[[I] - [B] \right]^{-1}
 \end{aligned}$$

Contrails

whereby Eq 47 reduces to

$$[Y_{o+f}] \{ \xi_{o+f} \} = [\Phi_{o+f}]^T \left[[I] - [R] [\Phi_{\infty}] [Y_{\infty}]^{-1} [\Phi_{\infty}]^T \right]^{-1} \left[[R] [\Phi_{o+f}] \{ \xi_{o+f} \} + \{ Q_{in} \} \right] \quad (48)$$

Now, define $[A] \equiv \left[[I] - [R] [\Phi_{\infty}] [Y_{\infty}]^{-1} [\Phi_{\infty}]^T \right]^{-1}$ (49)

Equation 48 then becomes

$$[Y_{o+f}] \{ \xi_{o+f} \} = [\Phi_{o+f}]^T [A] [R] [\Phi_{o+f}] \{ \xi_{o+f} \} + [\Phi_{o+f}]^T [A] \{ Q_{in} \} \quad (50)$$

Equation 50 is seen to be very similar to Eq 39. However, in Eq 50, the columns of modal coordinates contain only those coordinates which are of interest; therefore, this equation represents a fewer number of simultaneous differential equations to be solved. (In essence, the last r equations have been used to eliminate the last r variables from the set of n simultaneous equations.) Also, a new term appears in Eq 50 which was not found in Eq 39; this term is the $[A]$ matrix. It represents the modifications which must be made in the first n-r equations to include the effects of the higher-frequency modes. The $[A]$ matrix thus represents an aeroelastic correction factor to the system. It will theoretically account exactly for all influences of the higher-frequency modes. However, the exact calculation of $[A]$ requires all the information contained in a complete set of n equations and involves an unwieldy inversion of a matrix containing terms in s and s² (see Eq 49). At the frequencies of interest, ω , which are always much smaller than the higher mode eigenvalues, ω_k , by definition, the s and s² terms, relative to the stiffness term, are proportional to ω/ω_k^2 and $(\omega/\omega_k)^2$, respectively; thus they can be neglected. Even then, calculation of $[A]$ from Eq 49 would require knowledge of the higher-frequency mode shapes. Fortunately, however, by neglecting the s and s² terms, thereby making $[A]$ a quasi-static correction factor, it is possible (Ref. 1) to calculate the quantity

$$[\Phi_{\infty}] [Y_{\infty}]_{s=0}^{-1} [\Phi_{\infty}]^T \equiv [X_{\infty}] \quad (51)$$

from a knowledge of only the static deflection characteristics of the system. The details of this calculation are given in Appendix A.

C. AERODYNAMIC FORCES

So far, no mention has been made of methods whereby the $[R]$, $[Y]$, and $[\Phi]$ matrices may be calculated. Although the latter two are not necessarily simple to form, they will not be discussed because of extensive treatments in the literature (e.g., Ref. 3 and 4). The same might be said for the aerodynamic matrix, $[R]$, except for a significant major difference. While the $[Y]$ and $[\Phi]$ matrices may be derived in many ways, the results (for a given physical situation) will always be the same; this is not true of the $[R]$ matrix, which depends inherently on the assumptions made as to the origin of aerodynamic forces.

For purposes of the present study, a very complete formulation of $[R]$ is deemed unnecessary, because it can only affect certain of the numbers appearing in the equations of motion. Since these numbers are required to be only representative of the configurations involved, the aerodynamic matrix will be reduced to a very simple form. That is, almost all secondary aerodynamic and elastic effects (e.g., wing-body interference, unsteady aerodynamics, chordwise bending) will be neglected; and the air forces and moments will be represented by average derivatives associated with each lifting surface, or suitable portions thereof. Accordingly, the center of pressure (c.p.) for lift is assumed to be at a fixed fraction of the MAC for the surface or portion thereof (0.5 for Configurations 2 and 4 and 0.25 for Configuration 3); no downwash effects are considered on Configurations 2 and 4; the only (pure) moment is considered to result from pitching velocity; and the angle of attack for a section is defined by

$$\alpha = \theta + \frac{\dot{h}_{3/4}}{U_0} \quad (52)$$

where θ is the rigid chord rotation
 $h_{3/4}$ is the vertical displacement of the 3/4 chord

The selection of $h_{3/4}$ to define the section angle of attack is in accordance with theoretical aerodynamics [where, as a boundary condition, the flow velocities over the upper and lower surfaces of an airfoil are matched at the trailing edge (Ref. 6)].

To relate all this a little more specifically to $[R]$, refer to Eq 6 where the q 's are ordered as

Contrails

$$\{q\} = \begin{Bmatrix} h_{3/4} \\ \theta \end{Bmatrix} \quad (53)$$

and the Q 's are ordered as

$$\{Q_a\} = \begin{Bmatrix} \text{Z-force at c.p.} \\ \text{moment} \end{Bmatrix} \quad (54)$$

Note that the moment does not require specification of a point of application because the chord is assumed rigid. Now, partitioning the $[R]$ matrix,

$$[R] = \begin{bmatrix} a & \vdots & b \\ \dots & \vdots & \dots \\ c & \vdots & d \end{bmatrix} \quad (55)$$

where, in general,

a_{ij} is the Z-force (negative lift) at the c.p. of the i^{th} aerodynamic surface due to unit vertical displacement of the $3/4$ chord of the j^{th} surface

b_{ij} is the Z-force (negative lift) at the c.p. of the i^{th} aerodynamic surface due to unit rigid rotation of the chord of the j^{th} surface

c_{ij} is the moment on the i^{th} aerodynamic surface due to unit vertical displacement of the $3/4$ chord of the j^{th} surface

d_{ij} is the moment on the i^{th} aerodynamic surface due to unit rigid rotation of the chord of the j^{th} surface

The literal expressions for the partitions of $[R]$ are found from the general lift and moment equations. The Z-force at the c.p. (which for convenience is designated by the subscript "1/4") of section i is given by (excluding downwash)

$$L_{1/4 i} = -\frac{\rho U_0^2}{2} (s C_{L\alpha})_i \frac{s}{U_0} h_{3/4 i} - \frac{\rho U_0^2}{2} (s C_{L\alpha})_i \theta_i \quad (56)$$

The moment on section i is (excluding downwash)

$$M_i = \frac{\rho U_0^2}{2} \left(s \frac{c^2}{2} C_{m\dot{\theta}} \right)_i \frac{s}{U_0} \theta_i \quad (57)$$

Contrails

Therefore it is possible to write

$$\begin{pmatrix} L_{\frac{1}{4} 1} \\ L_{\frac{1}{4} 2} \\ \cdot \\ \cdot \\ L_{\frac{1}{4} m} \\ M_1 \\ M_2 \\ \cdot \\ \cdot \\ M_n \end{pmatrix} = \begin{bmatrix} a_{11} & 0 & & & 0 & b_{11} & 0 & & & 0 \\ 0 & a_{22} & & & 0 & 0 & b_{22} & & & 0 \\ \cdot & \cdot & \cdot & \cdot & \cdot & \cdot & \cdot & \cdot & \cdot & \cdot \\ \cdot & \cdot & \cdot & \cdot & \cdot & \cdot & \cdot & \cdot & \cdot & \cdot \\ 0 & 0 & \cdot & \cdot & \cdot & a_{mm} & 0 & 0 & \cdot & \cdot & b_{kk} \\ \cdot & \cdot & \cdot & \cdot & \cdot & \cdot & \cdot & \cdot & \cdot & \cdot & \cdot \\ 0 & 0 & & & 0 & d_{11} & 0 & & & 0 \\ 0 & 0 & & & 0 & 0 & d_{22} & & & 0 \\ \cdot & \cdot & \cdot & \cdot & \cdot & \cdot & \cdot & \cdot & \cdot & \cdot \\ \cdot & \cdot & \cdot & \cdot & \cdot & \cdot & \cdot & \cdot & \cdot & \cdot \\ 0 & 0 & \cdot & \cdot & \cdot & 0 & 0 & \cdot & \cdot & \cdot & d_{nn} \end{bmatrix} \begin{pmatrix} h_{\frac{3}{4} 1} \\ h_{\frac{3}{4} 2} \\ \cdot \\ \cdot \\ h_{\frac{3}{4} m} \\ \theta_1 \\ \cdot \\ \cdot \\ \cdot \\ \theta_n \end{pmatrix} \quad (58)$$

where the terms in the square matrix are those comprising [R] and are given by

$$\begin{aligned}
 a_{ij} &= -\frac{\rho U_0^2}{2} (SC_{L\alpha})_i \frac{s}{U_0} \delta_{ij} \\
 b_{ij} &= -\frac{\rho U_0^2}{2} (SC_{L\alpha})_i \delta_{ij} \\
 c_{ij} &= 0 \\
 d_{ij} &= \frac{\rho U_0^2}{2} \left(s \frac{c^2}{2} C_{m\theta} \right)_i \frac{s}{U_0} \delta_{ij}
 \end{aligned} \quad (59)$$

Contrails

where δ_{ij} is the Kronecker δ ($\delta = 1$ for $i = j$; $\delta = 0$ for $i \neq j$), and the other symbols are standard aerodynamic symbols.

The physical coordinates on the right side of Eq 58 can be written

$$\begin{Bmatrix} h_{3/4} \\ \theta \end{Bmatrix} = \begin{bmatrix} \Phi_{3/4} \\ \Phi' \end{bmatrix} \{\xi\} \quad (60)$$

Therefore Eq 54 becomes

$$\{Q_a\} = \begin{bmatrix} a & \vdots & b \\ \dots & \dots & \dots \\ c & \vdots & d \end{bmatrix} \begin{bmatrix} \Phi_{3/4} \\ \Phi' \end{bmatrix} \{\xi\} \quad (61)$$

and utilizing a compatible partitioning of $[\Phi]^T$, Eq 31 can be expressed as

$$\{F_a\} = \begin{bmatrix} \Phi_1^T/4 & \vdots & \Phi'^T \end{bmatrix} \begin{Bmatrix} \text{Z-force at c.p.} \\ \text{moment} \end{Bmatrix} \quad (62)$$

Therefore,

$$\{F_a\} = \begin{bmatrix} \Phi_1^T/4 & \vdots & \Phi'^T \end{bmatrix} \begin{bmatrix} a & \vdots & b \\ \dots & \dots & \dots \\ c & \vdots & d \end{bmatrix} \begin{bmatrix} \Phi_{3/4} \\ \Phi' \end{bmatrix} \{\xi\} \quad (63)$$

or in the terms desired here,

$$[F_\xi] = \begin{bmatrix} \Phi_1^T/4 & \vdots & \Phi'^T \end{bmatrix} \begin{bmatrix} a & \vdots & b \\ \dots & \dots & \dots \\ c & \vdots & d \end{bmatrix} \begin{bmatrix} \Phi_{3/4} \\ \Phi' \end{bmatrix} \quad (64)$$

where $[\Phi_k]$ is the matrix of mode deflections of the k-chord points
 $[\Phi']$ is the matrix of mode slopes of the rigid aerodynamic chords,
 i.e., $\Phi'_r = (d/dx)\Phi_r$, which is constant along a rigid chord

Expanding Eq 64 for the zero downwash case yields

$$[F_\xi] = [\Phi_1/4]^T [a] [\Phi_{3/4}] + [\Phi_1/4]^T [b] [\Phi'] + [\Phi']^T [d] [\Phi'] \quad (65)$$

Contrails

The ij^{th} element of the $[F_{\xi}]$ is found by adding the ij^{th} elements from each of the three components.

$$[a] [\phi_{3/4}]_{ij} = -q (SC_{L\alpha})_i \frac{s}{U_0} \phi_{i3/4j} \quad (66)$$

$$[\phi_{1/4}]^T [a] [\phi_{3/4}]_{ij} = -\sum_k q (SC_{L\alpha})_k \frac{s}{U_0} \phi_{k1/4i} \phi_{k3/4j} \quad (67)$$

$$[b] [\phi']_{ij} = -q (SC_{L\alpha})_i \phi'_{ij} \quad (68)$$

$$[\phi_{1/4}]^T [b] [\phi']_{ij} = -\sum_k q (SC_{L\alpha})_k \phi_{k1/4i} \phi'_{kj} \quad (69)$$

$$[d] [\phi']_{ij} = q \left(s \frac{c^2}{2} C_{m\dot{\theta}} \right)_i \frac{s}{U_0} \phi'_{ij} \quad (70)$$

$$[\phi']^T [d] [\phi']_{ij} = \sum_k q \left(s \frac{c^2}{2} C_{m\dot{\theta}} \right)_k \frac{s}{U_0} \phi'_{ki} \phi'_{kj} \quad (71)$$

Thus,

(72)

$$F_{\xi ij} = -\frac{\rho U_0}{2} \sum_n \left[\left([SC_{L\alpha}]_n \phi_{n1/4i} \phi_{n3/4j} - \left(\frac{sc^2 C_{m\dot{\theta}}}{2} \right)_n \phi'_{ni} \phi'_{nj} \right) s + U_0 (SC_{L\alpha})_n \phi_{n1/4i} \phi'_{nj} \right]$$

where the summation is over the n aerodynamic surfaces.

For situations involving downwash, $F_{\xi ij}$ includes terms involving off-diagonal elements of a_{ij} and b_{ij} (Eq 55). These added terms are shown in one version the final equations of motion, Eq 73.

D. FINAL EQUATIONS OF MOTION

With all the important elements now in hand, the final desired equations of motion can be formulated. To achieve a form consistent with aeronautical stability and control usage requires application of the $|W|$ transformation matrix (Eq 34 and 35), transferring all aerodynamic terms, except inputs, to the

$$\left\{ \begin{aligned}
 & \left\{ s^2 + \frac{\rho U_0}{2m} \left[\sum_n (S_n C_{T\alpha}^1) - S_4 C_{T\alpha} \frac{d\epsilon}{d\alpha} \right] s \right\} \\
 & \left\{ \frac{\rho U_0}{2I_y} \left[\sum_n (S_n C_{T\alpha}^1 n_{1/4}) - S_4 C_{T\alpha} \frac{d\epsilon}{d\alpha} 1_{4/3/4} \right] s \right\} \\
 & \left\{ \frac{\rho U_0}{2} \left[\sum_n (S_n C_{T\alpha}^1 n_{1/4}^2) - S_4 C_{T\alpha} \frac{d\epsilon}{d\alpha} \frac{1}{2} 1_{4/3/4} \right] s \right\} \\
 & \left\{ \frac{\rho U_0}{2} \left[\sum_n (S_n C_{T\alpha}^1 n_{1/4}^3) - S_4 C_{T\alpha} \frac{d\epsilon}{d\alpha} \frac{1}{2} 1_{4/3/4}^3 \right] s \right\}
 \end{aligned} \right\}$$

$$\left\{ \begin{aligned}
 & \left\{ \frac{\rho U_0}{2m} \left[\sum_n (S_n C_{T\alpha}^1 \phi_{n,3/4}^1) - S_4 C_{T\alpha} \frac{d\epsilon}{d\alpha} \phi_{1,3/4}^1 \right] s \right\} \\
 & \left\{ \frac{\rho U_0}{2I_y} \left[\sum_n (S_n C_{T\alpha}^1 n_{1/4} \phi_{n,3/4}^1) - S_4 C_{T\alpha} \frac{d\epsilon}{d\alpha} 1_{4/3/4} \phi_{1,3/4}^1 \right] s \right\} \\
 & \left\{ s^2 + \frac{\rho U_0}{2} \left[\sum_n (S_n C_{T\alpha}^1 n_{1/4}^2 \phi_{n,3/4}^1) - S_4 C_{T\alpha} \frac{d\epsilon}{d\alpha} \frac{1}{2} 1_{4/3/4}^2 \phi_{1,3/4}^1 \right] s \right\} \\
 & \left\{ \frac{\rho U_0}{2} \left[\sum_n (S_n C_{T\alpha}^1 n_{1/4}^3 \phi_{n,3/4}^1) - S_4 C_{T\alpha} \frac{d\epsilon}{d\alpha} \frac{1}{2} 1_{4/3/4}^3 \phi_{1,3/4}^1 \right] s \right\}
 \end{aligned} \right\}$$

U1

$$\left\{ \begin{aligned}
 & \left\{ \frac{\rho U_0}{2m} \left[\sum_n (S_n C_{T\alpha}^1 \phi_{n,3/4}^1) - S_4 C_{T\alpha} \frac{d\epsilon}{d\alpha} \phi_{1,3/4}^1 \right] s \right\} \\
 & \left\{ \frac{\rho U_0}{2I_y} \left[\sum_n (S_n C_{T\alpha}^1 n_{1/4} \phi_{n,3/4}^1) - S_4 C_{T\alpha} \frac{d\epsilon}{d\alpha} 1_{4/3/4} \phi_{1,3/4}^1 \right] s \right\} \\
 & \left\{ \frac{\rho U_0}{2} \left[\sum_n (S_n C_{T\alpha}^1 n_{1/4}^2 \phi_{n,3/4}^1) - S_4 C_{T\alpha} \frac{d\epsilon}{d\alpha} \frac{1}{2} 1_{4/3/4}^2 \phi_{1,3/4}^1 \right] s \right\} \\
 & \left\{ s^2 + \frac{\rho U_0}{2} \left[\sum_n (S_n C_{T\alpha}^1 n_{1/4}^3 \phi_{n,3/4}^1) - S_4 C_{T\alpha} \frac{d\epsilon}{d\alpha} \frac{1}{2} 1_{4/3/4}^3 \phi_{1,3/4}^1 \right] s \right\}
 \end{aligned} \right\}
 =
 \left\{ \begin{aligned}
 & \left\{ \frac{\rho U_0 S_n C_{T\alpha}^1}{2m} \right\} \\
 & \left\{ \frac{\rho U_0 S_n C_{T\alpha}^1}{2I_y} 1_{6,6} \right\} \\
 & \left\{ \frac{\rho U_0 S_n C_{T\alpha}^1}{2} \phi_{6,3} \right\} \\
 & \left\{ \frac{\rho U_0 S_n C_{T\alpha}^1}{2} \phi_{6,4} \right\}
 \end{aligned} \right\}$$

Contrails

(74)

$$\begin{array}{l}
 \left[\begin{array}{l}
 s - Z_4 \\
 -M_4 \\
 -F_{34} \\
 -F_{44}
 \end{array} \right]
 \begin{array}{l}
 -Z_q - U_0 \\
 s - M_q \\
 -F_{3q} \\
 -F_{4q}
 \end{array}
 \begin{array}{l}
 -Z_{k3}^s - Z_{k3} \\
 -M_{k3}^s - M_{k3} \\
 s^2 - F_{k3}^s - F_{k3} + \omega_k^2 \\
 -F_{4k3}^s - F_{4k3}
 \end{array}
 \begin{array}{l}
 -Z_{k4}^s - Z_{k4} \\
 -M_{k4}^s - M_{k4} \\
 -F_{k4}^s - F_{k4} + \omega_k^2 \\
 s^2 - F_{4k4}^s - F_{4k4} + \omega_k^2
 \end{array}
 \begin{array}{l}
 -Z_{k5}^s - Z_{k5} \\
 -M_{k5}^s - M_{k5} \\
 s^2 - F_{k5}^s - F_{k5} + \omega_k^2 \\
 -F_{4k5}^s - F_{4k5}
 \end{array}
 \begin{array}{l}
 -Z_{k6}^s - Z_{k6} \\
 -M_{k6}^s - M_{k6} \\
 -F_{k6}^s - F_{k6} \\
 -F_{4k6}^s - F_{4k6}
 \end{array}
 \begin{array}{l}
 \cdot \\
 \cdot \\
 \cdot \\
 \cdot
 \end{array}
 \begin{array}{l}
 \cdot \\
 \cdot \\
 \cdot \\
 \cdot
 \end{array}
 \begin{array}{l}
 \cdot \\
 \cdot \\
 \cdot \\
 \cdot
 \end{array}
 \begin{array}{l}
 \cdot \\
 \cdot \\
 \cdot \\
 \cdot
 \end{array}
 \end{array}
 =
 \begin{array}{l}
 v \\
 \delta \\
 \xi_3 \\
 \xi_4 \\
 \cdot \\
 \cdot \\
 \cdot \\
 \cdot \\
 \xi_k \\
 \cdot \\
 \cdot \\
 \cdot
 \end{array}
 \begin{array}{l}
 Z_{k8}^s \\
 M_{k8}^s \\
 F_{k8}^s \\
 F_{4k8}^s \\
 \cdot \\
 \cdot \\
 \cdot \\
 \cdot \\
 F_{k8}^s \\
 \cdot \\
 \cdot \\
 \cdot
 \end{array}$$

Contrails

left side, and nondimensionalizing by dividing each equation by the appropriate inertial quantity. Note that the mode shapes are normalized so that the generalized mass for each elastic mode is unity. Doing this for the case where only two flexible modes are included, and where downwash from the first aerodynamic surface affects the angle of attack of the fourth aerodynamic surface, results in Eq 73, which utilizes the following identities:

$$\begin{aligned}\varphi_{nk1}' &= 1 && \text{rigid-body translation imparts equal translation} \\ &&& \text{to all aerodynamic surfaces} \\ \varphi_{n1}' &= 0 && \text{rigid-body translation imparts no rotation to} \\ &&& \text{aerodynamic surfaces} \\ \varphi_{nk2}' &= l_{nk} && \text{rigid-body rotation imparts translation propor-} \\ &&& \text{tional to the distance from the center of rotation} \\ &&& \text{(} l_{nk} \text{ is the distance from the airframe center of} \\ &&& \text{gravity to the } k\text{-chord of the } n^{\text{th}} \text{ aerodynamic} \\ &&& \text{surface, positive aft)} \\ \varphi_{n2}' &= 1 && \text{rigid-body rotation imparts equal rotation to all} \\ &&& \text{aerodynamic surfaces}\end{aligned}$$

It should be noted that no aeroelastic correction, $[A]$, has yet been applied to Eq 73 and that to do so, in literal terms, would be a practical impossibility. Equation 73 is thus mainly illustrative of the form assumed by the various coefficients, which in an actual case would be modified by varying aeroelastic correction factors. By assigning a symbol (i.e., a stability derivative) to each of the terms (including the aeroelastic correction), Eq 73 can be simplified and extended to the general situation where an arbitrary number of flexible degrees of freedom are included, as in Eq 74, the final set of equations of motion.

SECTION III

FLEXIBLE AIRFRAME APPROXIMATE TRANSFER FUNCTIONS

The forms for the longitudinal transfer functions of a rigid airframe are well understood, and a summary of these forms may be found in Ref. 2. The addition of flexible degrees of freedom to a system has generally been treated to a lesser degree, but the forms for the transfer functions are nonetheless also well established. In general, the addition of each flexible mode will result in the addition of a pair of lightly damped roots to the numerator and denominator of each transfer function. Table I summarizes the forms expected for situations where two, one, or no elastic degrees of freedom are included in the equations, and forward speed is assumed constant.

In the current study, each of the transfer function factors shown in Table I was approximated by a limited number of terms involving directly the stability derivatives appearing in the equations of motion (Eq 74). These direct relationships allow the effects of parameter changes to be predicted with a reasonable degree of confidence without actually recalculating the transfer function.

A. DISCUSSION OF METHODS OF DERIVATION

Basically, the derivation of approximate transfer function factors involves determining the terms which are important for each airframe configuration considered. This is done by substituting a typical set of numerical values for speed, altitude, etc., into the equations, and then neglecting the small terms. In doing this, it is assumed implicitly that moderate changes in the parameters will not affect the segregation of small and large terms; that is, small terms remain small over a reasonable range of parameter variation. An exception to this was found in Configuration 4, where control reversal was noted for dynamic pressures of 20 psi.

Appendix B contains detailed descriptions of the two methods which were used to determine literal approximate factors for each of the configurations considered in the current study. Although the description of the first method considers the case of factoring a transfer function denominator, the technique used may be applied to numerators as well.

TABLE I

SUMMARY OF TRANSFER FUNCTION FACTORED FORMS

	RIGID AIRFRAME	FIRST ELASTIC MODE	SECOND ELASTIC MODE
Δ	$s \left[s^2 + (2\zeta\omega)_{sp} s + \omega_{sp}^2 \right]$	$\left[s^2 + (2\zeta\omega)_{1e} s + \omega_{1e}^2 \right]$	$\left[s^2 + (2\zeta\omega)_{2e} s + \omega_{2e}^2 \right]$
N_w	$A_w s \left(s + \frac{1}{T_{w1}} \right)$	$\left[s^2 + (2\zeta\omega)_{w1} s + \omega_{w1}^2 \right]$	$\left[s^2 + (2\zeta\omega)_{w2} s + \omega_{w2}^2 \right]$
N_θ	$A_\theta \left(s + \frac{1}{T_{\theta 2}} \right)$	$\left[s^2 + (2\zeta\omega)_{\theta 1} s + \omega_{\theta 1}^2 \right]$	$\left[s^2 + (2\zeta\omega)_{\theta 2} s + \omega_{\theta 2}^2 \right]$
N_{ξ_3}		$A_{\xi_3} s \left[s^2 + (2\zeta\omega)_{\xi_3 1} s + \omega_{\xi_3 1}^2 \right]$	$\left[s^2 + (2\zeta\omega)_{\xi_3 2} s + \omega_{\xi_3 2}^2 \right]$
N_{ξ_4}			$A_{\xi_4} s \left[s^2 + (2\zeta\omega)_{\xi_4 1} s + \omega_{\xi_4 1}^2 \right]$ $\times \left[s^2 + (2\zeta\omega)_{\xi_4 2} s + \omega_{\xi_4 2}^2 \right]$

B. APPROXIMATE FACTORS

The approximate factors for the denominator and numerators for each of the three configurations are presented in Tables II through VII. Inspection of these tables reveals that the transfer function factors for flexible airframes contain the rigid airframe factors derived in Ref. 2 (with aeroelastic corrections) along with the elastic-mode factors. It is noted that the literal factors for Configurations 2 and 3 are quite similar, and in some cases, are actually identical. The results for Configuration 4, however, are quite different.

Rather than including a list of validity conditions for each set of factors, it is suggested that the applicability of the approximations be determined by finding the exact numerical factors for a nominal case, and comparing them with the numbers obtained by using the approximate formulas. The reason for suggesting this approach is quite simple: the alternative of calculating the required validity conditions (those in Appendix B are just the start) would be unreasonably lengthy and complicated. It is therefore impractical and unnecessary to present a list of validity conditions. The justification for the method suggested lies in the assumption that moderate changes in parameters from the nominal values will not affect the segregation of large and small terms (except for Configuration 4).

C. ADEQUACY OF ONE- AND TWO-ELASTIC-MODE REPRESENTATIONS

Regardless of the validity of the approximations, there is still a basic question as to the number of modes required to adequately represent the system(s) under study. This subject was investigated in Ref. 1 for the three cases treated here and the results of this investigation are summarized below.

Configurations 2 and 3 were shown to be accurately represented with only one or two flexible modes, the frequency response curve being accurate (as determined by comparison with a five-elastic-mode case) up to the characteristic frequency of the last flexible mode included. However, Configuration 4 was shown to require considerably more flexible modes for an accurate representation. In an effort to obtain some usable data, Configuration 4 was investigated at several conditions of reduced dynamic pressures lower than those studied in Ref. 1. These lower pressures tend to minimize the dynamic effects of the higher-frequency modes, as indicated by the small changes which occurred in the exact factors for the

Contrails

TABLE II
TRANSFER FUNCTION APPROXIMATE FACTORS
CONFIGURATION 2
3 MODES

Δ	$\omega_{sp}^2 \doteq -U_0 M_w - \frac{U_0 M_{\xi 3} F_{3w}}{(\omega_3^2 - F_{3\xi 3}) + U_0 M_w}$ $(2\zeta\omega)_{sp} \doteq -Z_w - M_q - \frac{M_{\xi 3} F_{3q}}{(\omega_3^2 - F_{3\xi 3})}$ $\omega_{1e}^2 \doteq (\omega_3^2 - F_{3\xi 3}) + \frac{U_0 M_{\xi 3} F_{3w}}{(\omega_3^2 - F_{3\xi 3}) + U_0 M_w}$ $(2\zeta\omega)_{1e} \doteq -F_{3\xi 3} + \frac{M_{\xi 3} F_{3q}}{(\omega_3^2 - F_{3\xi 3})}$
N_w	$A_w = Z_\delta$ $\frac{1}{T_{w1}} \doteq \frac{U_0 M_\delta}{Z_\delta}$ $\omega_{w1}^2 \doteq (\omega_3^2 - F_{3\xi 3}) + M_{\xi 3} \frac{F_{3\delta}}{M_\delta}$ $(2\zeta\omega)_{w1} \doteq -F_{3\xi 3} + \left(M_{\xi 3} + \frac{Z_{\xi 3}}{U_0} - \frac{M_{\xi 3} Z_\delta}{U_0 M_\delta} \right) \frac{F_{3\delta}}{M_\delta}$
N_θ	$A_\theta = M_\delta$ $\frac{1}{T_{\theta 2}} \doteq -Z_w + M_w \frac{Z_\delta}{M_\delta} + \frac{Z_{\xi 3}}{(\omega_3^2 - F_{3\xi 3})} \frac{F_{3\delta}}{M_\delta}$ $\omega_{\theta 1}^2 \doteq (\omega_3^2 - F_{3\xi 3}) + M_{\xi 3} \frac{F_{3\delta}}{M_\delta}$ $(2\zeta\omega)_{\theta 1} \doteq -F_{3\xi 3} + M_{\xi 3} \frac{F_{3\delta}}{M_\delta} + \frac{(-F_{3w} + M_w \frac{F_{3\delta}}{M_\delta}) (-Z_{\xi 3} + M_{\xi 3} \frac{Z_\delta}{M_\delta})}{(\omega_3^2 - F_{3\xi 3}) + M_{\xi 3} \frac{F_{3\delta}}{M_\delta}}$
$N_{\xi 3}$	$A_{\xi 3} = F_{3\delta}$ $\omega_{\xi 3 1}^2 \doteq -U_0 M_w + U_0 F_{3w} \frac{M_\delta}{F_{3\delta}}$ $(2\zeta\omega)_{\xi 3 1} \doteq -Z_w - M_q + F_{3q} \frac{M_\delta}{F_{3\delta}}$

Contraails

TABLE III
TRANSFER FUNCTION APPROXIMATE FACTORS
CONFIGURATION 3
3 MODES

Δ	$\omega_{sp}^2 \doteq -U_0 M_w + Z_w M_q - \frac{U_0 M_{\xi 3} F_{3w}}{(\omega_3^2 - F_{3\xi 3}) + U_0 M_w}$ $(2\xi\omega)_{sp} \doteq -Z_w - M_q - \frac{F_{3w}(U_0 M_{\xi 3} + Z_{\xi 3})}{(\omega_3^2 - F_{3\xi 3})}$ $\omega_{1e}^2 \doteq (\omega_3^2 - F_{3\xi 3}) + \frac{U_0 M_{\xi 3} F_{3w}}{(\omega_3^2 - F_{3\xi 3}) + U_0 M_w}$ $(2\xi\omega)_{1e} \doteq -F_{3\xi 3} + \frac{F_{3w}(U_0 M_{\xi 3} + Z_{\xi 3})}{(\omega_3^2 - F_{3\xi 3})}$
N_w	$A_w = Z_0$ $\frac{1}{T_{w1}} \doteq \frac{U_0 M_0}{Z_0}$ $\omega_{w1}^2 \doteq (\omega_3^2 - F_{3\xi 3}) + M_{\xi 3} \frac{F_{30}}{M_0}$ $(2\xi\omega)_{w1} \doteq -F_{3\xi 3} + \left(M_{\xi 3} + \frac{Z_{\xi 3}}{U_0} \right) \frac{F_{30}}{M_0}$
N_θ	$A_\theta = M_0$ $\frac{1}{T_{\theta 2}} \doteq -Z_w + M_w \frac{Z_0}{M_0} + \frac{F_{3w} \left(M_{\xi 3} \frac{Z_0}{M_0} - Z_{\xi 3} \right)}{(\omega_3^2 - F_{3\xi 3})}$ $\omega_{\theta 1}^2 \doteq (\omega_3^2 - F_{3\xi 3}) + M_{\xi 3} \frac{F_{30}}{M_0}$ $(2\xi\omega)_{\theta 1} \doteq -F_{3\xi 3} + M_{\xi 3} \frac{F_{30}}{M_0} + \frac{Z_{\xi 3} F_{3w}}{(\omega_3^2 - F_{3\xi 3})}$
$N_{\xi 3}$	$A_{\xi 3} = F_{30}$ $\omega_{\xi 3 1}^2 \doteq U_0 F_{3w} \frac{M_0}{F_{30}}$ $(2\xi\omega)_{\xi 3 1} \doteq -Z_w - M_q + F_{3q} \frac{M_0}{F_{30}} + F_{3w} \frac{Z_0}{F_{30}}$

TABLE IV
TRANSFER FUNCTION APPROXIMATE FACTORS
CONFIGURATION 4
3 MODES

Δ	$\omega_{sp}^2 \doteq -\frac{1}{2} \left[U_0 M_w - (\omega_3^2 - F_{3\xi_3}) \right] + \left[U_0 M_{\xi_3} F_{3w} \right]^{1/2}$ $(2\zeta\omega)_{sp} \doteq -Z_w - M_q$ $\omega_{1e}^2 \doteq -\frac{1}{2} \left[U_0 M_w - (\omega_3^2 - F_{3\xi_3}) \right] - \left[U_0 M_{\xi_3} F_{3w} \right]^{1/2}$ $(2\zeta\omega)_{1e} \doteq -F_{3\xi_3}$
N_w	$A_w = Z_\delta$ $\frac{1}{T_{w1}} = \frac{U_0 M_\delta}{Z_\delta}$ $\omega_{w1}^2 \doteq (\omega_3^2 - F_{3\xi_3}) + M_{\xi_3} \frac{F_{3\delta}}{M_\delta}$ $(2\zeta\omega)_{w1} \doteq -F_{3\xi_3} + \frac{F_{3\delta}}{U_0 M_\delta} \left[Z_{\xi_3} + U_0 M_{\xi_3} - M_{\xi_3} \frac{Z_\delta}{M_\delta} \right]$
N_θ	$A_\theta = M_\delta$ $\frac{1}{T_{\theta 1}} \doteq -Z_w + M_w \frac{Z_\delta}{M_\delta} - \frac{(-F_{3w} + M_w \frac{F_{3\delta}}{M_\delta})(-Z_{\xi_3} + M_{\xi_3} \frac{Z_\delta}{M_\delta})}{\left[(\omega_3^2 - F_{3\xi_3}) + M_{\xi_3} \frac{F_{3\delta}}{M_\delta} \right]}$ $\omega_{\theta 1}^2 \doteq (\omega_3^2 - F_{3\xi_3}) + M_{\xi_3} \frac{F_{3\delta}}{M_\delta}$ $(2\zeta\omega)_{\theta 1} \doteq -F_{3\xi_3} + M_{\xi_3} \frac{F_{3\delta}}{M_\delta} + \frac{(-F_{3w} + M_w \frac{F_{3\delta}}{M_\delta})(-Z_{\xi_3} + M_{\xi_3} \frac{Z_\delta}{M_\delta})}{\left[(\omega_3^2 - F_{3\xi_3}) + M_{\xi_3} \frac{F_{3\delta}}{M_\delta} \right]}$
N_{ξ_3}	$A_\xi = F_{3\delta}$ $\omega_{\xi 3 1}^2 \doteq -U_0 M_w + U_0 F_{3w} \frac{M_\delta}{F_{3\delta}}$ $(2\zeta\omega)_{\xi 3 1} \doteq -Z_w - M_q$

TABLE V
TRANSFER FUNCTION APPROXIMATE FACTORS
CONFIGURATION 2

4 MODES

Δ	$\omega_{sp}^2 \doteq -U_0 M_w - \frac{U_0 M_{\xi_3} F_{\zeta_3 w}}{(\omega_3^2 - F_{\zeta_3 \xi_3}) + U_0 M_w} - \frac{U_0 M_{\xi_4} F_{\zeta_4 w}}{(\omega_4^2 - F_{\zeta_4 \xi_4})}$ $(2\zeta\omega)_{sp} \doteq -Z_w - M_q - \frac{M_{\xi_3} F_{\zeta_3 q}}{(\omega_3^2 - F_{\zeta_3 \xi_3}) + U_0 M_w}$ $\omega_{1e}^2 \doteq (\omega_3^2 - F_{\zeta_3 \xi_3}) + \frac{U_0 M_{\xi_3} F_{\zeta_3 w}}{(\omega_3^2 - F_{\zeta_3 \xi_3}) + U_0 M_w}$ $(2\zeta\omega)_{1e} \doteq -F_{\zeta_3 \xi_3} + \frac{M_{\xi_3} F_{\zeta_3 q}}{(\omega_3^2 - F_{\zeta_3 \xi_3}) + U_0 M_w}$ $\omega_{2e}^2 \doteq (\omega_4^2 - F_{\zeta_4 \xi_4})$ $(2\zeta\omega)_{2e} \doteq -F_{\zeta_4 \xi_4}$
N_w	$A_w = Z_\delta$ $\frac{1}{T_{w1}} \doteq \frac{U_0 M_\delta}{Z_\delta}$ $\omega_{w1}^2 \doteq (\omega_3^2 - F_{\zeta_3 \xi_3}) + M_{\xi_3} \frac{F_{\zeta_3 \delta}}{M_\delta}$ $(2\zeta\omega)_{w1} \doteq -F_{\zeta_3 \xi_3} + \left[M_{\xi_3} + \frac{Z_{\xi_3}}{U_0} - \frac{M_{\xi_3}}{U_0} \frac{Z_\delta}{M_\delta} \right] \frac{F_{\zeta_3 \delta}}{M_\delta}$ $\omega_{w2}^2 \doteq (\omega_4^2 - F_{\zeta_4 \xi_4}) + M_{\xi_4} \frac{F_{\zeta_4 \delta}}{M_\delta}$ $(2\zeta\omega)_{w2} \doteq -F_{\zeta_4 \xi_4} + \left[M_{\xi_4} + \frac{Z_{\xi_4}}{U_0} - \frac{M_{\xi_4}}{U_0} \frac{Z_\delta}{M_\delta} \right] \frac{F_{\zeta_4 \delta}}{M_\delta}$

Contrails

TABLE V CONCLUDED

N_{θ}	$A_{\theta} = M_{\delta}$ $\frac{1}{T_{\theta 2}} \doteq -Z_w + \left[\frac{M_w (\omega_3^2 - F_{3\xi 3})}{(\omega_3^2 - F_{3\xi 3}) + M_{\xi 3} \frac{F_{3\delta}}{M_{\delta}}} \right] \frac{Z_{\delta}}{M_{\delta}}$ $\omega_{\theta 1}^2 \doteq (\omega_3^2 - F_{3\xi 3}) + M_{\xi 3} \frac{F_{3\delta}}{M_{\delta}}$ $(2\xi\omega)_{\theta 1} \doteq -F_{3\xi 3} + M_{\xi 3} \frac{F_{3\delta}}{M_{\delta}} + \frac{(-F_{3w} + M_w \frac{F_{3\delta}}{M_{\delta}}) (-Z_{\xi 3} + M_{\xi 3} \frac{Z_{\delta}}{M_{\delta}})}{\left[(\omega_3^2 - F_{3\xi 3}) + M_{\xi 3} \frac{F_{3\delta}}{M_{\delta}} \right]}$ $\omega_{\theta 2}^2 \doteq (\omega_4^2 - F_{4\xi 4}) + M_{\xi 4} \frac{F_{4\delta}}{M_{\delta}}$ $(2\xi\omega)_{\theta 2} \doteq -F_{4\xi 4} + M_{\xi 4} \frac{F_{4\delta}}{M_{\delta}}$
$N_{\xi 3}$	$A_{\xi 3} = F_{3\delta}$ $\omega_{\xi 3 1}^2 \doteq -U_0 M_w + U_0 \left[F_{3w} \frac{M_{\delta}}{F_{3\delta}} - \frac{M_{\xi 4} F_{4w}}{(\omega_4^2 - F_{4\xi 4})} \right]$ $(2\xi\omega)_{\xi 3 1} \doteq -Z_w - M_d + \left[F_{3q} + F_{3w} \frac{Z_{\delta}}{M_{\delta}} \right] \frac{M_{\delta}}{F_{3\delta}}$ $\omega_{\xi 3 2}^2 \doteq (\omega_4^2 - F_{4\xi 4})$ $(2\xi\omega)_{\xi 3 2} \doteq -F_{4\xi 4} + \left[\frac{F_{4\delta}}{F_{3\delta}} F_{3\xi 4} - \frac{Z_{\delta}}{F_{3\delta}} F_{3w} \right]$
$N_{\xi 4}$	$A_{\xi 4} = F_{4\delta}$ $\frac{1}{T_{\xi 4 1}} \doteq -\frac{1}{2} (Z_w + M_d + F_{3\xi 3}) - (-U_0 M_w)^{1/2}$ $\frac{1}{T_{\xi 4 2}} \doteq (-U_0 M_w)^{1/2}$ $\omega_{\xi 4 1}^2 \doteq (\omega_3^2 - F_{3\xi 3}) - U_0 F_{4w} \frac{M_{\delta}}{F_{4\delta}}$

TABLE VI
TRANSFER FUNCTION APPROXIMATE FACTORS
CONFIGURATION 3

4 MODES

Δ	$\omega_{sp}^2 \doteq -U_0 M_w + Z_w M_q - \frac{U_0 M_{\xi_3} F_{3w}}{(\omega_3^2 - F_{3\xi_3})}$ $(2\zeta\omega)_{sp} \doteq -Z_w - M_q - \frac{F_{3w}(U_0 M_{\xi_3} + Z_{\xi_3})}{(\omega_3^2 - F_{3\xi_3})} - \frac{M_{\xi_4} F_{4q}}{(\omega_4^2 - F_{4\xi_4})}$ $\omega_{1e}^2 \doteq (\omega_3^2 - F_{3\xi_3}) - \frac{M_{\xi_4}(U_0 F_{4w} + F_{4q} F_{3\xi_3})}{(\omega_4^2 - F_{4\xi_4}) - (\omega_3^2 - F_{3\xi_3})}$ $(2\zeta\omega)_{1e} \doteq -F_{3\xi_3} + \frac{F_{3w}(U_0 M_{\xi_3} + Z_{\xi_3})}{(\omega_3^2 - F_{3\xi_3})} + \frac{M_{\xi_4} F_{4q} + F_{3\xi_4} F_{4\xi_3}}{(\omega_4^2 - F_{4\xi_4})}$ $\omega_{2e}^2 \doteq (\omega_4^2 - F_{4\xi_4})$ $(2\zeta\omega)_{2e} \doteq -F_{4\xi_4}$
N _w	$A_w = Z_\delta$ $\frac{1}{T_{w1}} \doteq \frac{U_0 M_\delta}{Z_\delta}$ $\omega_{w1}^2 \doteq (\omega_3^2 - F_{3\xi_3}) - \frac{F_{3\xi_4}}{(\omega_4^2 - F_{4\xi_4})} \left[F_{4\xi_3} - M_{\xi_3} \frac{F_{4\delta}}{M_\delta} \right]$ $(2\zeta\omega)_{w1} \doteq -F_{3\xi_3} + \left[\frac{Z_{\xi_4}(\omega_3^2 - F_{3\xi_3}) + U_0 M_{\xi_4} F_{3\xi_3}}{U_0(\omega_4^2 - F_{4\xi_4})} \right] \frac{F_{4\delta}}{M_\delta}$ $\omega_{w2}^2 \doteq (\omega_4^2 - F_{4\xi_4}) + M_{\xi_4} \frac{F_{4\delta}}{M_\delta}$ $(2\zeta\omega)_{w2} \doteq -F_{4\xi_4} + M_{\xi_4} \frac{F_{4\delta}}{M_\delta} + F_{3\xi_4} \left[\frac{M_{\xi_3} \frac{F_{4\delta}}{M_\delta} - F_{4\xi_3}}{(\omega_3^2 - F_{3\xi_3}) - (\omega_4^2 - F_{4\xi_4})} \right]$

Contrails

TABLE VI CONCLUDED

N_θ	$A_\theta = M_\delta$ $\frac{1}{T_{\theta 2}} \doteq -Z_w + M_w \frac{Z_\delta}{M_\delta} - \frac{Z_{\xi 3} F_{3w}}{(\omega_3^2 - F_{3\xi 3})}$ $\omega_{\theta 1}^2 \doteq (\omega_3^2 - F_{3\xi 3}) - \frac{F_{3\xi 4}}{(\omega_4^2 - F_{4\xi 4})} \left[F_{4\xi 3} - M_{\xi 3} \frac{F_{4\delta}}{M_\delta} \right]$ $(2\xi\omega)_{\theta 1} \doteq -F_{3\xi 3} + \left[\frac{Z_{\xi 4} (\omega_3^2 - F_{3\xi 3}) + U_0 M_{\xi 4} F_{3\xi 3}}{U_0 (\omega_4^2 - F_{4\xi 4})} \right] \frac{F_{4\delta}}{M_\delta}$ $\omega_{\theta 2}^2 \doteq (\omega_4^2 - F_{4\xi 4}) + M_{\xi 4} \frac{F_{4\delta}}{M_\delta}$ $(2\xi\omega)_{\theta 2} \doteq -F_{4\xi 4} + M_{\xi 4} \frac{F_{4\delta}}{M_\delta} + F_{3\xi 4} \left[\frac{M_{\xi 3} \frac{F_{4\delta}}{M_\delta} - F_{4\xi 3}}{(\omega_3^2 - F_{3\xi 3}) - (\omega_4^2 - F_{4\xi 4})} \right]$
$N_{\xi 3}$	$A_{\xi 3} = F_{3\delta}$ $\omega_{\xi 3 1}^2 \doteq \left[\frac{U_0 F_{3w} (\omega_4^2 - F_{4\xi 4})}{(\omega_4^2 - F_{4\xi 4}) \frac{F_{3\delta}}{M_\delta} + U_0 F_{3w} + F_{3\xi 4} \frac{F_{4\delta}}{M_\delta}} \right]$ $(2\xi\omega)_{\xi 3 1} \doteq -F_{4\xi 4} - M_q$ $\omega_{\xi 3 2}^2 \doteq (\omega_4^2 - F_{4\xi 4}) + \left[U_0 F_{3w} \frac{M_\delta}{F_{3\delta}} + F_{3\xi 4} \frac{F_{4\delta}}{F_{3\delta}} \right]$ $(2\xi\omega)_{\xi 3 2} \doteq -M_q + \left[F_{3q} + F_{3w} \frac{Z_\delta}{M_\delta} \right] \frac{M_\delta}{F_{3\delta}}$
$N_{\xi 4}$	$A_{\xi 4} = F_{4\delta}$ $\omega_{\xi 4 1}^2 \doteq -U_0 M_w + \left[U_0 F_{4w} + \frac{U_0 F_{3w} F_{4\xi 4}}{(\omega_3^2 - F_{3\xi 3})} - Z_w F_{4q} \right] \frac{M_\delta}{F_{4\delta}}$ $(2\xi\omega)_{\xi 4 1} \doteq -Z_w - M_q - \frac{U_0 M_w F_{3\xi 3}}{(\omega_3^2 - F_{3\xi 3})} + F_{4q} \frac{M_\delta}{F_{4\delta}}$ $\omega_{\xi 4 2}^2 \doteq (\omega_3^2 - F_{3\xi 3}) - \left[\frac{U_0 F_{3w} F_{4\xi 3}}{(\omega_3^2 - F_{3\xi 3})} \right] \frac{M_\delta}{F_{4\delta}}$ $(2\xi\omega)_{\xi 4 2} \doteq \frac{-(\omega_3^2 - F_{3\xi 3}) F_{3\xi 3}}{(\omega_3^2 - F_{3\xi 3}) + U_0 M_w} + F_{4w} \frac{Z_\delta}{F_{4\delta}}$

TABLE VII
TRANSFER FUNCTION APPROXIMATE FACTORS
CONFIGURATION 4
4 MODES

	$\omega_{sp}^2 \doteq (\omega_3^2 - F_{3\xi_3}) + \left[(\omega_4^2 - F_{4\xi_4}) - U_0 M_w \right]^{1/2}$ $(2\xi\omega)_{sp} \doteq -Z_w$ $\omega_{1e}^2 \doteq \frac{1}{2}(\omega_3^2 - F_{3\xi_3}) - \left[(\omega_4^2 - F_{4\xi_4}) - U_0 M_w \right]^{1/2}$ $\Delta (2\xi\omega)_{1e} \doteq Z_w - F_{3\xi_3} - F_{4\xi_4}$ $\omega_{2e}^2 \doteq -\frac{1}{2}(\omega_3^2 - F_{3\xi_3}) + \left[(\omega_4^2 - F_{4\xi_4}) - U_0 M_w \right]$ $(2\xi\omega)_{2e} \doteq -Z_w - M_d$
	$A_w = Z_8$ $\frac{1}{T_{w1}} \doteq \frac{U_0 M_8}{Z_8}$ $\omega_{w1}^2 \doteq (\omega_3^2 - F_{3\xi_3}) + M_{\xi_3} \frac{F_{38}}{M_8} - F_{4\xi_3} \left[\frac{F_{3\xi_4} - M_{\xi_4} \frac{F_{38}}{M_8}}{(\omega_4^2 - F_{4\xi_4}) - (\omega_3^2 - F_{3\xi_3}) - M_{\xi_3} \frac{F_{38}}{M_8}} \right]$ $(2\xi\omega)_{w1} \quad \text{Approximation not found}$ $\omega_{w2}^2 \doteq (\omega_4^2 - F_{4\xi_4}) + F_{4\xi_3} \left[\frac{F_{3\xi_4} - M_{\xi_4} \frac{F_{38}}{M_8}}{(\omega_4^2 - F_{4\xi_4}) - (\omega_3^2 - F_{3\xi_3}) - M_{\xi_3} \frac{F_{38}}{M_8}} \right]$ $(2\xi\omega)_{w2} \doteq -F_{4\xi_4} + \frac{F_{3\xi_4} F_{4\xi_3} - M_{\xi_4} F_{4\xi_3} \frac{F_{38}}{M_8}}{\omega_4^2 - F_{4\xi_4}}$
N_w	

Contrails

TABLE VII CONCLUDED

N_{θ}	$A_{\theta} = M_{\delta}$ $\frac{1}{T_{\theta 1}} \doteq -Z_w + M_w \frac{Z_{\delta}}{M_{\delta}}$ $\omega_{\theta 1}^2 \doteq (\omega_3^2 - F_{3\xi 3}) + M_{\xi 3} \frac{F_{3\delta}}{M_{\delta}} - F_{4\xi 3} \left[\frac{F_{3\xi 4} - M_{\xi 4} \frac{F_{3\delta}}{M_{\delta}}}{(\omega_4^2 - F_{4\xi 4}) - (\omega_3^2 - F_{3\xi 3}) - M_{\xi 3} \frac{F_{3\delta}}{M_{\delta}}} \right]$ $(2\xi\omega)_{\theta 1} \doteq -F_{3\xi 3} + M_{\xi 3} \frac{F_{3\delta}}{M_{\delta}} - \frac{F_{3\xi 4} F_{4\xi 3}}{(\omega_4^2 - F_{4\xi 4})}$ $\omega_{\theta 2}^2 \doteq (\omega_4^2 - F_{4\xi 4}) + F_{4\xi 3} \left[\frac{F_{3\xi 4} - M_{\xi 4} \frac{F_{3\delta}}{M_{\delta}}}{(\omega_4^2 - F_{4\xi 4}) - (\omega_3^2 - F_{3\xi 3}) - M_{\xi 3} \frac{F_{3\delta}}{M_{\delta}}} \right]$ $(2\xi\omega)_{\theta 2} \doteq -F_{4\xi 4} + \frac{F_{3\xi 4} F_{4\xi 3}}{(\omega_4^2 - F_{4\xi 4})}$
$N_{\xi 3}$	$A_{\xi 3} = F_{3\delta}$ $\omega_{\xi 3 1}^2 \doteq -U_{\theta} M_w + U_{\theta} F_{3w} \frac{M_{\delta}}{F_{3\delta}} - \frac{U_{\theta} F_{4w}}{(\omega_4^2 - F_{4\xi 4})} \left[M_{\xi 4} - F_{3\xi 4} \frac{M_{\delta}}{F_{3\delta}} \right]$ $(2\xi\omega)_{\xi 3 1} \doteq -Z_w - M_q + (F_{3q} + F_{3w} \frac{Z_{\delta}}{M_{\delta}}) \frac{M_{\delta}}{F_{3\delta}} - \frac{U_{\theta} M_{\xi 4} F_{4w}}{(\omega_4^2 - F_{4\xi 4})}$ $\omega_{\xi 3 2}^2 \doteq (\omega_4^2 - F_{4\xi 4})$ $(2\xi\omega)_{\xi 3 2} \doteq -F_{4\xi 4} + \frac{U_{\theta} M_{\xi 4} F_{4w}}{(\omega_4^2 - F_{4\xi 4})}$
$N_{\xi 4}$	$A_{\xi 4} = F_{4\delta}$ $\omega_{\xi 4 1}^2 \doteq \frac{U_{\theta} F_{4w}}{F_{4\xi 3}} (\omega_3^2 - F_{3\xi 3}) \frac{M_{\delta}}{F_{3\delta}}$ $(2\xi\omega)_{\xi 4 1} \doteq -Z_w + F_{3q} \frac{M_{\delta}}{F_{3\delta}}$ $\frac{1}{T_{\xi 4 2}} \doteq \frac{1}{2} (F_{4q} + F_{4w} \frac{Z_{\delta}}{M_{\delta}}) \frac{M_{\delta}}{F_{4\delta}} + (-F_{4\xi 3} \frac{F_{3\delta}}{F_{4\delta}})^{1/2}$ $\frac{1}{T_{\xi 4 3}} \doteq F_{4\xi 3} \frac{F_{3\delta}}{F_{4\delta}} - \left[- (U_{\theta} F_{4w} + F_{4\xi 3} \frac{F_{3\delta}}{M_{\delta}}) \frac{M_{\delta}}{F_{4\delta}} \right]^{1/2}$

Contrails

three- and four-mode transfer functions. The range of dynamic pressures for which the one- or two-elastic-mode representation is valid (regardless of the validity of the approximate factors) is thus strongly limited for this one configuration. Care should be exercised if this type of configuration is to be represented with only a few of its normal modes.

D. NUMERICAL COMPARISONS OF EXACT AND APPROXIMATE FACTORS

The excellent agreement between the approximate and the exact factors of Configurations 2 and 3 indicates that the approximation formulas for these configurations can be expected to remain valid for extreme ranges in dynamic pressure. However, the approximation formulas for Configuration 4 were not valid when the dynamic pressure was extended to 20 psi. Thus, those approximations should be used cautiously when conditions of high dynamic pressures are investigated.

SECTION IV

SINGLE SENSOR CONTROL LOOP SYSTEMS

A. INTRODUCTION

Control of the longitudinal axis in general implies control of the short period. Accordingly, the closed-loop bandwidth, or equivalently the open-loop crossover frequency, must be roughly equal to or greater than the short-period frequency. When flexibility effects are present such crossovers can sometimes lead to closed-loop instabilities because of structural "coupling" excited by the autopilot. Such incipient instabilities can easily be investigated by Bode analysis, and can in general be avoided.

Since the output quantity fed back to the controller senses all components of motion, rigid-body as well as elastic (unless filtered), the nature of the complete open-loop transfer function can often be drastically changed by a change in sensor location. Thus, whereas for a given sensor location it may be impossible to cross over near the short-period frequency without appreciable excitation of an elastic mode, a slight shift in sensor location may permit reasonable closures.

Both the general formulation of the output quantity as a function of sensor location and the process of selecting a "proper" location are discussed below, with specific reference to the use of vertical gyro feedback loops.

B. SENSOR OUTPUT

If the four-mode perturbation equations involve the vertical displacement, h , the pitch angle, θ , and the first two elastic modes, ξ_3 and ξ_4 , then the air-frame transfer functions are h/δ , θ/δ , ξ_3/δ , and ξ_4/δ . The rigid-body degrees of freedom are h and θ , while ξ_3 and ξ_4 represent the first two elastic degrees of freedom.

The deflection at any point i along the fuselage reference line will be

$$y_i = \phi_{i1}h + \phi_{i2}\theta + \phi_{i3}\xi_3 + \phi_{i4}\xi_4 \quad (75)$$

The slope, or pitch angle measured, for example, by a vertical gyro at any

Contrails

point i is found by differentiation:

$$\begin{aligned}\theta_i &= \left(\frac{dy}{dx}\right)_i \\ &= \frac{d\varphi_{i1}}{dx} h + \frac{d\varphi_{i2}}{dx} \theta + \frac{d\varphi_{i3}}{dx} \xi_3 + \frac{d\varphi_{i4}}{dx} \xi_4 \\ &= \varphi'_{i1} h + \varphi'_{i2} \theta + \varphi'_{i3} \xi_3 + \varphi'_{i4} \xi_4\end{aligned}\quad (76)$$

But for the rigid-body modes,

$$\begin{aligned}\varphi'_{i1} &= 0 \\ \varphi'_{i2} &= 1\end{aligned}\quad (77)$$

Thus,

$$\theta_i = \theta + \varphi'_{i3} \xi_3 + \varphi'_{i4} \xi_4\quad (78)$$

Because the sensor will detect the total physical motion, the transfer function which must be considered is

$$\frac{\theta_i}{\delta} = \frac{\theta}{\delta} + \varphi'_{i3} \frac{\xi_3}{\delta} + \varphi'_{i4} \frac{\xi_4}{\delta}\quad (79)$$

Following the transfer function factored forms given in Table I,

$$\begin{aligned}\frac{\theta}{\delta} &= \frac{N_\theta}{\Delta} \\ \frac{\xi_3}{\delta} &= \frac{N_{\xi_3}}{\Delta} \\ \frac{\xi_4}{\delta} &= \frac{N_{\xi_4}}{\Delta}\end{aligned}\quad (80)$$

Therefore,

$$\frac{\theta_i}{\delta} = \frac{N_\theta}{\Delta} + \varphi'_{i3} \frac{N_{\xi_3}}{\Delta} + \varphi'_{i4} \frac{N_{\xi_4}}{\Delta}\quad (81)$$

For convenience, this can be written in a slightly different form:

$$\frac{\theta_i}{\delta} = \left[1 + \varphi'_{i3} \frac{N_{\xi_3}}{N_\theta} + \varphi'_{i4} \frac{N_{\xi_4}}{N_\theta} \right] \frac{N_\theta}{\Delta}\quad (82)$$

Contrails

The sensed motion is thus the mean centerline motion (θ) modified by the bracketed factor of Eq 82. The mean centerline transfer function is, itself, different from the rigid-body transfer function obtained when the elastic modes are neglected. The difference is apparent from the following equations (cf. Table I).

Rigid Airframe

$$\frac{\theta}{\delta} = \frac{A_{\theta} \left(s + \frac{1}{T_{\theta 2}} \right)}{s \left[s^2 + (2\zeta\omega)_{sp} s + \omega_{sp}^2 \right]} \quad (83)$$

Elastic Airframe (Two Elastic Modes)

$$\frac{\theta}{\delta} = \frac{A_{\theta} \left(s + \frac{1}{T_{\theta 2}} \right) \left[s^2 + (2\zeta\omega)_{\theta_1} s + \omega_{\theta_1}^2 \right] \left[s^2 + (2\zeta\omega)_{\theta_2} s + \omega_{\theta_2}^2 \right]}{s \left[s^2 + (2\zeta\omega)_{sp} s + \omega_{sp}^2 \right] \left[s^2 + (2\zeta\omega)_{1e} s + \omega_{1e}^2 \right] \left[s^2 + (2\zeta\omega)_{2e} s + \omega_{2e}^2 \right]} \quad (84)$$

The addition of two elastic modes has added two pairs of second-order roots to the numerator and denominator of the mean centerline response, θ/δ . This is in addition to the elastic inputs which are added to θ/δ as shown in Eq 79.

C. CLOSED-LOOP CONSIDERATIONS

Assuming lead equalization of the gyro output ($T_e s + 1$) and neglecting actuator and sensor lags, the open-loop transfer function given by Eq 84 yields a frequency response curve of the form shown in Fig. 4. The actual curve will depend on the relative positions and degree of damping of each pair of complex roots shown. Closing the loop in this case is quite simple, requiring only that the zero db line intersect the amplitude curve at a frequency in the neighborhood of ω_{sp} and yet not intersect either of the higher-frequency "peaks." (Servo lags, unimportant at short period, will reduce the phase margin at higher frequencies.) Such a closure would be impossible if the θ/δ frequency response curve were of the form shown in Fig. 5 where ω_{1e} is assumed lower than ω_{θ_1} (and is very lightly damped). For this latter case, crossover near ω_{sp} would result in instability near ω_{1e} .

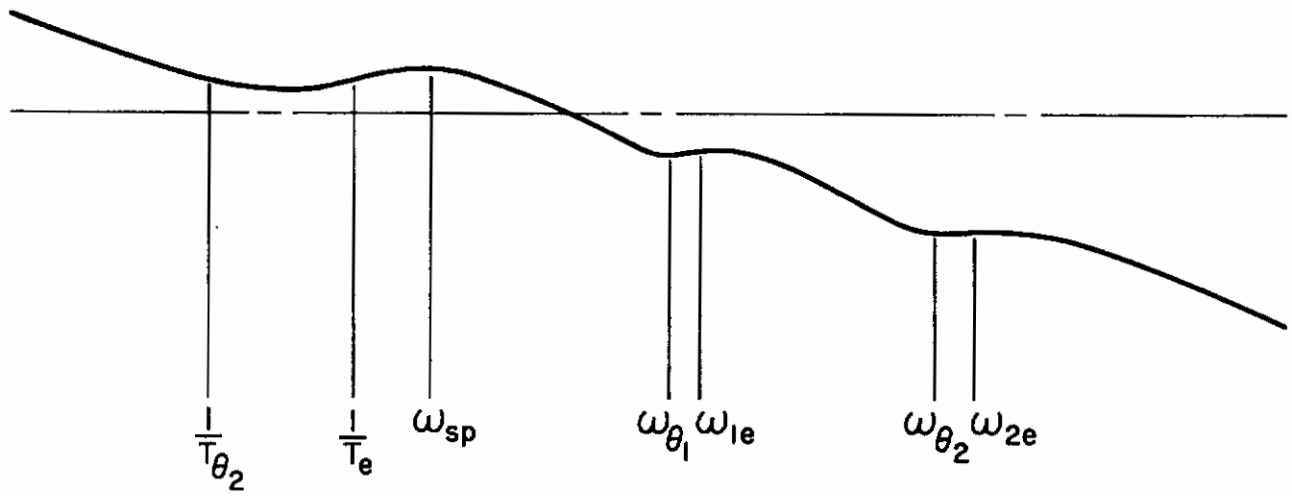


Figure 4. Bode ($j\omega$) Amplitude for Typical θ/δ with Lead Equalization

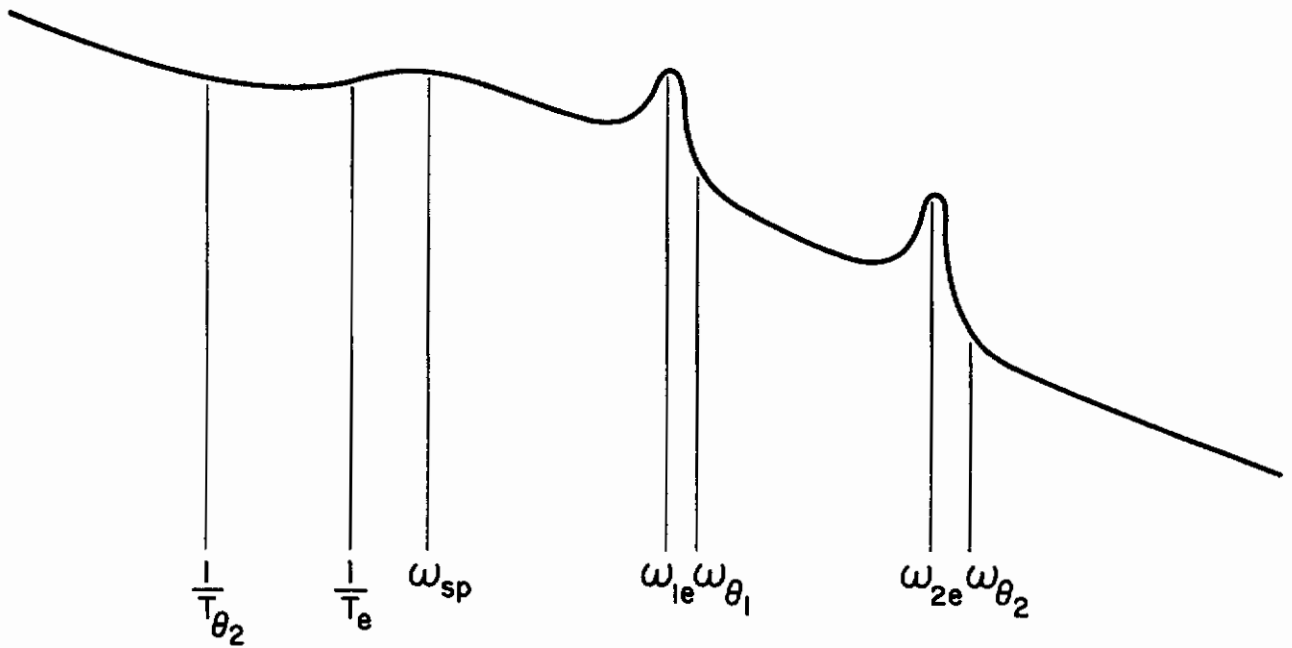


Figure 5. Bode ($j\omega$) Amplitude for θ/δ with $\omega_{1e} < \omega_{\theta_1}$ and ω_{sp} Near ω_{1e}

If the θ/δ response is favorable, as shown in Fig. 4, then the complete θ_1/δ response can also be made favorable by minimizing the dynamics of the bracketed term in Eq 82 (via the sensor location). If the θ/δ response is similar to that shown in Fig. 5, however, then the sensor should be located so the dynamics of the bracketed term reshape θ_1/δ to obtain a more desirable form.

D. OPTIMUM SENSOR LOCATION

Methods for locating the sensor to achieve desirable results for the two postulated situations will now be described. In the first case the sum of $\phi'_{13} N_{\xi_3} / N_\theta$ and $\phi'_{14} N_{\xi_4} / N_\theta$ will be held approximately constant over the frequency range of interest. Equation 82 shows that under these circumstances θ_1/δ will be equal to θ/δ with a gain change. In the second case a sensor location will be found which makes the combined dynamics of the terms in the brackets of Eq 82 just cancel the elastic modes found in the mean centerline transfer function, θ/δ (Eq 84).

The example chosen to demonstrate these methods is associated with the high q condition (1197 psf) for Configuration 3. The transfer functions given in Eq 82 can be obtained from Appendix D and are repeated below. (Note that the θ/δ transfer function will produce a frequency response similar to that shown in Fig. 4 and therefore is satisfactory.)

$$\begin{aligned}
 \frac{N_\theta}{A_\theta} &= (s + 1.53) [s^2 + 2(0.23)(12.8)s + 163] [s^2 + 2(0.015)(26)s + 673] \\
 \frac{N_{\xi_3}}{A_{\xi_3}} &= s [s^2 + 2(0.22)(15.1)s + 228] [s^2 + 2(0.39)(77.2)s + 5987] \\
 \frac{N_{\xi_4}}{A_{\xi_4}} &= s [s^2 + 2(0.17)(5.16)s + 26.7] [s^2 + 2(0.23)(13.1)s + 172] \\
 \Delta &= s [s^2 + 2(0.42)(4.59)s + 21.1] [s^2 + 2(0.22)(12.9)s + 166] \\
 &\quad \times [s^2 + 2(0.081)(29.7)s + 884]
 \end{aligned} \tag{85}$$

The process of locating the sensor to make the bracketed terms of Eq 82 independent of frequency is simplified by considering an alternate form.

$$\frac{\theta_1}{\delta} = \left[1 + \phi'_{14} \frac{N_{\xi_4}}{N_\theta} \left(1 + \frac{\phi'_{13}}{\phi'_{14}} \frac{N_{\xi_3}}{N_{\xi_4}} \right) \right] \frac{N_\theta}{\Delta} \tag{86}$$

Contrails

From Eq 86, it is obvious that mathematical operations equivalent to closing two loops will be performed, i.e., $\Phi'_{i3}N_{\xi3}/\Phi'_{i4}N_{\xi4}$ must be added to 1.0 and the result must be multiplied by $\Phi'_{i4}N_{\xi4}/N_{\theta}$ and added to 1.0. The solid line in Fig. 6 shows the Bode ($j\omega$) plot for the amplitude of $A_{\xi4}N_{\xi3}/A_{\xi3}N_{\xi4}$, and Fig. 7 shows the Bode ($j\omega$) plot for the amplitude of $A_{\theta}N_{\xi4}/A_{\xi4}N_{\theta}$. When the gain for the first closure ($\Phi'_{i3}A_{\xi3}/\Phi'_{i4}A_{\xi4}$) is chosen, then the curve for $1 + \Phi'_{i3}N_{\xi3}/\Phi'_{i4}N_{\xi4}$ will resemble that shown by the dashed line in Fig. 6. This is easily seen by noting that for any transfer function, G,

$$1 + G \doteq G \quad \text{for} \quad G \gg 1$$

$$1 + G \doteq 1 \quad \text{for} \quad G \ll 1$$

The closed-loop curve (corresponding to closing the first loop), is therefore closely approximated by $\Phi'_{i3}N_{\xi3}/\Phi'_{i4}N_{\xi4}$ when that quantity is much greater than unity (zero db), and by the zero db line when $\Phi'_{i3}N_{\xi3}/\Phi'_{i4}N_{\xi4}$ is much less than unity. For regions where $G \doteq 1$, the closed-loop can most conveniently be plotted using conventional Nichols charts.

Simultaneous inspection of the dashed line of Fig. 6 and the plot in Fig. 7 shows that the two curves have a mirror image resemblance. This is a result of a judicious closure of the first loop (i.e., properly locating the zero db line in Fig. 6). Because these two curves represent quantities which are to be multiplied (and thus their logarithmic, db, plots are to be added), the product is seen to be relatively independent of frequency. The key point here is that the gain of the first closure, $\Phi'_{i3}A_{\xi3}/\Phi'_{i4}A_{\xi4}$, was chosen to appropriately locate the zero db line in Fig. 6. The corresponding appropriate sensor location can now be determined from Fig. 8, which gives the value of $\Phi'_{i3}A_{\xi3}/\Phi'_{i4}A_{\xi4}$ as a function of fuselage station. Detailed numerical considerations show that the sensor should be placed at station 656 in order to make the value of

$$\Phi'_{i4} \frac{N_{\xi4}}{N_{\theta}} \left(1 + \frac{\Phi'_{i3}}{\Phi'_{i4}} \frac{N_{\xi3}}{N_{\xi4}} \right)$$

relatively independent of frequency. Closing the second loop is now trivial because it corresponds to adding a constant to 1.0.

Contrails

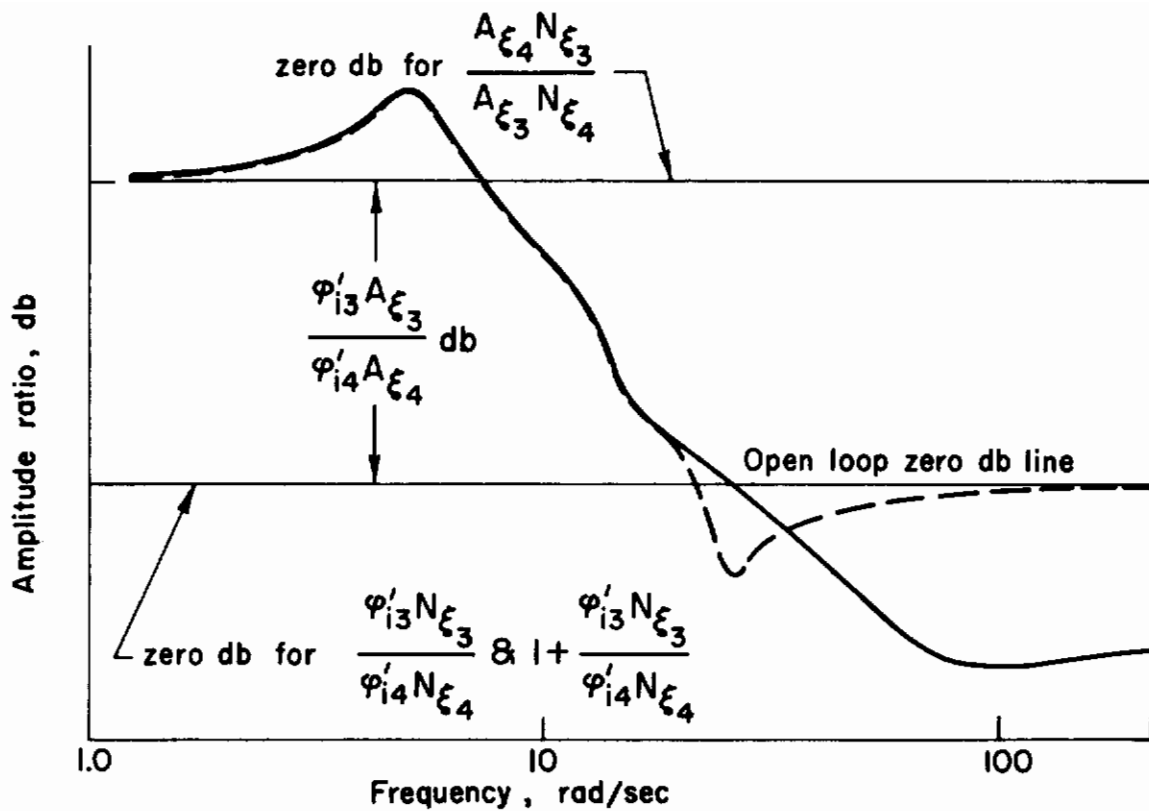


Figure 6. Bode ($j\omega$) Amplitude for $\frac{A_{\xi_4} N_{\xi_3}}{A_{\xi_3} N_{\xi_4}}$

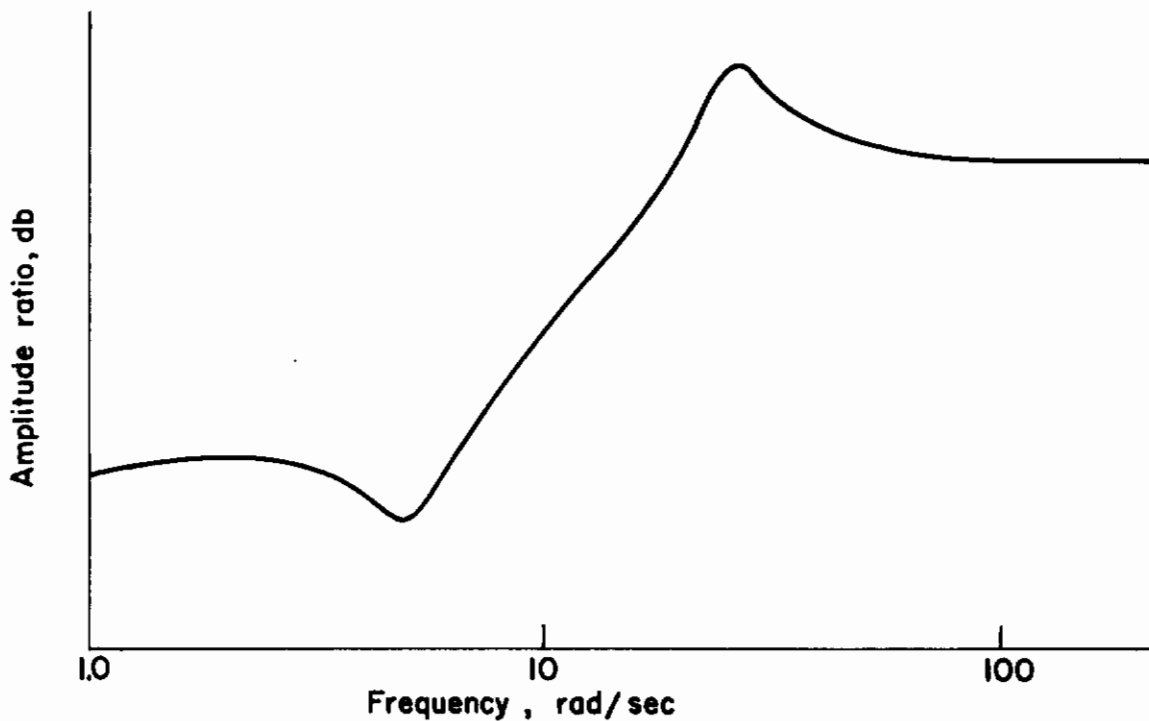


Figure 7. Bode ($j\omega$) Amplitude for $\frac{A_{\theta} N_{\xi_4}}{A_{\xi_4} N_{\theta}}$

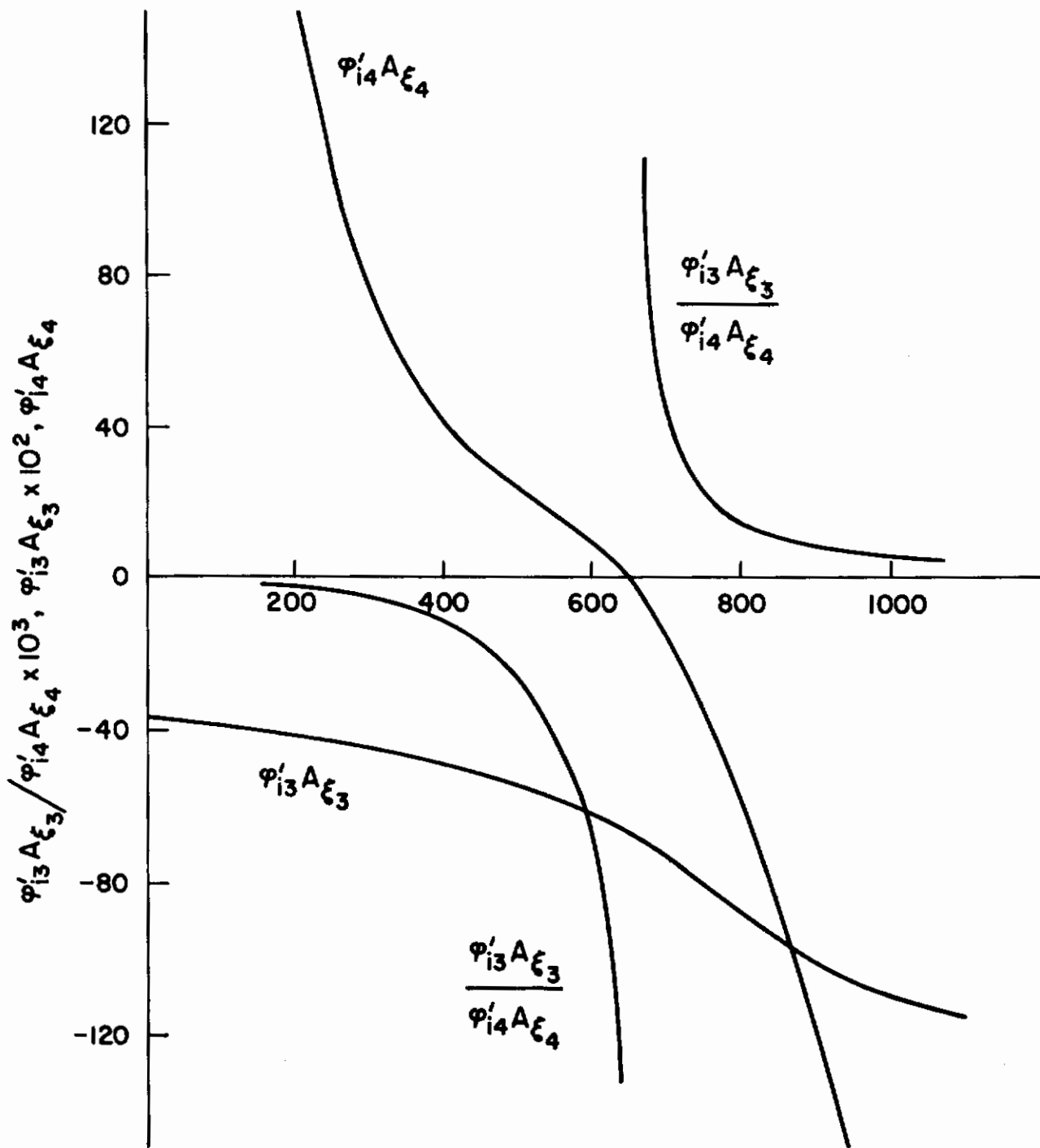


Figure 8. Variation of Mode Slopes Along the Fuselage

Contraails

It is noted that the mirror-image effect requires that a zero of N_{ξ_4}/N_θ and a pole of N_{ξ_3}/N_{ξ_4} occur at the same frequency with the same damping. However, this is always the case, because the zeros of the former are the poles of the latter. This method will therefore always theoretically reduce θ_1/δ_e to approximately θ/δ_e (when only two elastic modes are considered).

For the second situation postulated, i.e., a θ/δ frequency response as shown in Fig. 5, the dynamics of the elastic modes can be used to better shape the sensed pitch response. (Note that no such modification is required for the example picked.) Again, there are two closures involved (see Eq 86), with the location of the zeros for the second closure depending on the gain associated with the first closure. In turn, the gain is strictly dependent on the sensor location (mode shapes).

If the zeros resulting from the two closures are to be placed in close proximity to the elastic roots in Δ (Eq 85) with a resulting cancellation, the following considerations apply: The roots of the first closure will be the zeros for the second closure; one pair of these will be lightly damped and close to 13 rad/sec for any value of gain, as may be seen by inspecting Fig. 9. Since the roots of N_θ also include a pair near 13 rad/sec, the final zeros (which are the roots of the second closure) will include a lightly damped pair at approximately 13 rad/sec (see Fig. 10). This is true because a pole and zero in close proximity will always yield a root in that neighborhood for all values of gain (provided the remaining poles and zeros are relatively far removed, as they are in this case). Thus, for the example chosen the elastic poles of Δ at approximately 13 rad/sec will be cancelled for any sensor position selected. The placement of the sensor can thus be made with the intention of producing a pair of lightly damped zeros at approximately the location of the second elastic poles of Δ , 29.7 rad/sec. The second closure has a pair of lightly damped poles at approximately 26 rad/sec. The locus of the roots emanating from these poles must depart in the direction indicated in Fig. 10 if the locus is to include the desired location (29.7 rad/sec) for the zeros. The poles of the second closure (being the N_θ numerator) are not a function of sensor location; and of the four zeros resulting from the first closure, two are essentially independent of sensor location (the two lightly damped roots at approximately 13 rad/sec). Thus the problem is reduced to closing the first loop so that among the resulting roots

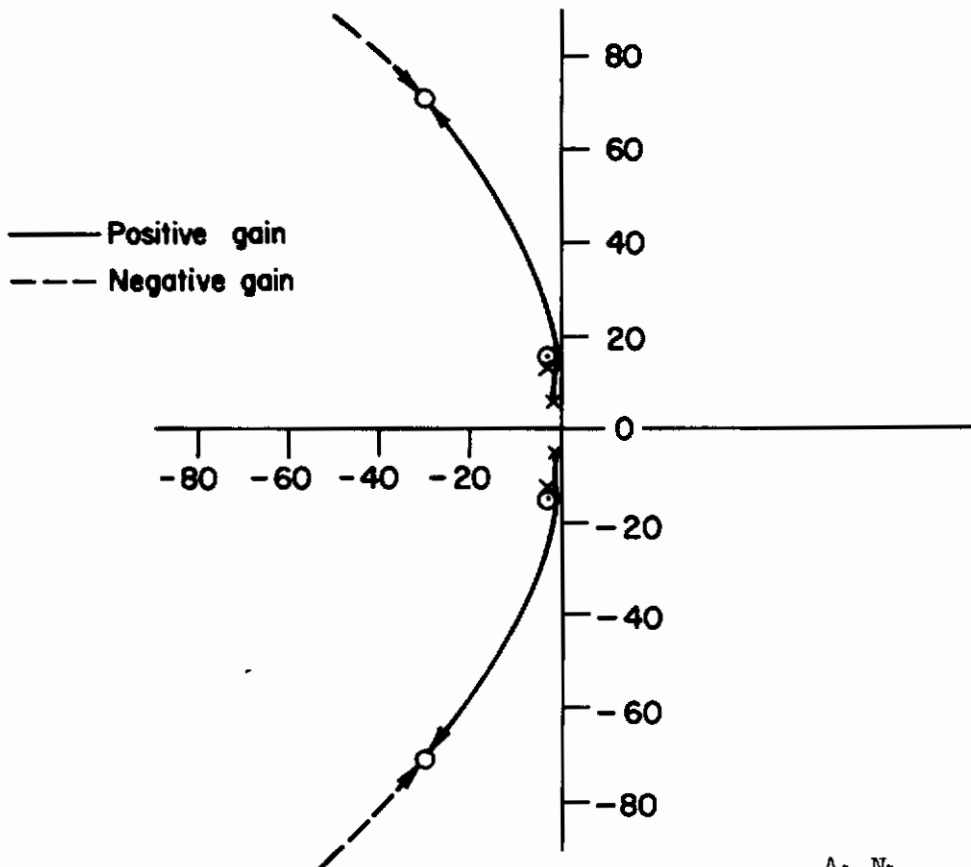


Figure 9. Locus of Roots for First Closure, $\frac{A_{E4} N_{E3}}{A_{E3} N_{E4}}$

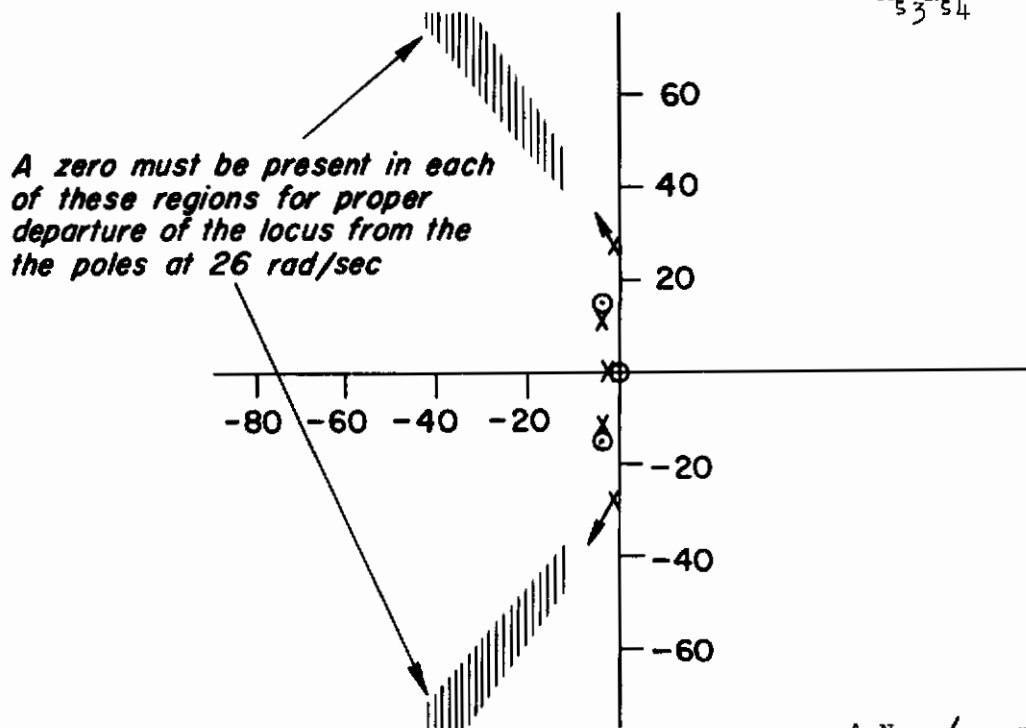


Figure 10. Pole Zero Configuration for Second Closure, $\frac{A_{E4} N_{E4}}{A_{E4} N_{E4}} \left(1 + \frac{\Phi_{i3} N_{E3}}{\Phi_{i4} N_{E4}} \right)$

Conclusions

(which will be zeros for the second closure) there will be a complex pair of zeros which yield the proper second-closure departure from the first-closure poles at 26 rad/sec. Figure 10 shows the required location of these zeros (cross-hatched area). There are two possible ways of producing roots in the cross-hatched area: the gain of the first closure, $\phi_{13}^1 A_{\xi_3} / \phi_{14}^1 A_{\xi_4}$, must be either positive or an extremely large negative number. The root locus for the first closure is shown in Fig. 9. If the gain is positive, it must be large enough to yield roots greater than 29.7 rad/sec. With this information, a number of positive gains are tried until the zeros resulting from the first closure fall in the desired position for the second closure. For the example chosen, the roots of the first closure need to be driven all the way to the zeros. Therefore, the sensor should be located at station 647 where the gain of the first closure takes on its largest value.

It is unfortunate that, for the example chosen, both methods result in placing the sensor at a fuselage station where the gain of the first closure, $\phi_{13}^1 A_{\xi_3} / \phi_{14}^1 A_{\xi_4}$, is changing quite rapidly. Any departure of the mode shapes from those expected may not result in the required gain and hence not achieve the desired flat response or the required cancellation of roots. The effects of such perturbations on the system can easily be estimated by applying the Bode techniques of Fig. 6 and 7. In any event, regardless of the validity of the examples chosen to illustrate the two approaches, the basic considerations involved are generally applicable to the closed-loop analysis and synthesis of flight control systems for flexible airframes. It is especially pertinent to note that a fairly complete set of transfer functions (including those of the coupled elastic modes themselves) is required for such analysis and synthesis activities.

SECTION V

RECOMMENDATIONS FOR FUTURE INVESTIGATIONS

The study leading to the results presented in this report has disclosed, or has investigated only partially, several potential areas of research, including the following:

1. the problem of finding the quasi-static aeroelastic correction for equations of motion which include a few elastic modes
2. the basic mechanics of mode interaction, and an understanding of what parameters can best be expected to provide an indication of the degree of coupling present
3. the possibility of representing the motion of an elastic airframe with a simplified set of equations of motion
4. if the transfer function approximate factors are a function of mode shape, what approximations can be made to adequately approximate the required modes?
5. when and how can the approximations developed in this study best be utilized?

As indicated by the manipulations outlined and demonstrated in Appendix A, any physical feeling for the meaning of $[X_{\infty}]$ is completely lost in the maze of relationships involved. This places the method in the category of being completely unsuited for use in the practical calculation of approximate transfer function factors. Nevertheless, the basic feeling exists that in one way or another, $[X_{\infty}]$ must correspond to "modified elastic properties." That is, the number of elastic modes already included must give rise to a correction of the basic static deflection properties; and the corrected properties (the "residual stiffness") must in some way be connected with $[X_{\infty}]$. These connections have to be formed, and a physically satisfying picture must be drawn before the process of obtaining simplified approximations to the aeroelastic corrections can proceed.

The desirability of obtaining such approximate corrections cannot be over-emphasized. This stems basically from the fact that if procedures akin to those described in Section II are required to establish proper aeroelastic corrections,

then much of the impact of approximate transfer functions is lost, because

1. the time and the machine methods required to compute $[X_{\infty}]$ might just as well be used to compute exact transfer functions
2. the basic possible physical insight which approximate transfer functions can potentially yield will not have been realized.

A second major consideration is the phenomenon of coupling. Better understanding of coupling is required, as evidenced by the results presented here on Configuration 3. In that instance, the equations proved to be weakly coupled, even though it was expected that strong coupling would be present. The reason for this is now known: coupling of two modes is not necessarily indicated by proximity of their frequencies. This is discussed in Ref. 8.

The equations of motion for flexible vehicles, including two rigid-body and an arbitrary number of flexible degrees of freedom, are given in their most compact form by Eq 74.

The approximate transfer functions derived in this study are a direct indication, for the cases studied, of the relative importance of the various terms in Eq 74. Unfortunately, as shown in Section III, all terms appear in one or another of the various factors involved in the complete set of transfer functions. Accordingly, the specification of the validity conditions for which the approximations apply becomes exceedingly complicated. Because all the parameters remain important (depending on the particular root involved), the most efficient way, currently, of determining the applicability of the approximations is to compute an "exact" check case. If the approximations are valid as shown by this comparison, they can be applied to gain the desired insight into sources of difficulty, effects of changes, etc.

An alternative approach to approximate factorization is to write sets of "simplified equations of motion," each set applicable to restricted-frequency regions (e.g., Ref. 9). The sets of simplified equations and the sets of approximate factors are complementary ways of specifying the important contributing terms; both approaches will theoretically yield similar results for the approximate transfer functions. Accordingly, the simplified equations can be used to specify, hopefully, more tractable validity conditions, and further to compute approximate transfer functions for other than control inputs (e.g., for gusts, as in Ref. 9). For these reasons, the simplified equations are highly desirable adjuncts to the approximate transfer function factors.

Contrails

The approximate factors for the transfer functions of a flexible airframe are given in terms of such quantities as airplane stability derivatives and mode deflections at various points on the airframe. A great many reports and papers deal with the subject of approximating such parameters, and many of those concerned with stability derivatives are directly applicable. The same is not true of all methods of estimating mode deflections, most of which are used only to establish an initial estimate for use in iterating to the exact value. Because the iteration procedures rapidly converge, the initial estimates need not be, and are not, very accurate. This is especially true of Galerkin's iteration method, and the method of Stodola and Vianello, where the iteration is continued until repeated iterations provide the same answer (Ref. 3). Other methods, such as Rayleigh-Ritz, modified Rayleigh-Ritz, collocation, and collocation using station functions (Ref. 3), rely somewhat more heavily on the original estimate if any accuracy is to be obtained. Thus, many techniques of varying accuracy (directed at these latter methods) have been formulated to provide a fairly reasonable estimate of the mode shape. Most of these, however, are usually content with merely satisfying boundary conditions. The importance of selecting or developing such approximations stems from the fact that fairly large errors in mode shape may be tolerable for the purpose of computing approximate transfer function factors. The effect of mode shape error on the accuracy of the approximate transfer functions is easily determined in a given case by finding the changes in the factors caused by variations in the values of the mode deflections.

It is desirable to apply the approximate transfer function formulas (Ref. 5) to some actual aircraft or missiles to demonstrate their application and utility on a tangible basis. Probably the most significant and useful results can be obtained for vehicles that are currently in the preliminary design stage. The information necessary for the evaluation of the approximate factors is generally most available at that time, and the resulting analysis would be useful to the vehicle manufacturer, inasmuch as some insight would be provided on the dominant factors affecting the aircraft modes.

Many of these problems may be resolved in the completion of Contract No. AF 33(657)-8374 which has recently been awarded specifically for study in these areas.

REFERENCES

1. Schwendler, Robert G. and Richard H. MacNeal, Optimum Structural Representation in Aeroelastic Analyses, ASD TR 61-680, January 1962.
2. Dynamics of the Airframe, BuAer Report AE-61-4-II, Northrop Aircraft, Inc., September 1952.
3. Bisplinghoff, Raymond L., Holt Ashley, and Robert L. Halfman, Aeroelasticity, Addison-Wesley Publishing Company, Inc., Reading, Massachusetts, 1955.
4. Scanlan, Robert H. and Robert Rosenbaum, Introduction to the Study of Aircraft Vibration and Flutter, The Macmillan Company, New York, 1951.
5. Hildebrand, F. B., Methods of Applied Mathematics, Prentice Hall, Inc., New York, 1952.
6. Milne-Thomson, L. M., Theoretical Aerodynamics, St Martin's Press, Inc., New York, 1958.
7. Methods of Analysis and Synthesis of Piloted Aircraft Flight Control Systems, BuAer Report AE-61-4-I, Northrop Aircraft, Inc., March 1952.
8. Continuing Investigation on Approximate Transfer Functions for a Flexible Airframe, Systems Technology, Inc., Technical Proposal No. 38, 15 December 1961.
9. Ashkenas, Irving L. and Duane T. McRuer, Approximate Airframe Transfer Functions and Application to Single Sensor Control Systems, WADC TR 58-82, June 1958.

APPENDIX A

AEROELASTIC CORRECTIONS

A method has been derived in Ref. 1 wherein $[X_{\infty}]$ can be calculated. It was not considered necessary to repeat that derivation in this report, but a summary of the method and an example of its use follow.

A. SUMMARY OF THE METHOD

To obtain the basic data required in these equations, the system is restrained at two points, and is then subjected to a unit acceleration field, first in translation and then in rotation. The resulting physical deflections are partitioned in matrix form as

$$\left\{ \begin{matrix} q_a \text{ trans} \end{matrix} \right\} = \left\{ \begin{matrix} q_g \text{ trans} \\ \dots\dots\dots \\ q_m \text{ trans} \end{matrix} \right\} \quad (A-1)$$

$$\left\{ \begin{matrix} q_a \text{ rot} \end{matrix} \right\} = \left\{ \begin{matrix} q_g \text{ rot} \\ \dots\dots\dots \\ q_m \text{ rot} \end{matrix} \right\} \quad (A-2)$$

where the subscripts a, g, and m denote acceleration deflections, grounded coordinates, and movable coordinates, respectively. These deflections are used in the calculation of $[X_{f+\infty}]$, where

$$[X_{\infty}] = [X_{f+\infty}] - [\Phi_f] [Y_f]_{s=0}^{-1} [\Phi_f]^T \quad (A-3)$$

In Eq A-3, the columns of $[\Phi_f]$ correspond to the finite-frequency mode shapes (those of interest as mentioned earlier); $[Y_f]$ represents the diagonal $[K + Ms^2]$ matrix for the corresponding finite frequency stiffness and mass matrices; and the elements of $[X_{f+\infty}]$ are found by calculating partitions of $[X_{f+\infty}]$ as follows:

Contrails

$$[X_{f+\omega}] = \begin{bmatrix} X_{(f+\omega)gg} & \cdots & X_{(f+\omega)gm} \\ \cdots & \cdots & \cdots \\ X_{(f+\omega)mg} & \cdots & X_{(f+\omega)mm} \end{bmatrix} \quad (A-4)$$

$$[X_{(f+\omega)gg}] = +[\Phi_{Or}][M_O]^{-1}[\Phi_O]^T[m][\{q_a \text{ trans}\}\{q_a \text{ rot}\}][M_O]^{-1}[\Phi_{Or}]^T \quad (A-5)$$

$$[X_{(f+\omega)mg}] = -[\{q_m \text{ trans}\}\{q_m \text{ rot}\}][M_O]^{-1}[\Phi_{Og}]^T \\ + [\Phi_{Om}][M_O]^{-1}[\Phi_O]^T[m][\{q_a \text{ trans}\}\{q_a \text{ rot}\}][M_O]^{-1}[\Phi_{Og}]^T \quad (A-6)$$

$$[X_{(f+\omega)gm}] = [X_{(f+\omega)mg}]^T \quad (A-7)$$

$$[X_{(f+\omega)mm}] = [Z_O] - [\Phi_{Om}][\Phi_{Og}]^{-1}[X_{(f+\omega)gg}][\Phi_{Og}]^{T^{-1}}[\Phi_{Om}]^T \\ + [\Phi_{Om}][\Phi_{Og}]^{-1}[X_{(f+\omega)gm}] + [X_{(f+\omega)mg}][\Phi_{Og}]^{T^{-1}}[\Phi_{Om}]^T \quad (A-8)$$

where $[Z_O]$ is the influence coefficient matrix of the system when restrained at the two points q_g ; and where $[\Phi_{Om}]$ and $[\Phi_{Og}]$ are found by partitioning the zero-frequency modal matrix into the elements corresponding to the restrained and unrestrained coordinates,

$$[\Phi_O] = \begin{bmatrix} \Phi_{Og} \\ \cdots \\ \Phi_{Om} \end{bmatrix} \quad (A-9)$$

Also, $[M_O]$ is the zero-frequency modal mass matrix

$[m]$ is the mass matrix of the physical system (defined previously)

B. EXEMPLARY DEVELOPMENT

The three masses shown in Fig. A-1 are rigidly attached to a weightless beam of length $2l$:

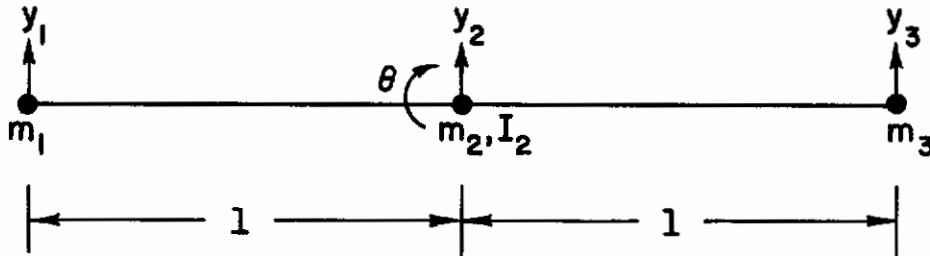


Figure A-1. Mechanical Model

The rotational inertia of the first and third masses in Fig. A-1 is negligible, and the rotational inertia of the second mass is I_2 . All deflections are measured inertially, and are positive as indicated. The angle θ is the inertial rotation of mass two, and is also positive as shown. Mass two is in the center of the beam which has a constant EI . The masses are assumed to be equal, m .

With this information, it will be possible to write the system equations of motion utilizing Lagrange's equation:

$$\frac{d}{dt} \left(\frac{\partial L}{\partial \dot{q}_r} \right) - \frac{\partial L}{\partial q_r} + \frac{\partial D}{\partial \dot{q}_r} = Q_r \quad (A-10)$$

where

- $L = T - U$
- $T =$ the kinetic energy of the system
- $U =$ the potential energy of the system
- $D =$ the damping energy of the system
- $Q_r =$ the generalized force on the r^{th} degree of freedom
- $q_r =$ the r^{th} degree of freedom

Following these definitions (an expression for the potential energy for the beams is derived in Ref. 3),

Contrails

$$\begin{aligned} L &= \frac{1}{2} m\dot{y}_1^2 + \frac{1}{2} m\dot{y}_2^2 + \frac{1}{2} m\dot{y}_3^2 + \frac{1}{2} I_2\dot{\theta}^2 \\ &\quad - \frac{3}{2} \frac{EI}{l^3} (y_1 - y_2 - l\theta)^2 \\ &\quad - \frac{3}{2} \frac{EI}{l^3} (y_3 - y_2 - l\theta)^2 \end{aligned} \quad (A-11)$$

It is not necessary to consider any external forces for the purposes of this example; thus, Q_r will be zero. Substituting in Lagrange's equation yields

$$\begin{aligned} m\ddot{y}_2 - 3 \frac{EI}{l^3} (y_1 - y_2 - l\theta) - 3 \frac{EI}{l^3} (y_3 - y_2 + l\theta) &= 0 \\ I_2\ddot{\theta} - 3 \frac{EI}{l^2} (y_1 - y_2 - l\theta) + 3 \frac{EI}{l^2} (y_3 - y_2 - l\theta) &= 0 \\ m\ddot{y}_3 + 3 \frac{EI}{l^3} (y_3 - y_2 + l\theta) &= 0 \\ m\ddot{y}_1 + 3 \frac{EI}{l^3} (y_1 - y_2 - l\theta) &= 0 \end{aligned} \quad (A-12)$$

Equations A-12 can be put into matrix form as indicated in Section II:

$$[ms^2 + k]\{q\} = \{Q\} \quad (A-13)$$

where

$$\{q\} = \begin{Bmatrix} y_2 \\ \theta \\ y_3 \\ y_1 \end{Bmatrix}$$
$$[m] = \begin{bmatrix} m & 0 & 0 & 0 \\ 0 & I_2 & 0 & 0 \\ 0 & 0 & m & 0 \\ 0 & 0 & 0 & m \end{bmatrix}$$

Contrails

$$[k] = \begin{bmatrix} 6 \frac{EI}{l^3} & 0 & -3 \frac{EI}{l^3} & -3 \frac{EI}{l^3} \\ 0 & 6 \frac{EI}{l} & 3 \frac{EI}{l^2} & -3 \frac{EI}{l^2} \\ -3 \frac{EI}{l^3} & 3 \frac{EI}{l^2} & 3 \frac{EI}{l^3} & 0 \\ -3 \frac{EI}{l^3} & -3 \frac{EI}{l^2} & 0 & 3 \frac{EI}{l^3} \end{bmatrix}$$

The modal matrix can now be found:

$$[\Phi] = \begin{bmatrix} 1 & 0 & -2 & 0 \\ 0 & \frac{1}{l} & 0 & -2 \frac{ml}{I_2} \\ 1 & -1 & 1 & -1 \\ 1 & 1 & 1 & 1 \end{bmatrix} \quad (A-14)$$

If the degrees of freedom of interest were limited to, for example, the two rigid-body modes and just one elastic mode, then, from Section II,

$$\begin{aligned} [\Phi_0] &= \begin{bmatrix} 1 & 0 \\ 0 & \frac{1}{l} \\ 1 & -1 \\ 1 & 1 \end{bmatrix} \\ [\Phi_f] &= \begin{bmatrix} -2 \\ 0 \\ 1 \\ 1 \end{bmatrix} \\ [\Phi_\infty] &= \begin{bmatrix} 0 \\ -2 \frac{ml}{I_2} \\ -1 \\ 1 \end{bmatrix} \end{aligned} \quad (A-15)$$

Contrails

The $[Y]$ matrix can also be calculated as described in Section II, and

$$[Y] = \begin{bmatrix} 3ms^2 & 0 & 0 & 0 \\ 0 & \left(2m + \frac{I_2}{l^2}\right)s^2 & 0 & 0 \\ 0 & 0 & 6ms^2 + 54 \frac{EI}{l^3} & 0 \\ 0 & 0 & 0 & \left(2m + 4 \frac{m^2 l^2}{I_2}\right)s^2 + \frac{61EI}{I_2^2} \left(2m + \frac{I_2}{l^2}\right)^2 \end{bmatrix} \quad (A-16)$$

Following Section II,

$$\begin{aligned} [Y_Q] &= \begin{bmatrix} 3ms^2 & 0 \\ 0 & \left(2m + \frac{I_2}{l^2}\right)s^2 \end{bmatrix} \\ [Y_f] &= \begin{bmatrix} 6ms^2 + 54 \frac{EI}{l^3} \end{bmatrix} \\ [Y_{\infty}] &= \begin{bmatrix} \left(2m + 4 \frac{m^2 l^2}{I_2}\right)s^2 + 3 \frac{EI}{l} \left(\frac{2}{I_2} + \frac{1}{ml^2}\right) \left(2m + 4 \frac{m^2 l^2}{I_2}\right) \end{bmatrix} \end{aligned} \quad (A-17)$$

From this information, $[X_{\infty}]$ can be calculated directly from Eq 47:

$$[X_{\infty}] = [\Phi_{\infty}] [Y_{\infty}]^{-1} [\Phi_{\infty}]^T \quad (47)$$

$$[X_{\infty}] = \frac{I_2^2}{61EI \left(2m + \frac{I_2}{l^2}\right)^2} \begin{bmatrix} 0 & 0 & 0 & 0 \\ 0 & 4 \frac{m^2 l^2}{I_2^2} & 2 \frac{ml}{I_2} & -2 \frac{ml}{I_2} \\ 0 & 2 \frac{ml}{I_2} & 1 & -1 \\ 0 & -2 \frac{ml}{I_2} & -1 & 1 \end{bmatrix} \quad (A-18)$$

Contrails

As described in Eq A-1 through A-9, $[X_{\infty}]$ can also be calculated without the knowledge of $[\Phi_{\infty}]$.

With the system restrained in translation, and rotation at the center of gravity (mass two):

$$\{q_m \text{ trans}\} = \begin{Bmatrix} \frac{ml^3}{3EI} \\ \frac{ml^3}{3EI} \end{Bmatrix}$$

$$\{q_m \text{ rot}\} = \begin{Bmatrix} -\frac{ml^3}{3EI} \\ \frac{ml^3}{3EI} \end{Bmatrix}$$

$$[Z_o] = \begin{bmatrix} \frac{l^3}{3EI} & 0 \\ 0 & \frac{l^3}{3EI} \end{bmatrix}$$

(A-19)

$$[\Phi_{om}] = \begin{bmatrix} 1 & -1 \\ 1 & 1 \end{bmatrix}$$

$$[\Phi_{og}] = \begin{bmatrix} 1 & 0 \\ 0 & \frac{1}{l} \end{bmatrix}$$

$$[M_o] = \begin{bmatrix} 3m & 0 \\ 0 & 2m + \frac{I_2}{l^2} \end{bmatrix}$$

Contrails

Equation A-5 yields

$$\begin{aligned}
 [X_{(f+\infty)gg}] &= \begin{bmatrix} 1 & 0 \\ 0 & \frac{1}{l} \end{bmatrix} \begin{bmatrix} \frac{1}{3m} & 0 \\ 0 & \frac{1}{2m + \frac{I_2}{l^2}} \end{bmatrix} \begin{bmatrix} 1 & 0 & 1 & 1 \\ 0 & \frac{1}{l} & -1 & 1 \end{bmatrix} \begin{bmatrix} m & 0 & 0 & 0 \\ 0 & I_2 & 0 & 0 \\ 0 & 0 & m & 0 \\ 0 & 0 & 0 & m \end{bmatrix} \\
 &\times \begin{bmatrix} 0 & 0 \\ 0 & 0 \\ \frac{ml^3}{3EI} & -\frac{ml^3}{3EI} \\ \frac{ml^3}{3EI} & \frac{ml^3}{3EI} \end{bmatrix} \begin{bmatrix} \frac{1}{3m} & 0 \\ 0 & \frac{1}{2m + \frac{I_2}{l^2}} \end{bmatrix} \begin{bmatrix} 1 & 0 \\ 0 & \frac{1}{l} \end{bmatrix} \quad (A-20)
 \end{aligned}$$

$$[X_{(f+\infty)gg}] = \begin{bmatrix} \frac{2l^3}{27EI} & 0 \\ 0 & \frac{2m^2 l I_2}{3EI \left(2m + \frac{I_2}{l^2}\right)^2} \end{bmatrix} \quad (A-21)$$

Contrails

Equation A-6 yields

$$\begin{aligned}
 [X_{(f+\infty)mg}] &= - \begin{bmatrix} \frac{ml^3}{3EI} & -\frac{ml^3}{3EI} \\ \frac{ml^3}{3EI} & \frac{ml^3}{3EI} \end{bmatrix} \begin{bmatrix} \frac{1}{3m} & 0 \\ 0 & \frac{1}{2m + \frac{I_2}{l^2}} \end{bmatrix} \begin{bmatrix} 1 & 0 \\ 0 & \frac{1}{l} \end{bmatrix} \\
 &+ \begin{bmatrix} 1 & -1 \\ 1 & 1 \end{bmatrix} \begin{bmatrix} \frac{1}{3m} & 0 \\ 0 & \frac{1}{2m + \frac{I_2}{l^2}} \end{bmatrix} \begin{bmatrix} 1 & 0 & 1 & 1 \\ 0 & \frac{1}{l} & -1 & 1 \end{bmatrix} \begin{bmatrix} m & 0 & 0 & 0 \\ 0 & I_2 & 0 & 0 \\ 0 & 0 & m & 0 \\ 0 & 0 & 0 & m \end{bmatrix} \\
 &\times \begin{bmatrix} 0 & 0 \\ 0 & 0 \\ \frac{ml^3}{3EI} & -\frac{ml^3}{3EI} \\ \frac{ml^3}{3EI} & \frac{ml^3}{3EI} \end{bmatrix} \begin{bmatrix} \frac{1}{3m} & 0 \\ 0 & \frac{1}{2m + \frac{I_2}{l^2}} \end{bmatrix} \begin{bmatrix} 1 & 0 \\ 0 & \frac{1}{l} \end{bmatrix} \tag{A-22}
 \end{aligned}$$

$$[X_{(f+\infty)mg}] = \begin{bmatrix} -\frac{l^3}{27EI} & -\frac{mI_2}{3EI \left(2m + \frac{I_2}{l^2}\right)^2} \\ -\frac{l^3}{27EI} & -\frac{mI_2}{3EI \left(2m + \frac{I_2}{l^2}\right)^2} \end{bmatrix} \tag{A-23}$$

Contrails

From Eq A-7,

$$[X_{(f+\infty)gm}] = \begin{bmatrix} -\frac{l^3}{27EI} & -\frac{l^3}{27EI} \\ \frac{mI_2}{3EI\left(2m + \frac{I_2}{l^2}\right)^2} & -\frac{mI_2}{3EI\left(2m + \frac{I_2}{l^2}\right)^2} \end{bmatrix} \quad (A-24)$$

Equation A-8 yields

$$[X_{(f+\infty)mm}] = \begin{bmatrix} \frac{l^3}{3EI} & 0 \\ 0 & \frac{l^3}{3EI} \end{bmatrix} - \begin{bmatrix} 1 & -1 \\ 1 & 1 \end{bmatrix} \begin{bmatrix} 1 & 0 \\ 0 & 1 \end{bmatrix} \begin{bmatrix} \frac{2l^3}{27EI} & 0 \\ 0 & \frac{2m^2l}{3EI\left(2m + \frac{I_2}{l^2}\right)^2} \end{bmatrix}$$

$$\times \begin{bmatrix} 1 & 0 \\ 0 & 1 \end{bmatrix} \begin{bmatrix} 1 & 1 \\ -1 & 1 \end{bmatrix} + \begin{bmatrix} 1 & -1 \\ 1 & 1 \end{bmatrix} \begin{bmatrix} 1 & 0 \\ 0 & 1 \end{bmatrix} \begin{bmatrix} -\frac{l^3}{27EI} & -\frac{l^3}{27EI} \\ \frac{mI_2}{3EI\left(2m + \frac{I_2}{l^2}\right)^2} & -\frac{mI_2}{3EI\left(2m + \frac{I_2}{l^2}\right)^2} \end{bmatrix}$$

$$+ \begin{bmatrix} -\frac{l^3}{27EI} & \frac{mI_2}{3EI\left(2m + \frac{I_2}{l^2}\right)^2} \\ -\frac{l^3}{27EI} & -\frac{mI_2}{3EI\left(2m + \frac{I_2}{l^2}\right)^2} \end{bmatrix} \begin{bmatrix} 1 & 0 \\ 0 & 1 \end{bmatrix} \begin{bmatrix} 1 & 1 \\ -1 & 1 \end{bmatrix} \quad (A-25)$$

Contrails

$$\left[X_{(f+\infty)mm} \right] = \begin{bmatrix} \frac{51^3}{27EI} - \frac{2m^2 1^3 + 2m1I_2}{3EI \left(2m + \frac{I_2}{1^2}\right)^2} & - \frac{41^3}{27EI} + \frac{2m^2 1^3 + 2m1I_2}{3EI \left(2m + \frac{I_2}{1^2}\right)^2} \\ - \frac{41^3}{27EI} + \frac{2m^2 1^3 + 2m1I_2}{3EI \left(2m + \frac{I_2}{1^2}\right)^2} & \frac{51^3}{27EI} - \frac{2m^2 1^3 + 2m1I_2}{3EI \left(2m + \frac{I_2}{1^2}\right)^2} \end{bmatrix} \quad (A-26)$$

Now $\left[X_{(f+\infty)} \right]$ can be constructed from Eq A-21, A-23, A-24, and A-26:

$$\left[X_{(f+\infty)} \right] = \begin{bmatrix} \frac{21^3}{27EI} & 0 & - \frac{1^3}{27EI} & - \frac{1^3}{27EI} \\ 0 & \frac{2m^2 1}{3EI \left(2m + \frac{I_2}{1^2}\right)^2} & \frac{mI_2}{3EI \left(2m + \frac{I_2}{1^2}\right)^2} & - \frac{mI_2}{3EI \left(2m + \frac{I_2}{1^2}\right)^2} \\ - \frac{1^3}{27EI} & \frac{mI_2}{3EI \left(2m + \frac{I_2}{1^2}\right)^2} & \frac{51^3}{27EI} - \frac{2m^2 1^3 + 2m1I_2}{3EI \left(2m + \frac{I_2}{1^2}\right)^2} & - \frac{41^3}{27EI} + \frac{2m^2 1^3 + 2m1I_2}{3EI \left(2m + \frac{I_2}{1^2}\right)^2} \\ - \frac{1^3}{27EI} & - \frac{mI_2}{3EI \left(2m + \frac{I_2}{1^2}\right)^2} & - \frac{41^3}{27EI} + \frac{2m^2 1^3 + 2m1I_2}{3EI \left(2m + \frac{I_2}{1^2}\right)^2} & \frac{51^3}{27EI} - \frac{2m^2 1^3 + 2m1I_2}{3EI \left(2m + \frac{I_2}{1^2}\right)^2} \end{bmatrix} \quad (A-27)$$

Before solving for $\left[X_{\infty} \right]$ from Eq A-3, it will be necessary to find $\left[X_f \right]$ from

$$\left[X_f \right] = \left[\phi_f \right] \left[Y_f \right]_{s=0}^{-1} \left[\phi_f \right]^T \quad (A-28)$$

Contrails

$$[X_f] = \frac{l^3}{54EI} \begin{bmatrix} 4 & 0 & -2 & -2 \\ 0 & 0 & 0 & 0 \\ -2 & 0 & 1 & 1 \\ -2 & 0 & 1 & 1 \end{bmatrix} \quad (A-29)$$

Subtracting Eq A-29 from Eq A-27,

$$[X_{\infty}] = \begin{bmatrix} 0 & 0 & 0 & 0 \\ 0 & \frac{2m^2 l}{3EI \left(2m + \frac{I_2}{l^2}\right)^2} & \frac{mI_2}{3EI \left(2m + \frac{I_2}{l^2}\right)^2} & -\frac{mI_2}{3EI \left(2m + \frac{I_2}{l^2}\right)^2} \\ 0 & \frac{mI_2}{3EI \left(2m + \frac{I_2}{l^2}\right)^2} & \frac{l^3}{6EI} - \frac{2m^2 l^3 + 2mlI_2}{3EI \left(2m + \frac{I_2}{l^2}\right)^2} & -\frac{l^3}{6EI} + \frac{2m^2 l^3 + 2mlI_2}{3EI \left(2m + \frac{I_2}{l^2}\right)^2} \\ 0 & -\frac{mI_2}{3EI \left(2m + \frac{I_2}{l^2}\right)^2} & -\frac{l^3}{6EI} + \frac{2m^2 l^3 + 2mlI_2}{3EI \left(2m + \frac{I_2}{l^2}\right)^2} & \frac{l^3}{6EI} - \frac{2m^2 l^3 + 2mlI_2}{3EI \left(2m + \frac{I_2}{l^2}\right)^2} \end{bmatrix}$$

(A-30)

Algebraic manipulation yields

$$[X_{\infty}] = \begin{bmatrix} 0 & 0 & 0 & 0 \\ 0 & \frac{2m^2 l}{3EI \left(2m + \frac{I_2}{l^2}\right)^2} & \frac{mI_2}{3EI \left(2m + \frac{I_2}{l^2}\right)^2} & -\frac{mI_2}{3EI \left(2m + \frac{I_2}{l^2}\right)^2} \\ 0 & \frac{mI_2}{3EI \left(2m + \frac{I_2}{l^2}\right)^2} & \frac{I_2^2}{61EI \left(2m + \frac{I_2}{l^2}\right)^2} & -\frac{I_2^2}{61EI \left(2m + \frac{I_2}{l^2}\right)^2} \\ 0 & -\frac{mI_2}{3EI \left(2m + \frac{I_2}{l^2}\right)^2} & -\frac{I_2^2}{61EI \left(2m + \frac{I_2}{l^2}\right)^2} & \frac{I_2^2}{61EI \left(2m + \frac{I_2}{l^2}\right)^2} \end{bmatrix} \quad (A-31)$$

Equation A-31 reduces to

$$[X_{\infty}] = \frac{I_2^2}{6lEI \left(2m + \frac{I_2}{l^2}\right)^2} \begin{bmatrix} 0 & 0 & 0 & 0 \\ 0 & \frac{4m^2 l^2}{I_2^2} & \frac{2ml}{I_2} & -\frac{2ml}{I_2} \\ 0 & \frac{2ml}{I_2} & 1 & -1 \\ 0 & -\frac{2ml}{I_2} & -1 & 1 \end{bmatrix} \quad (A-32)$$

The result obtained in Eq A-32 proves to be identical to the result obtain in Eq A-18, although no use has been made of the fourth-mode shape.

APPENDIX B

ANALYTICAL METHODS OF APPROXIMATE FACTORIZATION

A. CHARACTERISTIC POLYNOMIALS OF LIGHTLY COUPLED SYSTEMS

Approximate factors of a characteristic polynomial are found directly from the matrix of coefficients in the equations of motion, rather than by expanding the determinant of coefficients, and then factoring the resulting polynomial. The technique employed here involves determining those corrections that must be applied to a crude first-approximation to the factors. This method is particularly suitable to those cases where the diagonal elements of the determinant of coefficients are the major contributors to the characteristic polynomial. The case to be considered here is that of a 3-degree-of-freedom system having a determinant of coefficients of the following form:

$$\Delta(s) \equiv \begin{vmatrix} s + a_{11} & a_{12} & b_{13}s + a_{13} \\ a_{21} & s + a_{22} & b_{23}s + a_{23} \\ a_{31} & a_{32} & s^2 + b_{33}s + a_{33} \end{vmatrix} \quad (\text{B-1})$$

where $\Delta(s)$ is the characteristic polynomial, and a_{ij} and b_{ij} are real constants

This could represent an airframe with two rigid-body degrees of freedom and one elastic structural mode (as per Eq 74). $\Delta(s)$ can be expanded about the third column, giving

$$\Delta(s) = P(s) + R_1(s) + R_2(s) \quad (\text{B-2})$$

$$\text{where } P(s) = (s^2 + b_{33}s + a_{33}) \begin{vmatrix} s + a_{11} & a_{12} \\ a_{21} & s + a_{22} \end{vmatrix}$$

$$R_1(s) = -(b_{23}s + a_{23}) \begin{vmatrix} s + a_{11} & a_{12} \\ a_{31} & a_{32} \end{vmatrix}$$

$$\text{and } R_2(s) = (b_{13}s + a_{13}) \begin{vmatrix} a_{21} & s + a_{22} \\ a_{31} & a_{32} \end{vmatrix}$$

Contrails

P(s) can also be written

$$\begin{aligned} P(s) &= (s^2 + \beta s + y^2)(s^2 + \alpha s + x^2) \\ &= s^4 + (\alpha + \beta)s^3 + (x^2 + y^2 + \alpha\beta)s^2 + (\alpha y^2 + \beta x^2)s + x^2 y^2 \quad (B-3) \\ &= s^4 + Bs^3 + Cs^2 + Ds + E \end{aligned}$$

where by direct comparison

$$\begin{aligned} B &= \alpha + \beta \\ C &= x^2 + y^2 + \alpha\beta \\ D &= \alpha y^2 + \beta x^2 \\ E &= x^2 y^2 \end{aligned} \quad (B-4)$$

and by comparison with Eq B-2,

$$\begin{aligned} x^2 &= a_{11}a_{22} - a_{12}a_{21} \\ \alpha &= a_{11} + a_{22} \\ y^2 &= a_{33} \\ \beta &= b_{33} \end{aligned} \quad (B-5)$$

The complete $\Delta(s)$ is also of the form of Eq B-3, but with slightly modified factors and polynomial coefficients due to the added $R_1(s)$ and $R_2(s)$. Because the modified polynomial coefficients are directly available from Eq B-2, it is pertinent to relate increments in the coefficients to increments in the factors. Then the approximate factors of $\Delta(s)$ will be the factors of $P(s)$ as modified by these increments. Proceeding along these lines by taking differentials in Eq B-4,

$$\begin{aligned} dB &= d\alpha + d\beta \\ dC &= dx^2 + dy^2 + \alpha d\beta + \beta d\alpha \\ dD &= \alpha dy^2 + y^2 d\alpha + \beta dx^2 + x^2 d\beta \\ dE &= x^2 dy^2 + y^2 dx^2 \end{aligned} \quad (B-6)$$

Contrails

Because $R_1(s) + R_2(s)$ is of second degree, $dB = 0$, whereby

$$d\alpha = -d\beta \quad (B-7)$$

Substituting Eq B-7 into Eq B-6,

$$dC = dx^2 + dy^2 + (\alpha - \beta)d\beta \quad (B-8)$$

$$dD = \alpha dy^2 + \beta dx^2 + (x^2 - y^2)d\beta \quad (B-9)$$

$$dE = x^2 dy^2 + y^2 dx^2 \quad (B-10)$$

Eliminating $d\beta$ by combining Eq B-8 and B-9 gives

$$\frac{dC - dx^2 - dy^2}{\alpha - \beta} = \frac{dD - \alpha dy^2 - \beta dx^2}{x^2 - y^2} \quad (B-11)$$

Solving Eq B-10 for dx^2 ,

$$dx^2 = \frac{dE - x^2 dy^2}{y^2} \quad (B-12)$$

Substituting Eq B-12 into Eq B-11,

$$\frac{dC - \left(\frac{dE - x^2 dy^2}{y^2} \right) - dy^2}{\alpha - \beta} = \frac{dD - \alpha dy^2 - \beta \left(\frac{dE - x^2 dy^2}{y^2} \right)}{x^2 - y^2} \quad (B-13)$$

Then, solving Eq B-13 for dy^2 ,

$$dy^2 = \frac{(y^2 - x^2)(y^2 dC - dE) + (\alpha - \beta)(y^2 dD - \beta dE)}{(y^2 - x^2)^2 + (\alpha - \beta)(\alpha y^2 - \beta x^2)} \quad (B-14)$$

By solving Eq B-10 for dy^2 , and by substituting the result into Eq B-11, a similar expression for dx^2 can be found:

$$dx^2 = \frac{(y^2 - x^2)(dE - x^2 dC) + (\alpha - \beta)(\alpha dE - x^2 dD)}{(y^2 - x^2)^2 + (\alpha - \beta)(\alpha y^2 - \beta x^2)} \quad (B-15)$$

Contrails

Expressing Eq B-14 and B-15 in terms of finite differentials (rather than infinitesimal), and collecting terms,

$$\Delta x^2 = \frac{[y^2 - x^2 + \alpha(\alpha - \beta)]\Delta E - [x^2(y^2 - x^2)]\Delta C - [x^2(\alpha - \beta)]\Delta D}{(y^2 - x^2)^2 + (\alpha - \beta)(\alpha y^2 - \beta x^2)} \quad (B-16)$$

$$\Delta y^2 = \frac{-[y^2 - x^2 + \beta(\alpha - \beta)]\Delta E + [y^2(y^2 - x^2)]\Delta C + [y^2(\alpha - \beta)]\Delta D}{(y^2 - x^2)^2 + (\alpha - \beta)(\alpha y^2 - \beta x^2)} \quad (B-17)$$

Considering that Eq B-1 is representative of an airframe with one elastic mode included in the equations of motion, $\Delta(s)$, in terms of the factored forms of Table I, would be given by

$$\Delta(s) = [s^2 + (2\xi\omega)_{sp}s + \omega_{sp}^2][s^2 + (2\xi\omega)_{1e}s + \omega_{1e}^2] \quad (B-18)$$

where

$$\omega_{sp}^2 = x^2 + \Delta x^2$$

$$(2\xi\omega)_{sp} = \alpha + \Delta\alpha$$

$$\omega_{1e}^2 = y^2 + \Delta y^2$$

$$(2\xi\omega)_{1e} = \beta + \Delta\beta$$

Therefore, using Eq B-5, B-16, and B-17, the approximations to the characteristic frequencies are given in terms of the matrix elements by

$$\omega_{sp}^2 = a_{11}a_{22} - a_{12}a_{21} + \frac{\left\{ \begin{aligned} & [a_{33} - a_{11}a_{22} + a_{12}a_{21} + (a_{11} + a_{22})(a_{11} + a_{22} - b_{33})]\Delta E \\ & - [(a_{11}a_{22} - a_{12}a_{21})(a_{33} - a_{11}a_{22} + a_{12}a_{21})]\Delta C \\ & - [(a_{11}a_{22} - a_{12}a_{21})(a_{11} + a_{22} - b_{33})]\Delta D \end{aligned} \right\}}{(a_{33} - a_{11}a_{22} + a_{12}a_{21})^2} + (a_{11} + a_{22} - b_{33})[(a_{11} + a_{22})a_{33} - b_{33}(a_{11}a_{22} - a_{12}a_{21})] \quad (B-19)$$

Contrails

$$\omega_{1e}^2 = a_{33} + \frac{\left\{ \begin{array}{l} -[a_{33} - a_{11}a_{22} + a_{12}a_{21} + b_{33}(a_{11} + a_{22} - b_{33})]\Delta E \\ + [a_{33}(a_{33} - a_{11}a_{22} + a_{12}a_{21})]\Delta C \\ + [a_{33}(a_{11} + a_{22} - b_{33})]\Delta D \end{array} \right\}}{\left\{ \begin{array}{l} (a_{33} - a_{11}a_{22} + a_{12}a_{21})^2 \\ + (a_{11} + a_{22} - b_{33}) [(a_{11} + a_{22})a_{33} - b_{33}(a_{11}a_{22} - a_{12}a_{21})] \end{array} \right\}} \quad (B-20)$$

$$\Delta C = -a_{31}b_{13} - a_{32}b_{23}$$

$$\Delta D = -a_{13}a_{31} - a_{23}a_{32} + a_{31}(a_{12}b_{23} - a_{22}b_{13}) + a_{32}(a_{21}b_{13} - a_{11}b_{23}) \quad (B-21)$$

$$\Delta E = a_{13}(a_{21}a_{32} - a_{22}a_{31}) - a_{23}(a_{11}a_{32} - a_{12}a_{31})$$

Equations B-19 and B-20 represent first-order corrected values for the squares of the short-period and first elastic-mode frequencies when $R_1(s)$ and $R_2(s)$ are added to $P(s)$ to give $\Delta(s)$ (Eq B-2). However, because Eq B-19 and B-20 are very unwieldy, it is desirable to simplify the two corrections. Subject to a reasonable set of validity conditions, some relatively simple relations can be found. Consider the following:

Dividing Eq B-14 by Eq B-15 gives

$$\frac{dy^2}{dx^2} = \frac{-(y^2 - x^2)(dE - y^2dC) - (\alpha - \beta)(\beta dE - y^2dD)}{(y^2 - x^2)(dE - x^2dC) + (\alpha - \beta)(\alpha dE - x^2dD)} \quad (B-22)$$

Dividing numerator and denominator by $(y^2 - x^2)(dE - x^2dC)$,

$$\frac{dy^2}{-dx^2} = \frac{\left(\frac{dE - y^2dC}{dE - x^2dC} \right) + \left(\frac{\alpha - \beta}{y^2 - x^2} \right) \left(\frac{\beta dE - y^2dD}{dE - x^2dC} \right)}{1 + \left(\frac{\alpha - \beta}{y^2 - x^2} \right) \left(\frac{\alpha dE - x^2dD}{dE - x^2dC} \right)} \quad (B-23)$$

This can be greatly simplified by making the following assumptions (which have been observed to be true in many instances):

$$y^2dC \ll dE$$

$$x^2dC \ll dE$$

Contrails

Equation B-23 then becomes

$$\frac{dy^2}{-dx^2} = \frac{1 + \left(\frac{\alpha - \beta}{y^2 - x^2}\right)\left(\beta - y^2 \frac{dD}{dE}\right)}{1 + \left(\frac{\alpha - \beta}{y^2 - x^2}\right)\left(\alpha - x^2 \frac{dD}{dE}\right)} \quad (\text{B-24})$$

The following assumptions have also proven to be quite reasonable and will further reduce the complexity of the approximation:

Further, assume
$$\left(\frac{\alpha - \beta}{y^2 - x^2}\right)\left(\beta - y^2 \frac{dD}{dE}\right) \ll 1$$

and
$$\left(\frac{\alpha - \beta}{y^2 - x^2}\right)\left(\alpha - x^2 \frac{dD}{dE}\right) \ll 1$$

whereby
$$dx^2 = -dy^2 \quad (\text{B-25})$$

Substituting Eq B-25 into Eq B-10 gives

$$dx^2 = -dy^2 = \frac{dE}{y^2 - x^2} \quad (\text{B-26})$$

Thus,
$$\omega_{sp}^2 = a_{11}a_{22} - a_{12}a_{21} + \frac{\Delta E}{a_{33} - a_{11}a_{22} + a_{12}a_{21}} \quad (\text{B-27})$$

and,
$$\omega_{1e}^2 = a_{33} - \frac{\Delta E}{a_{33} - a_{11}a_{22} + a_{12}a_{21}} \quad (\text{B-28})$$

Equations B-27 and B-28 are the desired simplifications of Eq B-19 and B-20.

The remaining task is to find corrections to the damping terms in Eq B-3. Because the frequency corrections are now known, either Eq B-8 or Eq B-9 can be solved directly for the two damping corrections which (Eq B-7) are simply of opposite sign. Because of the relative magnitudes of the quantities involved, it is presumed that Eq B-9 will give a more accurate result than will Eq B-8; accordingly,

$$d\beta = -d\alpha = \frac{-dD + \alpha dy^2 + \beta dx^2}{y^2 - x^2} \quad (\text{B-29})$$

Transforming back into the variables of interest, and replacing differentials with finite differences,

Contrails

$$(2\xi\omega)_{sp} \doteq a_{11} + a_{22} + \frac{\Delta D - (a_{11} + a_{22})\Delta y^2 - b_{33}\Delta x^2}{a_{33} - a_{11}a_{22} + a_{12}a_{21}} \quad (B-30)$$

$$(2\xi\omega)_{1e} \doteq b_{33} - \frac{\Delta D - (a_{11} + a_{22})\Delta y^2 - b_{33}\Delta x^2}{a_{33} - a_{11}a_{22} + a_{12}a_{21}} \quad (B-31)$$

where ΔD is given in Eq B-21 and Δx^2 and Δy^2 are the correction terms in Eq B-19 and B-20 or in B-27 and B-28.

It is now desirable to have a simpler expression for the damping correction. Using Eq B-25 in Eq B-29 gives

$$d\beta = -d\alpha \doteq \frac{-dD - (\alpha - \beta)dx^2}{y^2 - x^2} \quad (B-32)$$

Now Eq B-26 can be substituted into Eq B-32, giving

$$d\beta = -d\alpha \doteq \frac{-dD - \left(\frac{\alpha - \beta}{y^2 - x^2}\right)dE}{y^2 - x^2} \quad (B-33)$$

Therefore, Eq B-30 and B-31 can be written

$$(2\xi\omega)_{sp} \doteq a_{11} + a_{22} + \frac{\Delta D + \left(\frac{a_{11} + a_{22} - b_{33}}{a_{33} - a_{11}a_{22} + a_{12}a_{21}}\right)\Delta E}{a_{33} - a_{11}a_{22} + a_{12}a_{21}} \quad (B-34)$$

and

$$(2\xi\omega)_{1e} \doteq b_{33} - \frac{\Delta D + \left(\frac{a_{11} + a_{22} - b_{33}}{a_{33} - a_{11}a_{22} + a_{12}a_{21}}\right)\Delta E}{a_{33} - a_{11}a_{22} + a_{12}a_{21}} \quad (B-35)$$

The following is a summary of validity conditions which allow use of the simple approximations given by Eq B-27, B-28, B-34, and B-35. If these validity conditions are not satisfied, then Eq B-19, B-20, B-30, and B-31 must be used; in this case only the first validity condition listed below is necessary.

Validity Conditions

1. The correction terms are all small (on a percent basis).

$$2. \left| \frac{a_{33}\Delta C}{\Delta E} \right| \ll 1 \quad \text{and} \quad \left| \frac{(a_{11}a_{22} - a_{12}a_{21})\Delta C}{\Delta E} \right| \ll 1$$

$$3. \left| \left[\frac{a_{11} + a_{22} - b_{33}}{a_{33} - a_{11}a_{22} + a_{12}a_{21}} \right] \left[b_{33} - a_{33} \frac{\Delta D}{\Delta E} \right] \right| \ll 1$$

and

$$\left| \left[\frac{a_{11} + a_{22} - b_{33}}{a_{33} - a_{11}a_{22} + a_{12}a_{21}} \right] \left[a_{11} + a_{22} - (a_{11}a_{22} - a_{12}a_{21}) \frac{\Delta D}{\Delta E} \right] \right| \ll 1$$

The method described above is directly applicable to the case where the equations of motion include 3 degrees of freedom. If 4 degrees of freedom are included, a similar technique can be used, but must be applied twice—once to get approximate factors for the upper left 3 x 3 part of the 4 x 4 determinant, and once again to correct these factors.

B. APPROXIMATE FACTORS FOR HIGHLY COUPLED SYSTEMS

The fundamentals of this method can be summarized briefly as follows. First, the exact factors (in numerical terms) must be known for a case where the parameters in the equations of motion take on typical values. Then, approximate literal factors (in terms of the polynomial coefficients) are found by solving the simultaneous equations which relate factors and polynomial coefficients; in this process, numerically small terms have had to be neglected. Then, because the polynomial coefficients are defined in terms of the stability derivatives in the equations of motion, the approximate factors can also be expressed in these terms. A more detailed description of this method is best presented in the form of a set of instructions. Although a transfer function denominator is considered in the following set of instructions, the method is also applicable for finding numerator factors:

1. obtain exact transfer function factors in numerical terms for a typical set of parameter values

Contrails

2. assume the denominator of the transfer function factors as (e.g., for a sixth-order denominator)

$$\begin{aligned} s^6 + Bs^5 + Cs^4 + Ds^3 + Es^2 + Fs + G &= \left[s^2 + (2\zeta\omega)_{sp}s + \omega_{sp}^2 \right] \\ &\times \left[s^2 + (2\zeta\omega)_{1e}s + \omega_{1e}^2 \right] \\ &\times \left[s^2 + (2\zeta\omega)_{2e}s + \omega_{2e}^2 \right] \end{aligned}$$

3. expand the factors in Step 2, and match coefficients of s , giving six equations in six unknowns to solve
4. throw away those terms in Step 3 that are very small (by knowing exact numbers)
5. solve simplified equations (from Step 4) for $(2\zeta\omega)_{sp}$, ω_{sp}^2 , etc., in terms of B , C , D , E , F , and G . This gives approximate frequency and damping terms as functions of polynomial coefficients
6. expand the determinant of coefficients in the equations of motion in literal terms
7. match coefficients of s from Step 6 with those in the polynomial on the left side of the equation in Step 2
8. throw away terms that are very small (by knowing exact numbers) in Step 7. This gives approximate expressions for the polynomial coefficients in terms of coefficients in the equations of motion
9. combine results of Steps 5 and 8 to get approximate expressions for frequency and damping terms as functions of coefficients in the equations of motion.

The applicability of this method is contingent on one being able to solve the equations in Step 5; these equations proved to be solvable in all cases considered in this study.

APPENDIX C

DESCRIPTION OF CONFIGURATIONS

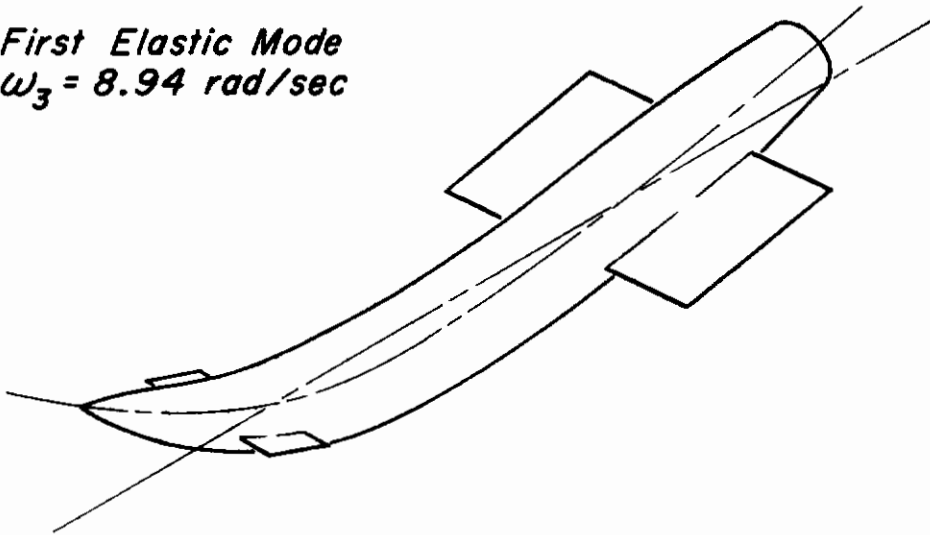
The data presented in this appendix describe the vehicles and the flight conditions which were investigated. No data are shown for Configuration 1 because the study of that vehicle was discontinued early in the project.

The information necessary for the calculation of the aerodynamic matrices may be found in Table C-I (the aerodynamic parameters), and Table C-VIII (the flight conditions). Tables C-II, C-III, and C-IV present the mode shapes and slopes for the three configurations, and Tables C-V, C-VI, and C-VII present the $[X_{(f+\infty)}]$ matrices. A profile view of each airframe with the control surfaces shown may be found in Fig. C-4 through C-8.

TABLE C-1
DESCRIPTION OF CONFIGURATIONS

ITEM	CONFIGURATION 2 MISSILE WITH CANARD AND LOW ASPECT RATIO WING	CONFIGURATION 3 HIGH ASPECT RATIO, SWEEPING AIRPLANE	CONFIGURATION 4 DELTA WING AIRPLANE
Planform	Fig. C-1	Fig. C-2	Fig. C-4
Total mass (slugs)	9324	3902	4656
Total pitch inertia (slug-ft ²)	5.833 x 10 ⁶	1.692 x 10 ⁶	1.246 x 10 ⁶
Body flexible in bending	Yes	Yes	Yes
Wing spanwise bending (no chordwise bending consid.)	No	Yes	Yes
Lifting surfaces	Canard and wing, Fig. C-4	Six rigid wing strips and horizontal tail, Fig. C-6	Five rigid wing strips one symmetrical about δ , Fig. C-7
Control	Canard at fuselage sta. 250	All-movable elevators at fuselage sta. 1100	Elevons
c.p.	Mid-chord	Quarter-chord	Mid-chord
Lift on each surface	←	→	→
Moment on lifting surface	$\frac{1}{4} \rho U_0^2 S c^2 C_{m\dot{\theta}}$	$-\frac{1}{2} \rho U_0^2 S C_{L\alpha} \left(\theta + \frac{h}{U_0} + \frac{d\alpha}{d\delta} \delta \right)$	$\frac{1}{2} \rho U_0^2 S c \left(\frac{c}{2U_0} C_{m\dot{\theta}} \dot{\theta} - 0.64\delta \right)$
$d\alpha/d\delta$	1.0 for canard	1.0 for elevators	0.505 for elevons
Downwash	No	$\frac{d\epsilon}{d\alpha} = 0.6$ (for inner wing strips on elevators)	No
$C_{L\alpha}$	1.5	6.0	5.0
$C_{m\dot{\theta}}$	$-\frac{\pi}{4}$	$-\frac{\pi}{4}$	$-\frac{\pi}{4}$

First Elastic Mode
 $\omega_3 = 8.94 \text{ rad/sec}$



Second Elastic Mode
 $\omega_4 = 21.45 \text{ rad/sec}$

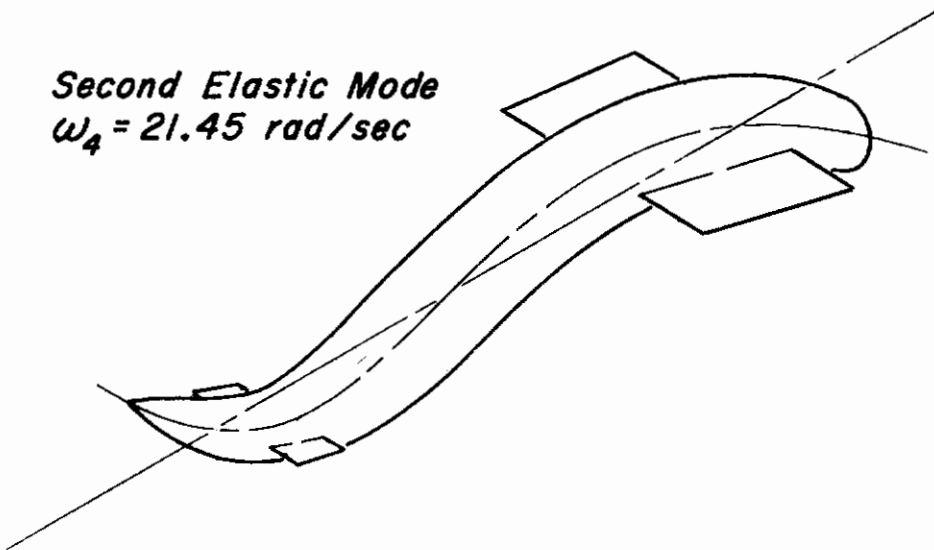
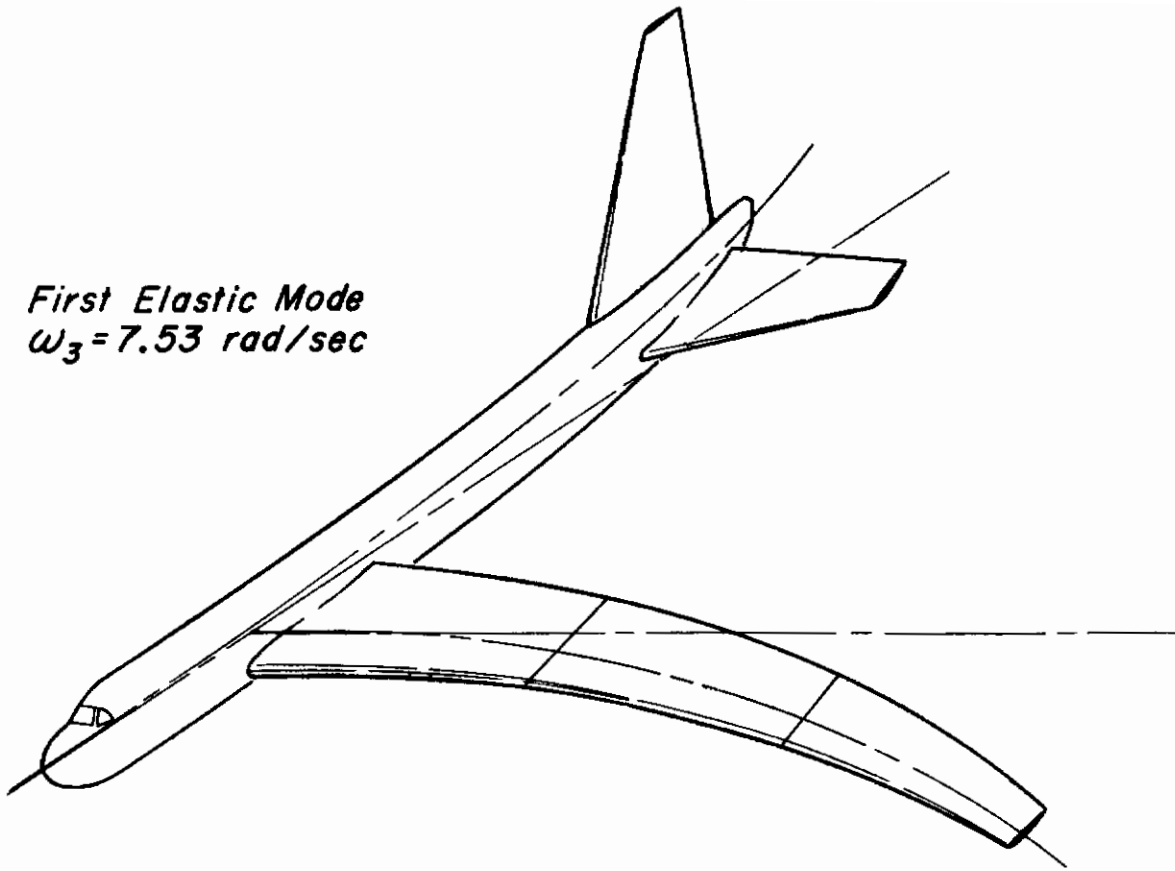


FIGURE C-1. ELASTIC MODES FOR CONFIGURATION 2

TABLE C-II
MODE SHAPES AND FREQUENCIES
CONFIGURATION 2

MODE NO.	1	2	3	4
FREQUENCY, cps	0	0	1.421	3.42
<u>Mode Deflections</u>				
Canard	1.0	-453	-0.0241	0.0464
Wing	1.0	197	0.00418	-0.0388
<u>Mode Slopes</u>				
Canard	0	1.0	0.000432	0.000262
Wing	0	1.0	-0.000158	0.000188

First Elastic Mode
 $\omega_3 = 7.53 \text{ rad/sec}$



Second Elastic Mode
 $\omega_4 = 27.02 \text{ rad/sec}$

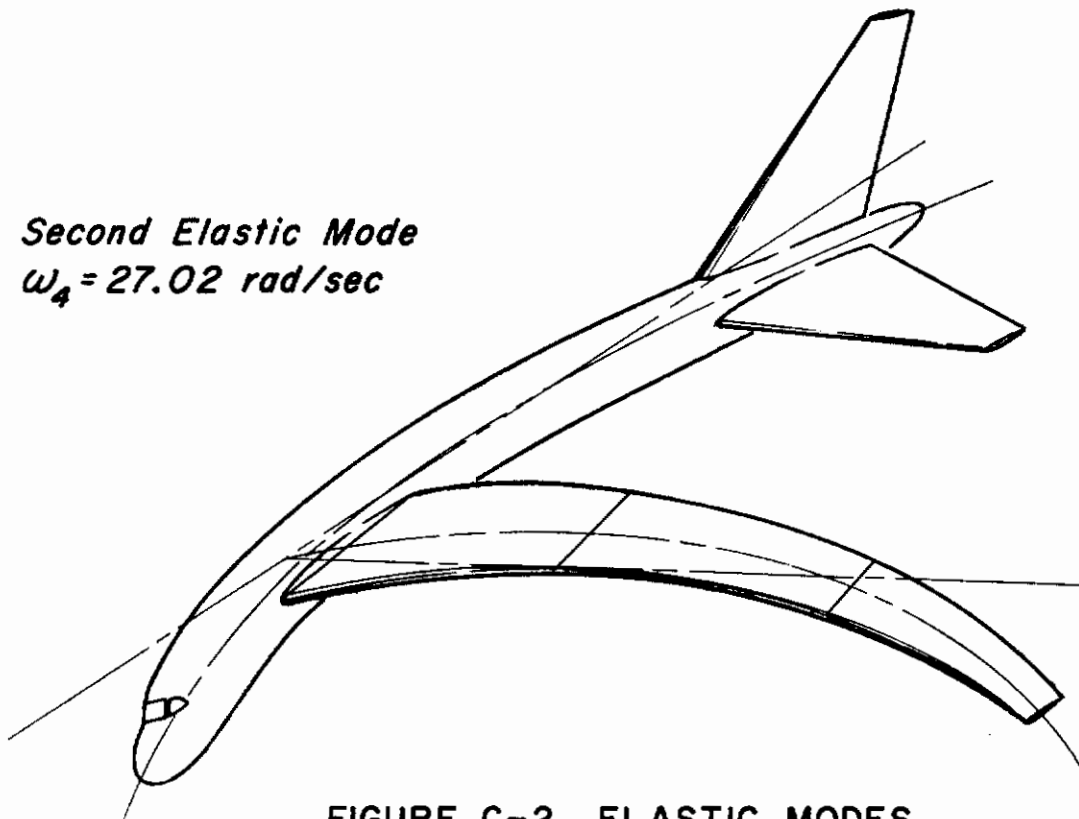
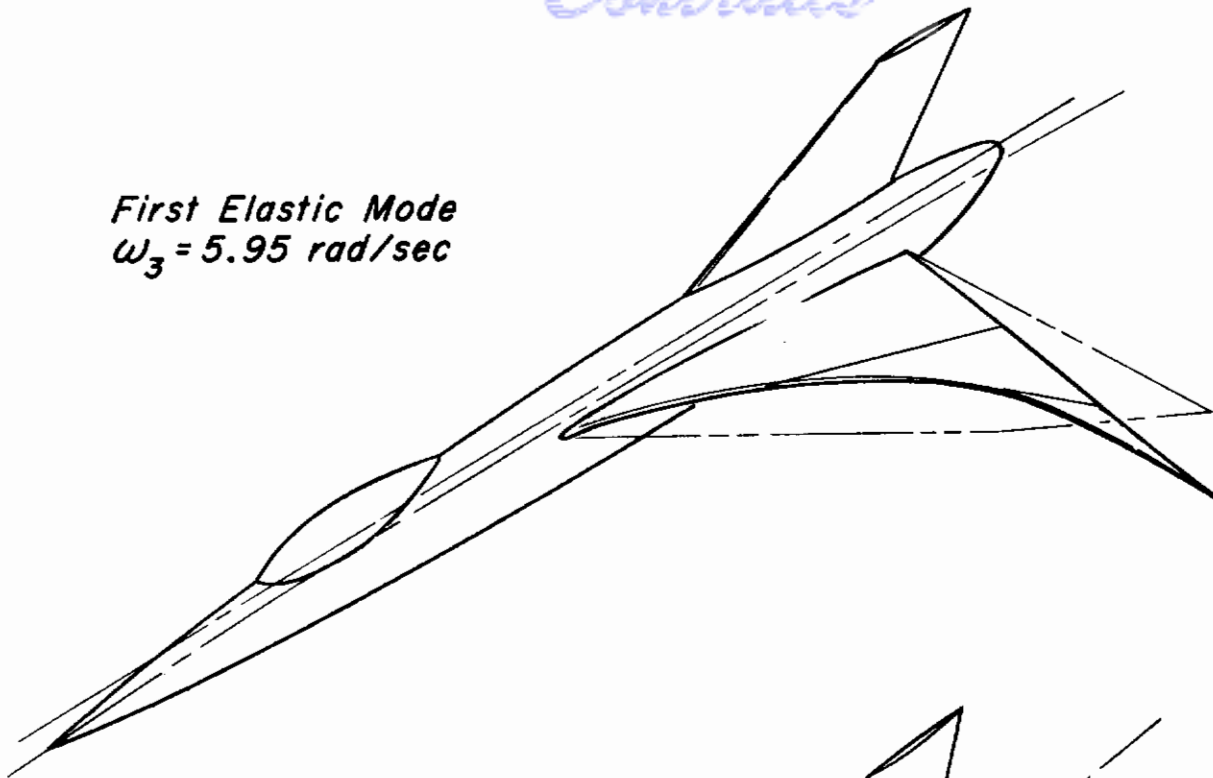


**FIGURE C-2. ELASTIC MODES
FOR CONFIGURATION 3**

TABLE C-III
MODE SHAPES AND FREQUENCIES
CONFIGURATION 3

MODE NO.	1	2	3	4
FREQUENCY, cps	0	0	1.199	4.3
<u>Mode Deflections</u>				
Tail	1.0	573	-0.0592	0.130
1/4 Chord Strip I	1.0	-120	-0.00976	-0.0212
1/4 Chord Strip II	1.0	44.3	0.0455	-0.0749
1/4 Chord Strip III	1.0	208	0.178	0.0283
<u>Mode Slopes</u>				
Tail	0	1.0	-0.0863×10^{-3}	0.707×10^{-3}
Stream Slope Strip I	0	1.0	0.0197×10^{-3}	-0.204×10^{-3}
Stream Slope Strip II	0	1.0	0.159×10^{-3}	0.168×10^{-3}
Stream Slope Strip III	0	1.0	0.262×10^{-3}	0.580×10^{-3}

First Elastic Mode
 $\omega_3 = 5.95 \text{ rad/sec}$



Second Elastic Mode
 $\omega_4 = 7.74 \text{ rad/sec}$

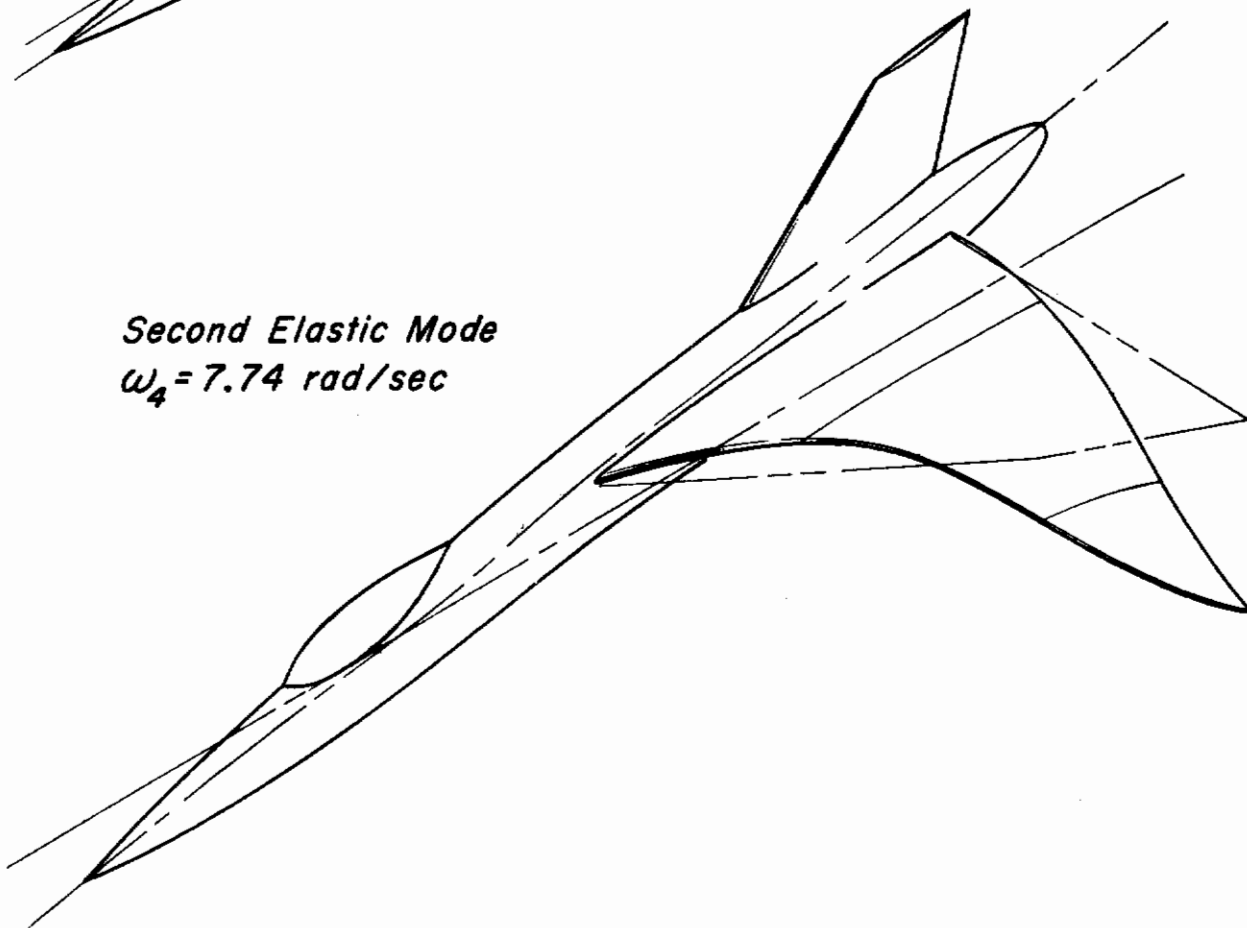


FIGURE C-3. ELASTIC MODES FOR CONFIGURATION 4

TABLE C-IV
 MODE SHAPES AND FREQUENCIES
 CONFIGURATION 4

MODE NO.	1	2	3	4
FREQUENCY, cps	0	0	0.948	1.231
<u>Mode Deflections</u>				
1/4 Chord Strip I	1.0	-50.0	0.0122	-0.0258
1/4 Chord Strip II	1.0	25.0	-0.00385	-0.0143
1/4 Chord Strip III	1.0	100	-0.0410	0.0644
3/4 Chord Strip I	1.0	150	0.0133	-0.0477
3/4 Chord Strip II	1.0	175	0.0241	0.00212
3/4 Chord Strip III	1.0	200	0.0682	0.115

TABLE C-V

$$\left[X(f+\infty) \right] \times 10^6$$

CONFIGURATION 2

	Canard Deflection	Wing Deflection	Canard Slope	Wing Slope
Canard Deflection	39	-2.932	-0.12	0.06712
Wing Deflection	-2.932	19.55	0.003890	-0.02532
Canard Slope	-0.12	0.003890	0.00321	-0.0007384
Wing Slope	0.06712	-0.02532	-0.0007384	0.00302

TABLE C-VI
 $\left[X_{(f+\infty)} \right] \times 10^6$
 CONFIGURATION 3

	Tail Deflection	1/4 Chord Strip I	1/4 Chord Strip II	1/4 Chord Strip III	Tail Slope	Stream Slope Strip I	Stream Slope Strip II	Stream Slope Strip III
Tail Deflection	124.5	6.765	-60.15	-200.0	0.3783	-0.0803	-0.2200	-0.3307
1/4 Chord Strip I	6.765	6.300	-5.145	-31.56	0.00354	0.0072	-0.00844	-0.02560
1/4 Chord Strip II	-60.15	-5.145	89.5	157.1	-0.09525	0.0825	0.1720	0.1327
1/4 Chord Strip III	-200.0	-31.56	157.1	628.5	-0.2786	0.0712	0.564	1.0475
Tail Slope	0.3783	0.00354	-0.09525	-0.2786	0.002842	-0.0003079	-0.0004855	-0.000620
Stream Slope Strip I	-0.0803	0.0072	0.0825	0.0712	-0.0003079	0.000785	0.000737	0.000603
Stream Slope Strip II	-0.2200	-0.00844	0.1720	0.564	-0.0004855	0.000737	0.003865	0.003730
Stream Slope Strip III	-0.3307	-0.02560	0.1327	1.0475	-0.000620	0.000603	0.003730	0.01744

TABLE C-VII

$$\left[X_{(f+\infty)} \right] \times 10^6$$

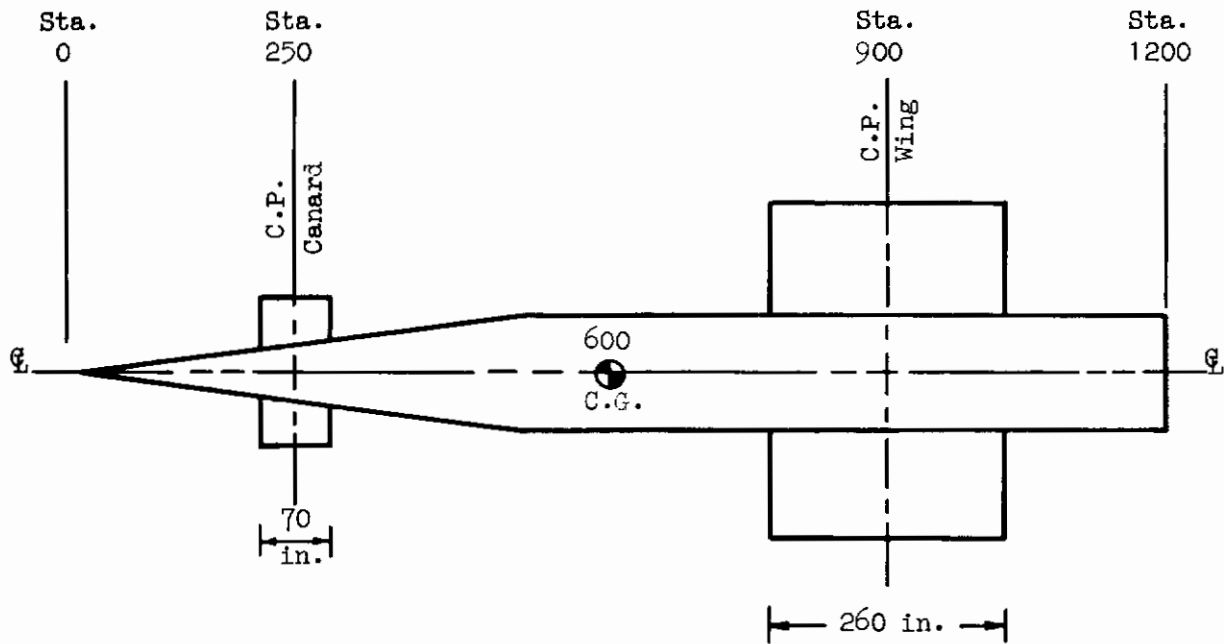
CONFIGURATION 4

	1/4 Chord Strip I	1/4 Chord Strip II	1/4 Chord Strip III	3/4 Chord Strip I	3/4 Chord Strip II	3/4 Chord Strip III
1/4 Chord Strip I	24.63	10.39	-42.03	21.98	3.852	-25.48
1/4 Chord Strip II	10.39	60.3	-11.40	7.81	-3.093	-34.51
1/4 Chord Strip III	-42.03	-11.40	117.2	-66.85	-25.63	45.50
3/4 Chord Strip I	21.98	7.81	-66.85	45.39	7.39	-66.75
3/4 Chord Strip II	3.852	-3.093	-25.63	7.39	66.25	50.2
3/4 Chord Strip III	-25.48	-34.51	45.50	-66.75	50.2	353.6

TABLE C-VIII
FLIGHT CONDITIONS

CONFIGURATION	DYNAMIC PRESSURE, psf	FORWARD SPEED, ft/sec	MACH NO.	ALTITUDE, ft
2	5,050	2,060	1.84	0
	12,960	3,300	2.96	0
3	639	1,003	0.97	20,000
	1,197	1,003	0.90	0
4	858	2,430	2.37	22,500
	1,717	2,430	2.50	40,000
	4,250	2,490	2.50	20,000

Contrails



Note: Stations shown in inches

Area of canard (total for both sides) = 7000 in.²

Area of wing (total for both sides) = 62,400 in.²

Figure C-4. Configuration 2

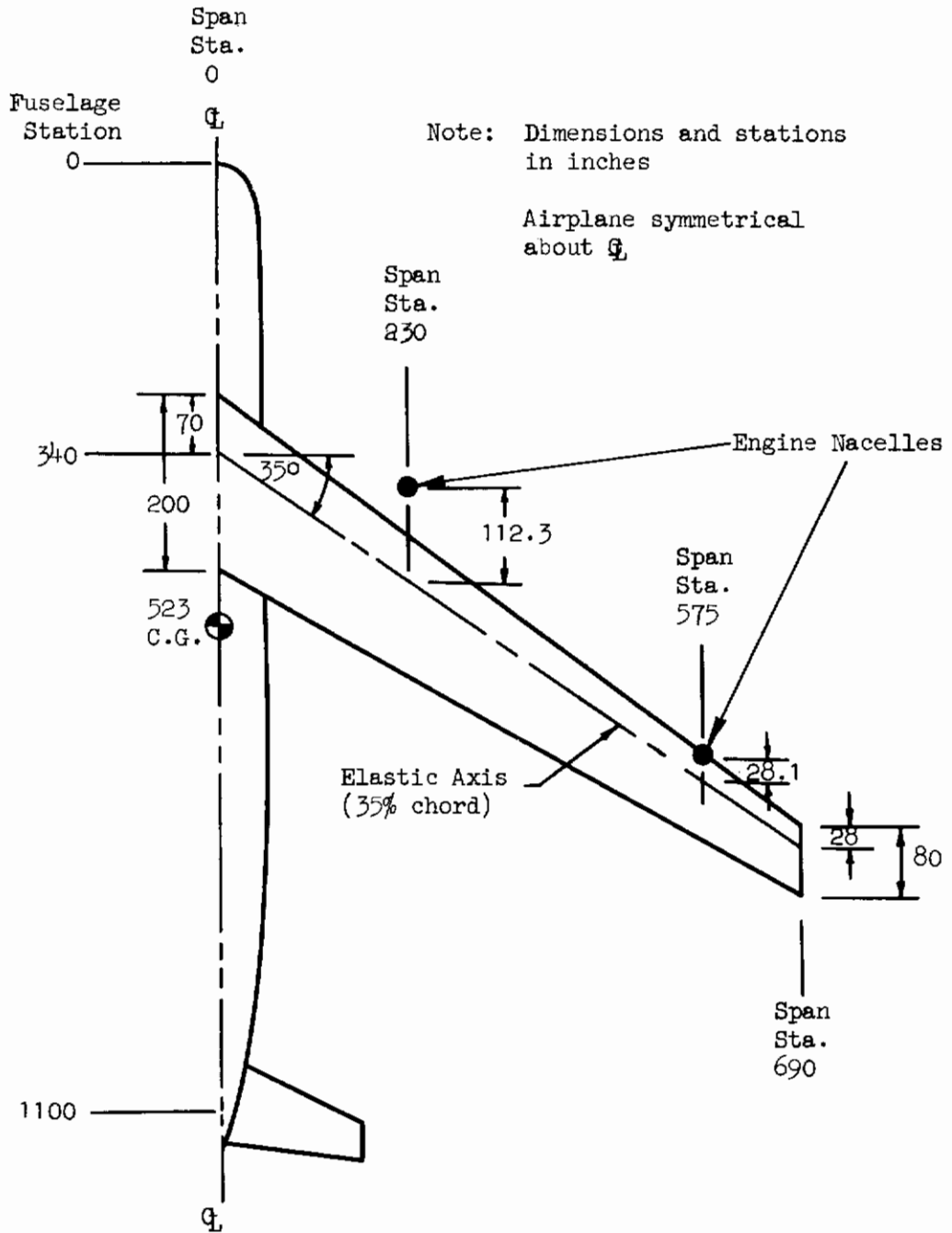


Figure C-5. Configuration 3

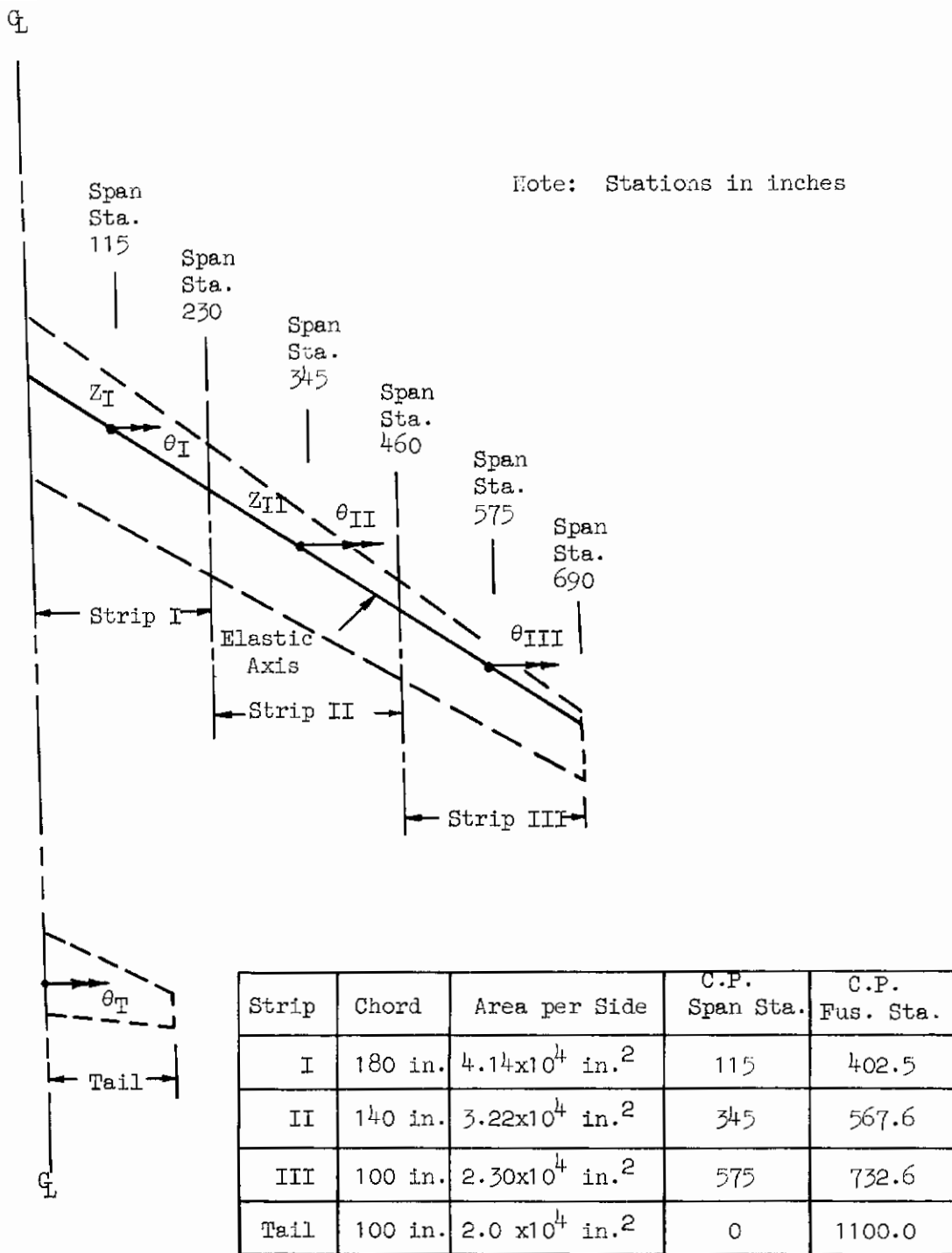


Figure C-6. Aerodynamic Strips for Configuration 3

Contours

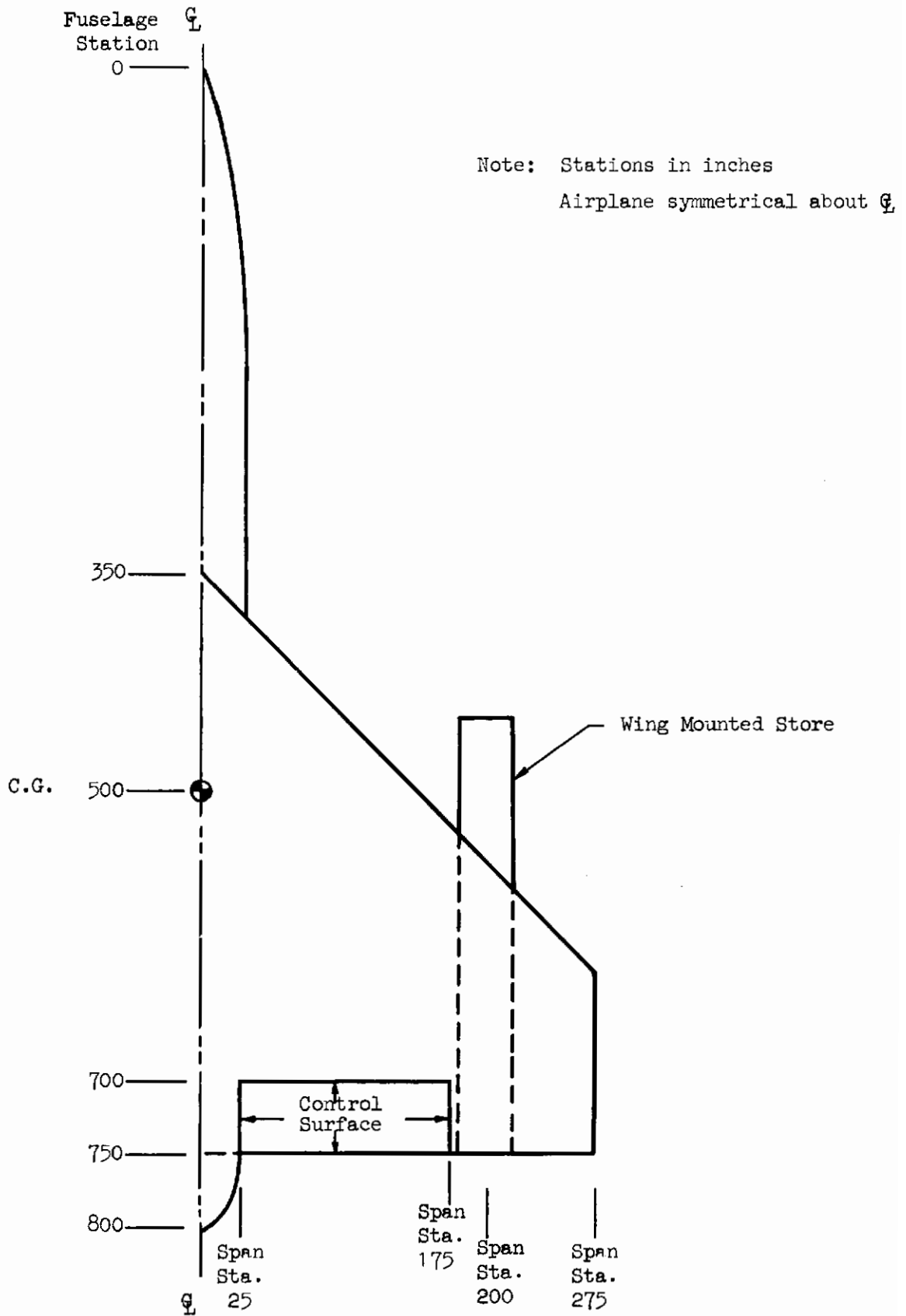


Figure C-7. Configuration 4

Contours

Strip	Chord	Area per side	Span Sta. of C.P.
I	400 in.	20,000 in. ²	0
II	300 in.	30,000 in. ²	100
III	200 in.	20,000 in. ²	200
Control Surface	50 in.	7,500 in. ²	-

Note: Stations in inches

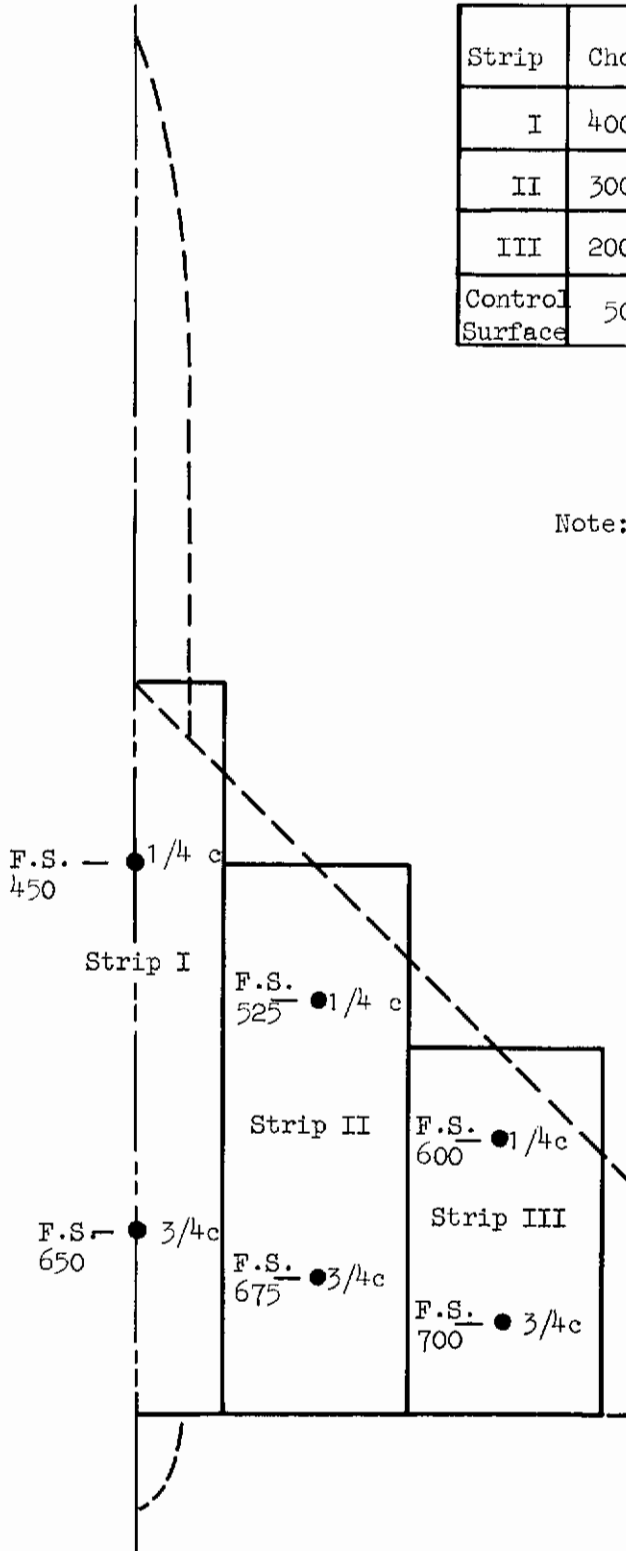


Figure C-8. Aerodynamic Strips for Configuration 4

APPENDIX D

NUMERICAL EQUATIONS OF MOTION, APPROXIMATE FACTORS AND EXACT FACTORS

This appendix presents the majority of the numerical data for the report. The numerical equations of motion of the three vehicles are given in Fig. D-1, D-2, and D-3, and include the static aeroelastic correction for the modes not included. Tables D-I, D-II, and D-III present the exact factors for the equations and the values obtained with the approximation formulas presented in Section III.

$q = 35.0 \text{ psi}$

THREE
DEGREES
OF
FREEDOM

$$\begin{bmatrix} s + 0.1982 & -24680 & 0.001375s - 0.519 \\ 0.0002885 & s + 0.141 & -0.000001097s - 0.002567 \\ 0.202 & -111.0 & s^2 + 0.0696s + 73.65 \end{bmatrix} \begin{bmatrix} w \\ \dot{\theta} \\ \xi_3 \end{bmatrix} = \begin{bmatrix} -4388 \\ 2.4358 \\ 89208 \end{bmatrix}$$

FOUR
DEGREES
OF
FREEDOM

$$\begin{bmatrix} s + 0.1912 & -24680 & 0.001152s - 0.4673 & -0.005664s + 0.9237 \\ 0.0002805 & s + 0.1407 & -0.000001380s - 0.002511 & -0.00001367s + 0.001126 \\ 0.2002 & -111.9 & s^2 + 0.06954s + 73.67 & -0.1088s + 0.272 \\ -3.974 & -657.7 & -0.1094s + 25.47 & s^2 + 0.3028s + 443.8 \end{bmatrix} \begin{bmatrix} w \\ \dot{\theta} \\ \xi_3 \\ \xi_4 \end{bmatrix} = \begin{bmatrix} -474.58 \\ 2.4038 \\ 89118 \\ -168806 \end{bmatrix}$$

$q = 90.0 \text{ psi}$

THREE
DEGREES
OF
FREEDOM

$$\begin{bmatrix} s + 0.347 & -39560 & 0.01519s - 1.605 \\ 0.000502 & s + 0.0749 & 0.0000245s - 0.00700 \\ 0.344 & -395 & s^2 + 0.148s + 63.86 \end{bmatrix} \begin{bmatrix} w \\ \dot{\theta} \\ \xi_3 \end{bmatrix} = \begin{bmatrix} -9778 \\ 6.538 \\ 232108 \end{bmatrix}$$

FOUR
DEGREES
OF
FREEDOM

$$\begin{bmatrix} s + 0.3115 & -39630 & 0.01252s - 1.223 & -0.02193s + 2.406 \\ 0.0004594 & s + 0.08077 & 0.00002126s - 0.006551 & -0.00005021s + 0.002949 \\ 0.3334 & -395.5 & s^2 + 0.1470s + 63.97 & -0.2174s + 0.7557 \\ -6.495 & 742.3 & -0.4656s + 66.47 & s^2 + 0.8552s + 416.0 \end{bmatrix} \begin{bmatrix} w \\ \dot{\theta} \\ \xi_3 \\ \xi_4 \end{bmatrix} = \begin{bmatrix} -12268 \\ 6.2458 \\ 231308 \\ -439408 \end{bmatrix}$$

Figure D-1. Equations of Motion in Numerical Terms
Configuration 2

$q = 4.43 \text{ psi}$

$$\begin{bmatrix} s + 1.257 \\ 0.001205 \\ 17.44 \end{bmatrix} \begin{bmatrix} -11800 \\ s + 1.539 \\ 2191 \end{bmatrix} \begin{bmatrix} 0.04428s + 1.395 \\ 0.0000927s + 0.00161 \\ s^2 + 3.211s + 119.7 \end{bmatrix} \begin{bmatrix} w \\ \dot{\theta} \\ \xi_3 \end{bmatrix} = \begin{bmatrix} -30576 \\ -22.526 \\ 371808 \end{bmatrix}$$

THREE
DEGREES
OF
FREEDOM

$$\begin{bmatrix} s + 1.227 \\ 0.0009635 \\ 16.69 \\ -6.224 \end{bmatrix} \begin{bmatrix} 0.04180s + 1.195 \\ 0.00007589s + 0.000665 \\ s^2 + 3.153s + 115.4 \\ -0.4043s - 19.75 \end{bmatrix} \begin{bmatrix} 0.02489s + 4.099 \\ 0.0004958s + 0.03247 \\ 0.005064s + 100.4 \\ s^2 + 2.771s + 835.6 \end{bmatrix} \begin{bmatrix} w \\ \dot{\theta} \\ \xi_3 \\ \xi_4 \end{bmatrix} = \begin{bmatrix} -36106 \\ -26.908 \\ 236308 \\ -1127008 \end{bmatrix}$$

FOUR
DEGREES
OF
FREEDOM

$q = 8.31 \text{ psi}$

$$\begin{bmatrix} s + 2.149 \\ 0.002094 \\ 28.74 \end{bmatrix} \begin{bmatrix} -11650 \\ s + 2.513 \\ 3636 \end{bmatrix} \begin{bmatrix} 0.06095s + 2.204 \\ 0.000169s + 0.003648 \\ s^2 + 4.988s + 160.1 \end{bmatrix} \begin{bmatrix} w \\ \dot{\theta} \\ \xi_3 \end{bmatrix} = \begin{bmatrix} -54048 \\ -35.088 \\ 482708 \end{bmatrix}$$

THREE
DEGREES
OF
FREEDOM

$$\begin{bmatrix} s + 2.067 \\ 0.001433 \\ 26.49 \\ -10.63 \end{bmatrix} \begin{bmatrix} -11560 \\ s + 3.168 \\ 5866 \\ 10550 \end{bmatrix} \begin{bmatrix} 0.05651s + 1.794 \\ 0.0001367s + 0.00133 \\ s^2 + 4.870s + 149.6 \\ -0.4816s - 30.34 \end{bmatrix} \begin{bmatrix} 0.04663s + 7.021 \\ 0.000830s + 0.05643 \\ 0.3510s + 192.6 \\ s^2 + 4.564s + 907.8 \end{bmatrix} \begin{bmatrix} w \\ \dot{\theta} \\ \xi_3 \\ \xi_4 \end{bmatrix} = \begin{bmatrix} -68296 \\ -46.536 \\ 91808 \\ -1843008 \end{bmatrix}$$

FOUR
DEGREES
OF
FREEDOM

Figure D-2. Equations of Motion in Numerical Terms
Configuration 3

$q = 5.95 \text{ psi}$

THREE DEGREES OF FREEDOM	$\begin{bmatrix} s + 0.3390 \\ 0.000840 \\ 1.546 \end{bmatrix}$	$\begin{bmatrix} -31050 \\ s + 0.1802 \\ 419.9 \end{bmatrix}$	$\begin{bmatrix} 0.005953s + 2.613 \\ 0.00003061s + 0.00870 \\ s^2 + 0.1880s + 48.50 \end{bmatrix}$	$\begin{bmatrix} \dot{w} \\ \dot{\theta} \\ \xi_3 \end{bmatrix} = \begin{bmatrix} -16308 \\ -6.5668 \\ -128208 \end{bmatrix}$
FOUR DEGREES OF FREEDOM	$\begin{bmatrix} s + 0.3487 \\ 0.0008798 \\ 1.5940 \\ 1.076 \end{bmatrix}$	$\begin{bmatrix} 0.007856s + 3.380 \\ s + 0.1934 \\ 435.9 \\ 356.2 \end{bmatrix}$	$\begin{bmatrix} 0.001562s + 1.202 \\ 0.00002284s + 0.00496 \\ s^2 + 0.1975s + 52.33 \\ 0.2122s + 85.52 \end{bmatrix}$	$\begin{bmatrix} \dot{w} \\ \dot{\theta} \\ \xi_3 \\ \xi_4 \end{bmatrix} = \begin{bmatrix} -16168 \\ -6.5096 \\ -127508 \\ 15538 \end{bmatrix}$

$q = 11.9 \text{ psi}$

THREE DEGREES OF FREEDOM	$\begin{bmatrix} s + 0.7401 \\ 0.001804 \\ 3.355 \end{bmatrix}$	$\begin{bmatrix} -29080 \\ s + 0.3021 \\ 771.0 \end{bmatrix}$	$\begin{bmatrix} 0.005818s + 4.174 \\ 0.0000428s + 0.01301 \\ s^2 + 0.3679s + 56.31 \end{bmatrix}$	$\begin{bmatrix} \dot{w} \\ \dot{\theta} \\ \xi_3 \end{bmatrix} = \begin{bmatrix} -15836 \\ -8.7158 \\ -187808 \end{bmatrix}$
FOUR DEGREES OF FREEDOM	$\begin{bmatrix} s + 0.7579 \\ 0.001879 \\ 3.446 \\ 1.555 \end{bmatrix}$	$\begin{bmatrix} -29080 \\ s + 0.3335 \\ 808.9 \\ 652.9 \end{bmatrix}$	$\begin{bmatrix} 0.01004s + 5.737 \\ 0.00006047s + 0.01956 \\ s^2 + 0.3892s + 64.21 \\ 0.3672s + 135.8 \end{bmatrix}$	$\begin{bmatrix} \dot{w} \\ \dot{\theta} \\ \xi_3 \\ \xi_4 \end{bmatrix} = \begin{bmatrix} -15888 \\ -8.7358 \\ -188108 \\ -403.78 \end{bmatrix}$

$q = 29.5 \text{ psi}$

THREE DEGREES OF FREEDOM	$\begin{bmatrix} s + 2.055 \\ 0.004956 \\ 9.199 \end{bmatrix}$	$\begin{bmatrix} -31160 \\ s + 0.1198 \\ 880.8 \end{bmatrix}$	$\begin{bmatrix} -0.027772s + 8.580 \\ -0.00001777s + 0.02345 \\ s^2 + 0.6848s + 77.75 \end{bmatrix}$	$\begin{bmatrix} \dot{w} \\ \dot{\theta} \\ \xi_3 \end{bmatrix} = \begin{bmatrix} 122308 \\ 20.308 \\ 193608 \end{bmatrix}$
FOUR DEGREES OF FREEDOM	$\begin{bmatrix} s + 2.053 \\ 0.004969 \\ 9.208 \\ 0.7114 \end{bmatrix}$	$\begin{bmatrix} -31150 \\ s + 0.1953 \\ 967.0 \\ 1414 \end{bmatrix}$	$\begin{bmatrix} -0.02046s + 11.03 \\ 0.00001466s + 0.03459 \\ s^2 + 0.7189s + 90.80 \\ 0.6127s + 208.3 \end{bmatrix}$	$\begin{bmatrix} \dot{w} \\ \dot{\theta} \\ \xi_3 \\ \xi_4 \end{bmatrix} = \begin{bmatrix} 117708 \\ 18.428 \\ 171608 \\ -331408 \end{bmatrix}$

Figure D-3. Equations of Motion in Numerical Terms
Configuration 4

Contrails

TABLE D-I
 NUMERICAL VALUES FOR EXACT AND APPROXIMATE TRANSFER FUNCTION FACTORS
 CONFIGURATION 2

Transfer Function Factor	q = 35.0 psi				q = 90.0 psi			
	3 Modes		4 Modes		3 Modes		4 Modes	
	Approx.	Exact	Approx.	Exact	Approx.	Exact	Approx.	Exact
ω_{sp}^2	7.31	7.33	7.36	7.40	22.0	22.1	21.9	22.4
$(2\zeta\omega)_{sp}$.335	.338	.328	.336	.379	.373	.336	.309
ω_{1e}^2	73.5	73.5	73.5	73.5	61.7	61.6	62.1	61.5
$(2\zeta\omega)_{1e}$.074	.072	.074	.080	.200	.196	.204	.276
ω_{2e}^2	-	-	444	444	-	-	416	414
$(2\zeta\omega)_{2e}$	-	-	.303	.288	-	-	.835	.790
$1/T_{w1}$	-137	-137	-125	-125	-264	-264	-202	-201
ω_{w1}^2	83.0	83.0	83.0	83.0	88.8	88.7	88.2	88.9
$(2\zeta\omega)_{w1}$.219	.219	.219	.219	.299	.299	.302	.298
ω_{w2}^2	-	-	452	451	-	-	437	437
$(2\zeta\omega)_{w2}$	-	-	.532	.531	-	-	1.01	1.03
$1/T_{\theta1}$.236	.242	.240	.241	.377	.381	.377	.381
$\omega_{\theta1}^2$	83.1	83.2	83.0	83.1	88.8	88.7	88.2	89.0
$(2\zeta\omega)_{\theta1}$.084	.084	.085	.085	.104	.104	.107	.104
$\omega_{\theta2}^2$	-	-	452	452	-	-	437	436
$(2\zeta\omega)_{\theta2}$	-	-	.207	.202	-	-	.482	.466
$\omega_{\xi31}^2$	5.77	5.85	5.84	5.85	16.2	16.2	16.5	16.3
$(2\zeta\omega)_{\xi31}$.370	.382	.373	.386	.533	.551	.517	.558
$\omega_{\xi32}^2$	-	-	444	444	-	-	416	416
$(2\zeta\omega)_{\xi32}$	-	-	.086	.084	-	-	.405	.381
$1/T_{\xi41}$	-	-	-2.43	-2.39	-	-	-3.99	-3.62
$1/T_{\xi42}$	-	-	2.63	2.71	-	-	4.26	4.19
$\omega_{\xi42}^2$	-	-	87.6	86.5	-	-	101	95.9
$(2\zeta\omega)_{\xi42}$	-	-		.0370	-	-		.0150

TABLE D-II
 NUMERICAL VALUES FOR EXACT AND APPROXIMATE TRANSFER FUNCTION FACTORS
 CONFIGURATION 3

Transfer Function Factor	q = 4.43 psi				q = 8.31 psi			
	3 Modes		4 Modes		3 Modes		4 Modes	
	Approx.	Exact	Approx.	Exact	Approx.	Exact	Approx.	Exact
ω_{sp}^2	13.05	12.78	12.6	13.2	21.2	19.6	21.0	21.1
$(2\xi\omega)_{sp}$	2.43	2.38	2.46	2.42	3.61	3.84	3.97	3.85
ω_{1e}^2	123	123	120	121	170	169	163	166
$(2\xi\omega)_{1e}$	3.58	3.62	3.64	3.65	6.03	5.86	6.03	6.00
ω_{2e}^2	-	-	836	827	-	-	908	884
$(2\xi\omega)_{2e}$	-	-	2.77	2.86	-	-	4.56	4.82
$1/T_{w1}$	88.7	89.0	91.5	90.8	78.2	78.3	85.2	83.5
ω_{w1}^2	122	122	118	121	165	166	157	163
$(2\xi\omega)_{w1}$	3.55	3.53	3.47	3.58	5.47	5.43	5.69	5.62
ω_{w2}^2	-	-	699	688	-	-	684	664
$(2\xi\omega)_{w2}$	-	-	.593	.588	-	-	1.02	1.12
$1/T_{\theta1}$.920	.910	.924	.918	1.53	1.51	1.54	1.53
$\omega_{\theta1}^2$	122	122	118	121	165	165	157	163
$(2\xi\omega)_{\theta1}$	3.57	3.55	3.47	3.60	5.62	5.54	5.69	5.73
$\omega_{\theta2}^2$	-	-	699	695	-	-	684	673
$(2\xi\omega)_{\theta2}$	-	-	.593	.496	-	-	1.02	.780
$\omega_{\xi31}^2$	127	145	124	135	251	286	230	228
$(2\xi\omega)_{\xi31}$	5.56	5.56	4.54	4.68	10.52	10.52	7.73	6.55
$\omega_{\xi32}^2$	-	-	1543	1404	-	-	6390	5987
$(2\xi\omega)_{\xi32}$	-	-	7.64	7.20	-	-	52.6	59.7
$\omega_{\xi41}^2$	-	-	19.5	18.9	-	-	27.7	26.7
$(2\xi\omega)_{\xi41}$	-	-	1.25	1.10	-	-	2.02	1.78
$\omega_{\xi42}^2$	-	-	124	122	-	-	166	172
$(2\xi\omega)_{\xi42}$	-	-	1.25	1.10	-	-	2.02	1.78

TABLE D-III
NUMERICAL VALUES FOR EXACT AND APPROXIMATE TRANSFER FUNCTION FACTORS
CONFIGURATION 4

Transfer Function Factor	q = 5.95 psi				q = 11.9 psi				q = 29.5 psi			
	3 Modes		4 Modes		3 Modes		4 Modes		3 Modes		4 Modes	
	Approx.	Exact	Approx.	Exact	Approx.	Exact	Approx.	Exact	Approx.	Exact	Approx.	Exact
ω_{sp}^2	57.8	60.6	65.0	55.7	93.4	90.3	78.9	76.0	209	207	110	140
$(2\xi\omega)_{sp}$.519	.471	.349	.332	1.04	1.08	.758	.767	2.18	2.27	2.05	1.70
ω_{1e}^2	16.9	14.02	13.5	14.2	18.8	18.8	17.5	19.5	34.1	25.5	26.6	26.9
$(2\xi\omega)_{1e}$.188	.237	.232	.238	.368	.327	.291	.280	.685	.591	.144	.252
ω_{2e}^2	-	-	134	144	-	-	183	184	-	-	308	278
$(2\xi\omega)_{2e}$	-	-	.542	.554	-	-	1.09	1.09	-	-	2.25	2.05
$1/T_{w1}$	125	125	125	125	160	161	160	160	51.6	51.7	48.7	48.9
ω_{w1}^2	31.5	31.5	32.1	32.25	28.3	28.2	29.3	29.7	55.4	55.4	54.9	54.3
$(2\xi\omega)_{w1}$.100	.0997	-	.0951	.142	.141	-	.00777	.872	.873	-	.439
ω_{w2}^2	-	-	131	132	-	-	153	152	-	-	203	222
$(2\xi\omega)_{w2}$	-	-	.423	.428	-	-	.747	.747	-	-	1.17	1.24
$1/T_{\theta 1}$.132	.132	.130	.132	.447	.447	.416	.446	-.482	-.486	-1.12	-.482
$\omega_{\theta 1}^2$	31.5	31.5	32.1	32.3	28.3	28.3	29.3	29.7	55.4	55.0	54.9	54.3
$(2\xi\omega)_{\theta 1}$.129	.127	.0669	.0836	.242	.242	.134	.113	.254	.258	.544	.0356
$\omega_{\theta 2}^2$	-	-	131	132	-	-	153	152	-	-	203	222
$(2\xi\omega)_{\theta 2}$	-	-	.438	.425	-	-	.785	.775	-	-	1.20	.923
$\omega_{\xi 1}^2$	1.52	1.51	1.59	1.50	7.23	7.23	7.17	7.18	*	*	*	*
$(2\xi\omega)_{\xi 1}$.108	.108	.112	.115	.402	.400	.419	.414	*	*	*	*
$\omega_{\xi 2}^2$	-	-	134	135	-	-	160	161	-	-	199	219
$(2\xi\omega)_{\xi 2}$	-	-	.389	.396	-	-	.666	.666	-	-	1.03	.689
$\omega_{\xi 4}^2$	-	-	10.45	6.97	-	-	9.97	9.99	-	-	*	*
$(2\xi\omega)_{\xi 4}$	-	-	.126	.177	-	-	.382	.409	-	-	*	*
$1/T_{\xi 4 2}$	-	-	**	**	-	-	69.4	68.7	-	-	**	**
$1/T_{\xi 4 3}$	-	-	**	**	-	-	-103	-105	-	-	**	**

* Complex pair breaks into real roots
** Real roots become complex pair